EMBRY-RIDDLE
Aeronautical University™
SCHOLARLY COMMONS

Theses - Daytona Beach   Dissertations and Theses

4-1997

Development and Initial Evaluation of an Acoustic Apparatus Used For Testing of Farfield Noise Emitted by a Propeller in a Short Duct

R. Duane Oleson
Embry-Riddle Aeronautical University - Daytona Beach

Follow this and additional works at: https://commons.erau.edu/db-theses

Part of the Aerospace Engineering Commons

DEVELOPMENT AND INITIAL EVALUATION OF AN ACOUSTIC

APPARATUS USED FOR TESTING OF FARFIELD NOISE

EMITTED BY A PROPELLER IN A SHORT DUCT

by

R. Duane Oleson

A Thesis Submitted to the
Office of Graduate Programs
in Partial Fulfillment of the Requirements for the Degree of
Master of Science in Aerospace Engineering

Embry-Riddle Aeronautical University
Daytona Beach, Florida
April 1997

UMI Number: EP31828

INFORMATION TO USERS

The quality of this reproduction is dependent upon the quality of the copy
submitted.   Broken or indistinct print, colored or poor quality illustrations
and photographs, print bleed-through, substandard margins, and improper
alignment can adversely affect reproduction.
In the unlikely event that the author did not send a complete manuscript
and there are missing pages, these will be noted.   Also, if unauthorized
copyright material had to be removed, a note will indicate the deletion.

UMI®

DEVELOPMENT AND INITIAL EVALUATION OF AN ACOUSTIC

APPARATUS USED FOR TESTING OF FARFIELD NOISE EMITTED

BY A PROPELLER IN A SHORT DUCT

by

R. Duane Oleson

This thesis was prepared under the direction of the candidate's thesis committee chairman, Dr. Howard Patrick, Department of Aerospace Engineering, and has been approved by the members of his thesis committee. It was submitted to the Office of Graduate Studies and was accepted in partial fulfillment of the requirements for the degree of Master of Science in Aerospace Engineering.

THESIS COMMITTEE:

Dr. Howard Patrick
Chairman

Dr. Allen Ormsbee
Member

Mr. Charles Eastlake
Member

Department Chair, Aeronautical Engineering

ACKNOWLEDGMENTS

ABSTRACT

Author: R. Duane Oleson

Title: Development and Initial Evaluation of an Acoustic Apparatus Used For Testing of Farfield Noise Emitted by a Propeller in a Short Duct

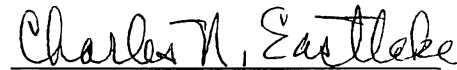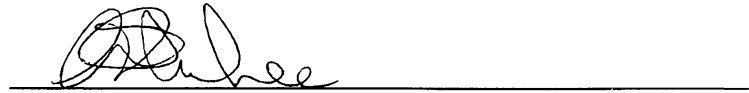Institution: Embry-Riddle Aeronautical University

Degree: Master of Science in Aerospace Engineering

Year: 1997

The purpose of this thesis was to design, construct and evaluate an apparatus which was used for testing of acoustic emissions by a propeller in a short duct. An apparatus was designed based on a combination of acoustic principles and a desire to be able apply the knowledge gained to a practical application such as an ultralight aircraft in an effort to reduce the overall noise levels emitted. The apparatus consisted of a 35 horsepower ultralight engine, a four bladed ultralight propeller, and a duct constructed of a foam core covered with fiberglass. Initial evaluations compared noise levels from the apparatus both with and without the shroud in place, as well as various engine silencer configurations. The data gathered proved the apparatus was actually about 6 dB louder with the shroud than without the shroud as a result of strong rotor-stator interactions. Based on the initial evaluations, this apparatus demonstrated its potential for further testing and acoustical work in the principles of rotor-stator interactions, short duct acoustics, and active noise control applications with the long range goal being to reduce the acoustic emissions from propeller driven aircraft.

TABLE OF CONTENTS

LIST OF TABLES

LIST OF FIGURES

CHAPTER 1

INTRODUCTION

1.1 BACKGROUND

Since the early 1970's, noise pollution has been a slowly increasing worldwide problem. Areas surrounding airports especially, have "taken a beating" due to increased public objections to the noise levels related to the airport traffic [1]. While much of the concern lies with large commercial jets airliners, the fact is that much of the "fly-over" noise is generated by smaller propeller driven aircraft. In order to control the noise emissions from propellers, there has been pressure to employ stricter regulations than already exist on the aviation industry in an effort to force the airplane manufactures to further reduce the overall noise levels due to the propellers. The work contained herein addresses this issue by further researching new methods for lowering the noise emitted from propellers, without decreasing their performance.

Propeller noise is going to continue to become a concern in the future as propellers are relied upon in almost all facets of aviation. Within the general aviation (GA) industry which relies almost solely upon propellers as a means for propulsion, recent liability reforms have spurred the manufacture of new aircraft again, and it is expected that the GA aircraft fleet will start to see an increase in the number of planes flying over the next ten

1

years or so. In the airline industry, many companies tend to rely upon smaller turbo-prop

driven aircraft to fly many of their feeder routes, and as the airline industry continues to

expand, so will the number of commuter flights. Finally, recent technologies have brought

fourth the prop-fan engine, which implements two sets of counter-rotating propeller

blades, providing higher efficiencies, as well as higher perceived noise levels than previous

equivalent turbo-fan engines which could pose a potential problem should the prop-fan

engine make it on to production aircraft.

Control of increasing levels of noise at airports has been divided into three areas:

quantification of airport noise, noise abatement at specific airports, and reduction of

aircraft noise at the source [2]. It is the reduction of aircraft noise at the source that is the

primary concern to the aircraft industry and the Federal Aviation Administration (FAA).

(Although noise abatement procedures at airports have also been receiving attention

recently.) Federal Aviation Regulation (FAR) 36 spells out the limitations on aircraft

noise, both for existing and new aircraft [3]. For new propeller driven aircraft, the FAR

restricts the total flyover sound emissions at a height of 1000 feet to between 68 and 82

decibels (dBA), based on the exact gross weight of the airplane. With stricter limitations

possible towards the beginning of the 21st century, methods for reducing propeller noise

are becoming more critical.

When examining how to reduce the total noise emitted from an object into the

surrounding area, there are two basic approaches that can be taken. The first is to reduce

the amount of noise that is generated by the source; however, this is not always practical

as much of the time, this could result in adversely altering the amount of performance by

the noise generator. The second approach is to control the noise after it has been generated and prevent it from traveling beyond the source. This is referred to as noise suppression. Optimally, both approaches should be used in parallel to achieve the greatest overall sound reduction.

Using the first approach, noise emitted from a propeller can be reduced by altering its shape and size, or by lowering its rotational speed, both of which can alter the performance of the propeller. There is currently ongoing work in this area, through the National Aeronautics and Space Administration (NASA) working in conjunction with some universities. To date, this method has proven to be successful, although the amount of reduction that will be able to be achieved in the future while maintaining the performance level is questionable.

In the past, noise suppression methods have not been used very extensively in the aviation industry to quiet the noise emitted from the propeller, but due to the recent advancements in materials and technologies, noise suppression methods must be considered. Noise suppression methods can be divided into two basic types: passive noise control and active noise control (ANC). Passive noise control is the suppression of noise through the use of passive means such as insulating barriers, redirection methods, and noise absorption materials. Passive noise control tends to work better with higher frequency sounds, since as a general rule, the lower the frequencies, the more material is needed to dampen out the noise. This can result in great weight and size penalties.

Active noise control uses sound waves to cancel out unwanted sound waves. It generally works best with lower frequency sounds (<500 Hz) that are of constant or

repeatable tones. Using active control methods generally tends to be much more complex than using passive means, but theoretically a 100% reduction can be achieved. While this might not ever be the case in real life situations, it is still possible to see reductions on the order of 25 dB in certain cases which is quite significant. It is for this reason that research into the use of active noise control to cancel out lower frequency tones generated by propellers becomes important.

As of now, ANC has been performed and tested on propellers in a long duct (long duct implies the length is approximately ten times the diameter) [4]. The next logical step is to try to apply that work to a short duct (length is about one half the diameter). Using such a short duct though brings up the question of how many of the concepts applicable to longer ducts still apply for a short duct? Can it be assumed that the frequencies below the cut-off, which would normally decay before exiting into the open atmosphere, will still decay and play a negligible role in the overall-sound-pressure-level (OASPL)?

The work that needs to be performed consists of two major developmental areas. One is the design and building of the experimental apparatus and the second is the development and implementation of the active noise control that will be used. The primary purpose of this thesis is the construction and evaluation of a platform which will be able to be used for active noise control testing on a short duct. A thorough description of the initial design, as well as reasoning will be provided. Initial performance and acoustical data will be presented and analyzed for the cases of the unshrouded propeller and the shrouded propeller. Finally, discussion of the implementation of future active noise control as well as other possible applications for the apparatus will be provided.

1.2 THEORY

The general theory presented in this section is divided into three headings: active noise control, duct acoustics, and rotor-stator interaction. The design of the apparatus is based on theoretical principles from each of these areas.

1.2.1 Active Noise Control Theory

Acoustical noise occurs due to pressure fluctuations that are generated by a source and proceed to travel through a medium as a pressure wave. Basic wave theory states that a wave of frequency (Ω), amplitude (A), and phase (ϕ), when added to a second wave of identical frequency and amplitude, but 180 degrees out of phase with the original, will provide a net resultant of zero. This basic concept, applied to acoustical pressure waves is known as active noise control.

In theory, any acoustical noise emitted from a primary source can be canceled out by a secondary source provided that the secondary source is capable of producing an identical sound wave fully out of phase and of equal magnitude to that of the primary source. In a 3-dimensional freefield system though, this requires the secondary source to be placed at the exact same location as the primary source. Notice, from Figure 1A, when the sources are placed at different locations, the sound waves emitted from each source do not line up, but in Figure 1B, when the sources are placed at the same location, it is possible for the sound waves emitted to fully overlap as they propagate from the sources.

PRIMARY SOURCE

SECONDARY SOURCE

Fig. 1A

Fig. 1B
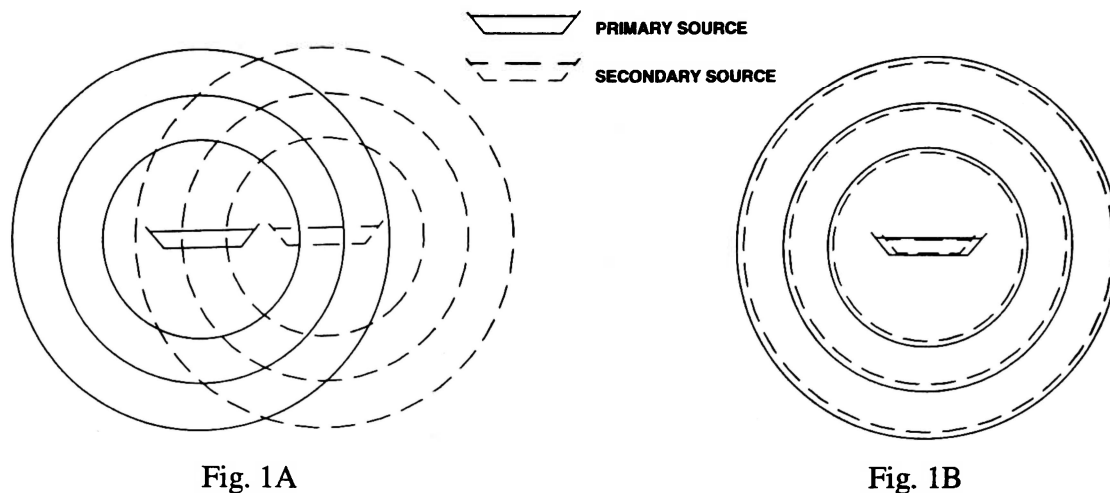
Figure 1. Emission of Sound Waves From Two Sources

Since it is not physically possible to place a secondary source at the same location

as the primary source, the other option is to model the noise as an infinite set of sources

placed around the primary source. In theory, by using an infinite number of secondary

sources, primary noise can be kept from passing beyond the set of anti-noise sources. This

concept is known as Huygen's principle [5] and is shown in Figure 2. While full noise

ZONE OF SILENCE
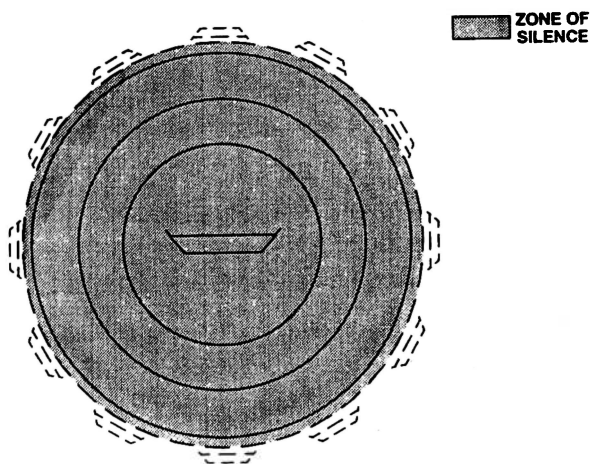
Figure 2. Huygen's Principle

cancellation will never be achieved in the practical sense using ANC due to the need for an infinite number of sources, partial noise attenuation is still possible through careful application of ANC principles.

The most common means of employing ANC takes place through use of destructive wave interference. This concept was first demonstrated by Thomas Young [6] in the early nineteenth century through use of his famous "two slit" experiment in which he demonstrated that two identical light beams that were out of phase would create alternating dark stripes and light stripes on a screen. The dark bands were where the light waves canceled each other out, and the light bands were the areas where the light beams intensified each other. The concept remains unchanged for acoustical wave theory.

Almost all commercial ANC systems today are based on destructive wave interference at the receiver. This type of system works well for noise cancellation within small enclosed regions, generally around a person's ears and/or head. The basic system detects the unwanted noise, and using the unwanted noise, generates an anti-noise which drives the overall level down in one particular region. These type systems have proven to be very successful within limited regions, but, while the noise is reduced in certain areas due to destructive interference, it inevitably ends up being increased in other areas due to constructive interference [7]. Generally the area of cancellation tends to cover only about one tenth of the primary wavelength distance from the center of cancellation. Even with the lowest audible frequency of 20 Hz, this only accounts for a sphere of cancellation with a radius of approximately 2.5 feet [6].

A second approach provides for a more global cancellation of noise. By placing the secondary source as close as possible to the primary source, the acoustic waves emitted from the secondary source blanket those from the primary source. This type of noise cancellation can be thought of as a true suppression of noise at the source. It occurs due to an unloading of the primary source. Essentially, by driving the medium at the surface of the primary source in phase with the primary source, no sound emissions take place since the primary source no longer has a medium to perform work on. Acoustically speaking, the impedance of the system is driven towards infinity. In free field conditions, this type of cancellation requires that the secondary source be placed very close to the primary source, in essence creating a dipole source. In ducts, however, the secondary source can be placed further upstream or downstream of the primary source, as long as the phase is adjusted to account for the time it takes the secondary source wave to reach the primary source.

A final strategy of active noise control involves absorption of noise using a secondary source. The secondary source is now emitting no power, but rather absorbing energy from the system. However, since most noise generators act as poor acoustical absorbers due to low transfer efficiencies, the secondary source usually still has to be driven by an external source to keep it at the same frequency as the primary frequency and when examining the effects this has on the impedance at the primary source, it can be seen that this type of system actually increases the power emitted at the primary source. Overall, this method is not very efficient, and has been shown to work only in some limited cases involving plane waves in ducts [8].

Early ANC systems generally were based around simple feedback loops. A pure

feedback system, shown in Figure 3, works by introducing a secondary noise source into

the medium and through use of a microphone detects the difference between the primary

noise source and the secondary source. Based on the differences between the primary
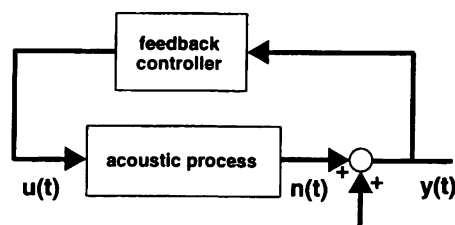
Figure 3. Feedback Loop

source and secondary source, the secondary source is then appropriately adjusted to

minimize the error detected by the microphone. As is often the case, however, with pure

feedback systems, stability of the system becomes an issue. Often, an ANC system based

solely on feedback will not be able to respond fast enough to keep up with changes in the

primary noise source, unless the changes are slow enough to allow the system to make

appropriate adjustments without over-compensating in the process. In a feedback system,

it is advantageous to place the microphone as close to the secondary source as possible to

provide tight coupling between the source and the detector.

Feedforward systems require the detection of the primary noise, before reaching

the secondary source. Feedforward systems are widely used in ducts, and often in systems

where the noise is of repetitive nature. A feedforward system can use a microphone to
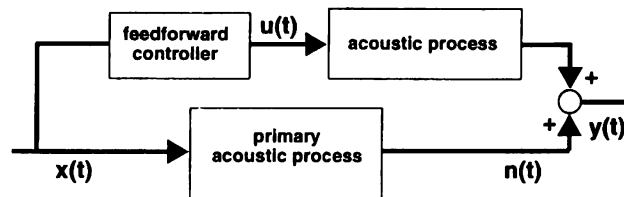
Figure 4. Feedforward Loop

detect the noise upstream, and provide for an appropriate anti-noise to cancel out the unwanted noise further downstream. For the cases of repetitive noise sources, such as rotating blades or vibrating surfaces, other input signals from a tachometer or accelerometer can be used to determine the frequency that the noise to be canceled is occurring at.

A variation on the straight feedforward system is known as the Essex method [9]. The Essex method, depicted in Figure 5 uses an upstream microphone to detect random noise, and a downstream microphone to detect any residual error. The Essex method is basically a combination feedforward and feedback system, which used the feedforward signal to determine the anti-noise frequency and phase, and the feedback signal to adjust the filters to minimize residual error. While other microphone-speaker setups have been attempted with various degrees of success, both in ducts and in the freefield, the basic ANC concepts and control theories remained constant throughout.
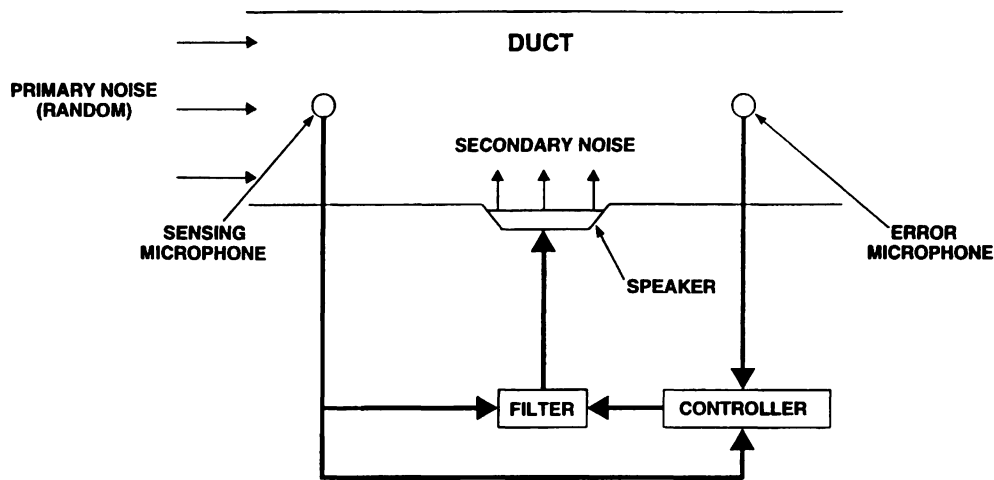
Figure 5. Essex System

1.2.2 Basic Duct Theory and Cutoff Concepts

1.2.2.1 One Dimensional Duct

Lets consider a one dimensional wave traveling down a channel. The channel is made up of two solid boundaries. Basic wave theory states that the tangent of the wave at the wall has to be perpendicular to the wall, due to the boundary conditions at the wall. Because of the this, it can be seen that any wave traveling down the channel will be constricted to an even integer of half-wavelengths, known as q. The wavelength of a wave traveling down the channel will be constricted by the distance between the two walls, d, and can be seen to have a wavelength in the y-direction of $\lambda_y = 2d / q$. When q equals zero, λ_y goes to infinity, and a plane wave is formed. This is essentially just a

pressure disturbance traveling down the duct. In the First Cross Mode, as can be seen in

Figure 6, q will equal one, and so on.

The cutoff frequency for the q th mode is defined by c / λ_y, where c is the local

speed of sound. If the free space frequency of the wave traveling down the channel, that

q = 0   PLANE WAVE

q = 1   FIRST CROSS MODE

q = 2   SECOND CROSS MODE
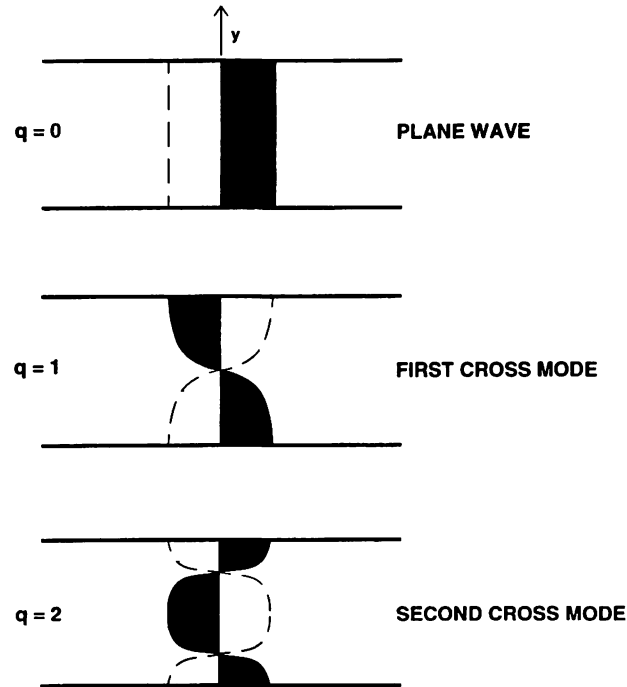
Figure 6. One Dimensional Waves

is the frequency of the wave in a medium with no boundaries, is larger than this, as

illustrated in Figure 7, the wave will not be able to propagate and will decay exponentially.

It can also be shown mathematically that the wave will decay exponentially [10]. From

the wave number equation,

$$k_x = \frac{2\pi}{c}\sqrt{f^2 - f_q^2}$$ Eq. 1

a relation between the freestream frequency and the cutoff frequency can be seen. If

$f < f_q$, k_x will become imaginary which will cause the wave equation to decay

exponentially, as shown in Figure 7. If the frequency is greater than the cutoff frequency,

then k_x will be a real number. When plotted, it can be seen that the amplitude of the wave

follows a cosine distribution. This is shown in Figure 8.
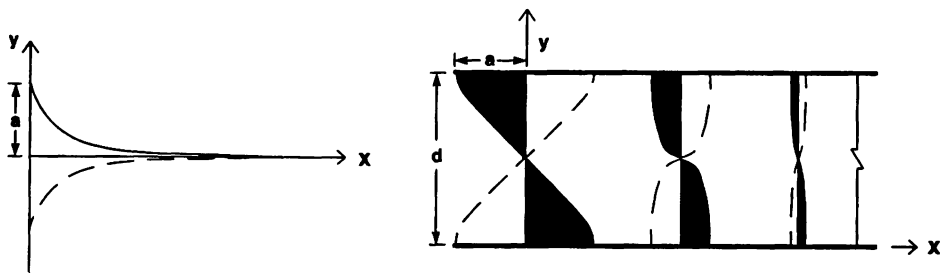
Figure 7. First Cross Mode Decaying Field
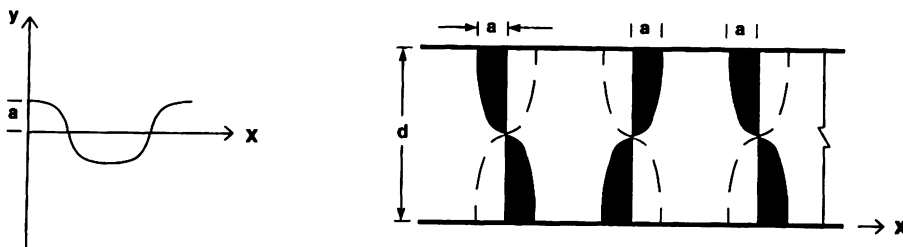
Figure 8. First Cross Mode Propagating Field

1.2.2.2 Axisymetric Ducts

When considering a duct with a rotating propeller or with rotating compressor

blades, Ω defines the rotational frequency of the main shaft. Thus, the blade passing

frequency (BPF) is defined as the rotational speed multiplied by the number of blades, B,

$$BPF = \Omega B. \hspace{3cm} Eq. 2$$

The circumferential velocity, defined by $c_s = r\Omega$, is the speed at which the wave travels

around the duct. Since with each passing of a blade, a pressure disturbance is introduced,

the circumferential velocity is based on the rotational velocity. It follows that the

circumferential Mach number is simply the ratio c_s / c and is abbreviated M_s.
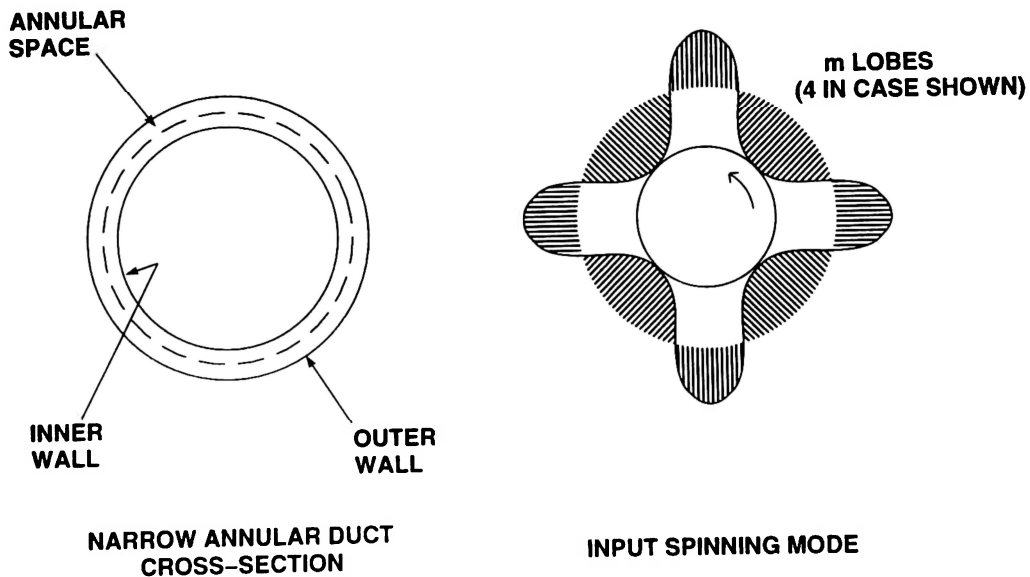
Figure 9. Modes in an Annular Duct

The same concepts from the one dimensional case can be applied to axisymetric ducts, the only difference being that the wave travels around the circumference of the cylinder now. The distance between the two boundaries is simply the circumference of the cylinder, or $2\pi r$, where r is the radius. Instead of q wave-halflengths, the wave is said to contain m number of lobes in the circumferential mode, as in Figure 9. Thus, the cutoff wavelength is now given by $\lambda_s = 2\pi r / m$ and the corresponding cutoff frequency is given by the formula,

$$f^*_m = 1.84c / \pi D \qquad\qquad Eq. 3$$

where 1.84 is the eigenvalue (or zero value) of the Bessel function of the first kind for the m = 1 mode [4]. Other values are listed in Figure 10. The number of radial modes is given as n. Generally, radial modes will not propagate unless the frequencies are much higher than the cutoff frequencies, and thus do not have to be considered [4,10].

To get a better idea of how various waves propagate down a duct, Figures 11A - 11D, taken from Taylor and Sofrin's paper,[10] have been provided. In Figure 11A, the wave can be seen to be decaying. Note how it decays exponentially, just as in the one dimensional case. In Figure 11B, the frequency of the wave is equal to the cutoff frequency. Thus the wave fits perfectly within its boundaries, and will rotate with no spiral angle and will neither propagate nor decay. Figure 11C contains a wave with a frequency larger than the cutoff, so it will propagate with a spiral angle, α. From Figure 11D, it is seen that the spiral angle decreases as the frequency increases. This is
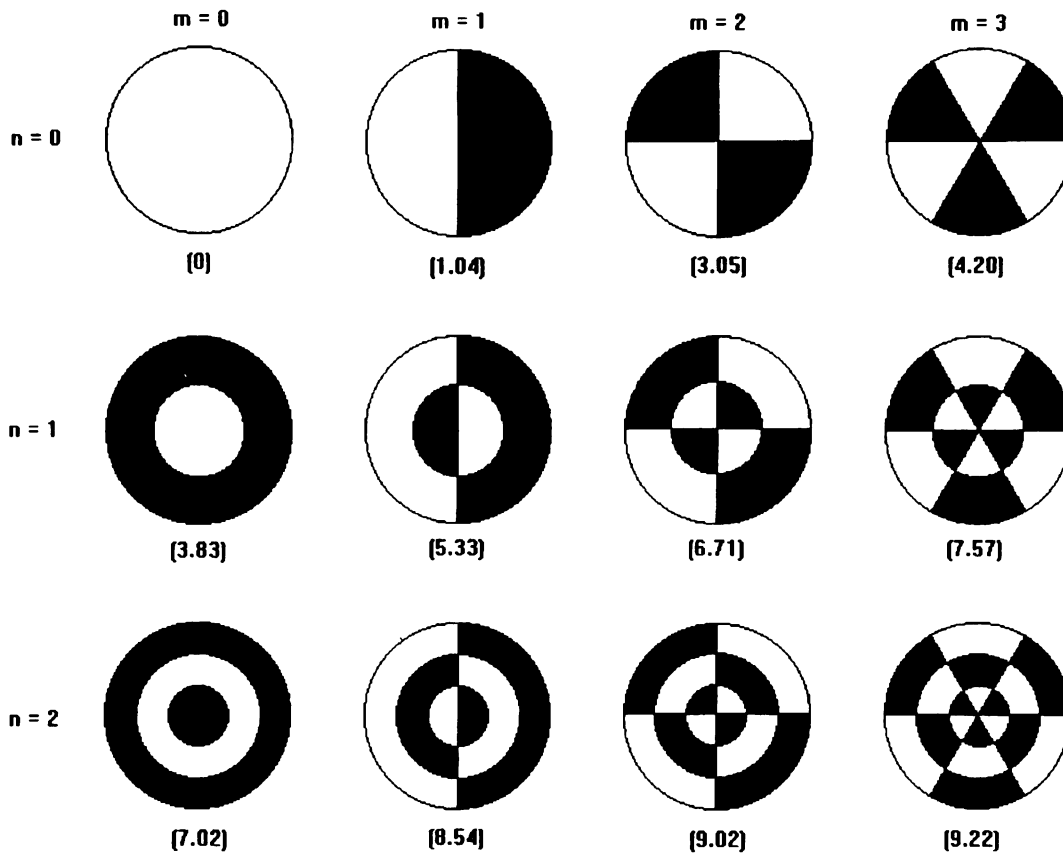
Figure 10. Eigenvalues for Circumferential Modes

due to the fact that the circumferential component of the wave has to equal the frequency for that particular mode. Thus, as the wave frequency increases, the circumferential component (or the sin α component) of the wave frequency decreases in proportion, causing the spiral angle to also decrease accordingly.
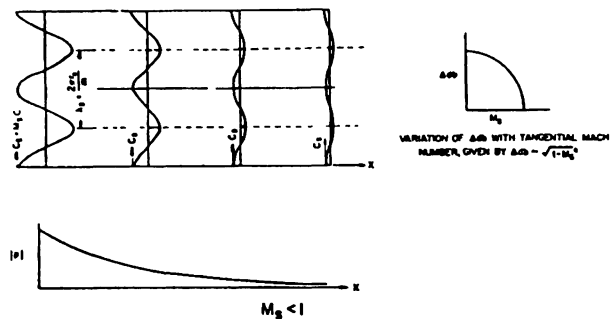
Figure 11A. Properties of Decaying Field; $M_s < 1$
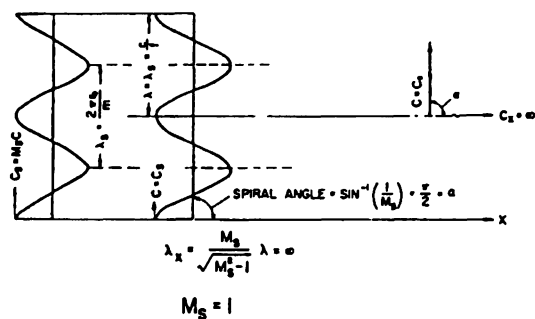
Tyler and Sofrin

Figure 11B. Properties of Stationary Field; $M_s = 1$
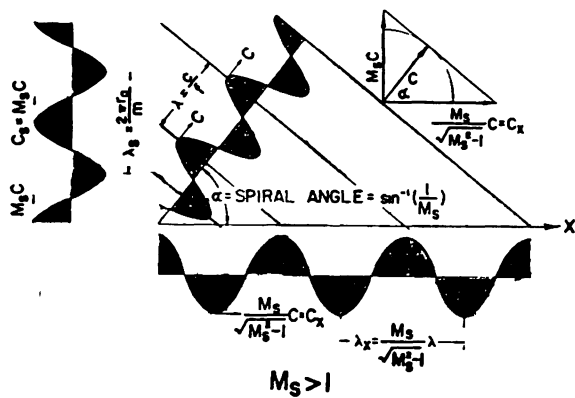
Figure 11C. Properties in a Propagating Field; $M_s > 1$
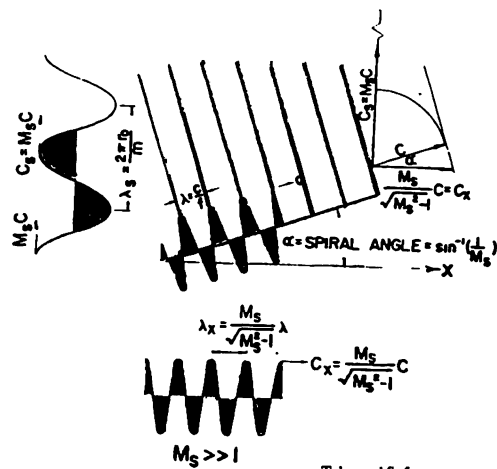
Tyler and Sofrin

Figure 11D. Properties in a Propagating Field; $M_s \gg 1$

1.2.3 Rotor-Stator Interaction Tones

The number of circumferential modes associated with any rotating pressure field in a cylindrical duct is given by the standard equation,

$$m = sB \qquad\qquad \text{Eq. 4}$$

where s is called the harmonic number (1, 2, 3, ...) and B is the number of rotating pressure disturbances. In the case of a rotating fan or propeller, B is the number of blades. If the duct contains stator blades, then additional interaction tones will be formed and the circumferential mode can be found using Equation 5,

$$m = sB + kV \qquad\qquad \text{Eq. 5}$$

where V is the number of stator blades and k is an integer multiplier (0, ±1, ±2, ...). As was shown in the previous section, a given circumferential mode will not propagate unless it is traveling at supersonic speeds. With stators in place, it is possible for these interaction tones to be supersonic even if the blade tip speed is subsonic, indicating that they could propagate down a duct. The rotational velocity of any particular mode is given by

$$\Omega_m = \Omega \Big/ \left(1 + \frac{kV}{sB}\right). \qquad\qquad \text{Eq. 6}$$

Considering Ω_m will only propagate if it is supersonic, then it can be seen that

$|1 + kV / sB| < 1$. To find out which modes will propagate, the first step is to figure out

which k values will provide for $\Omega_m > \Omega$ for a given mode and number of stators and

propellers. Once appropriate k values have been found, the corresponding Ω_m's can be

found using Equation 6. If this value is greater then the cutoff frequency, the wave will

most likely propagate. Examples of this case, based on actual data accumulated for this

report are worked out in Section 3.2.2.1.

In their paper, Tyler and Sofrin were able to show that, in theory, a stator to rotor

blade ratio of two or greater, will provide for the minimal number of tones that propagate

down a circular duct [10]. This can be verified rather easily using the above equations.

For the case of the first harmonic, s = 1 and a stator-rotor blade ratio of V / B = 2,

Equation 6 yields $-1 < 1+2k < 1$, or simplified, $-1 < k < 0$. In this case, k has no values

that can satisfy it. This demonstrates that given twice the number of stator blades to rotor

blades, all modes of the first harmonic will be cut off and will decay. Of course, this might

not always be a practical situation. For example, a compressor with 28 blades would

require 56 stator blades which is not very plausible. In the case of a propeller with three

blades though, the use of six or seven stator blades is very plausible. To date there has

been no published experimental data using a ducted propeller to back this theory up.

1.3 PAST WORK

A review of past work is presented in this section. First, past work with ducted propellers is examined. Then, a review of work with ANC in ducts is provided.

1.3.1 Shrouded Propellers

Most initial work with shrouded propellers was driven by performance increases that could be achieved by placing a shroud, or duct, around a propeller. It was not until the 1950's when the acoustical benefits of placing a shroud around a propeller were first examined by Hubbard when he performed a series of static condition tests, designed to measure the acoustical characteristics of various propeller/shroud configurations [11]. By varying the shroud airfoil, as well as the propeller configurations, Hubbard achieved shrouded noise reductions of up to 6 dB under smooth flow conditions. He was even able to achieve up to 20 dB reductions among some of the higher frequencies. He found, however, that when a crosswind was introduced into the inflow, an inlet stall condition would occur, increasing the noise levels by 6 dB. Further results of his work are summarized in Table 1, in which the effects of different variables tested are given. Much of the initial shroud design for the apparatus being reported was based on the shrouds used in Hubbard's experimentation.

More recent work with shrouded propellers has examined their practical application to GA airplanes [12]. Tests were performed in NASA's full scale tunnel, using

Table 1. Results from Hubbard's testing on shrouded propellers

Configuration Parameter	Acoustical Effect
Unseparated Flow vs. Separated Flow	With unseparated flow, noise was dominated by low-frequency tones, while under separated flow, overall noise increased and all rotational frequencies were exaggerated.
Shroud Chord	Acoustically, shroud chord did not affect noise levels. Aerodynamically, the longer chords were more stable.
Tip Clearance	No appreciable change in sound levels up to a tip-clearance ratio of 1% of the radius. Greater than 1%, sound pressures rapidly approached those of the unshrouded condition.
Tip Speed	Fundamental freq. and second harmonic demonstrated increases as the 4.5 power and 5.5 power of the tip speed, as predicted for unshrouded propellers.
Number of Blades	As number of blades increased, fundamental frequencies of the rotational sound decreased while vortex noise increased.

a Cessna 337, a light twin that uses a push-pull engine configuration. Only the pusher

propeller was used for these tests, which examined an unshrouded 2-bladed propeller as

well as various 3 and 5 bladed shrouded configurations. Results concluded that the

shroud did not provide any significant noise reduction under tunnel flow conditions for

most power and thrust settings measured. At static conditions the propeller in-plane noise

levels were less for the shrouded propeller than for the unshrouded propeller, but still

remained equal for other locations. Shroud shielding was most likely the largest contributor to the in-plane noise reduction.

While those initial set of NASA tests were not extremely encouraging, they did serve the purpose of setting up further testing, using the same tunnel and airplane, of a quiet-fan (Q-fan) design [13]. The Q-fan has some of the characteristics of both a shrouded propeller and a turbo fan. It has seven wide chord blades. The diameter of these blades is smaller than that of a standard propeller which allows for higher RPM's without higher tip speeds. The Q-fan also incorporates inlet guide vanes to help increase thrust. The acoustic conclusions using the Q-fan appeared to be favorable. The Q-fan reduced the extrapolated fly-over noise level to 65 dBA for 1,000 ft. This compares to levels of 75 dBA with the shrouded propeller used in the earlier test. It was felt that further increases in noise reduction could be achieved by installing duct acoustic treatment and by installing the Q-fan in a tractor arrangement rather than a pusher arrangement which could reduce some of the inlet turbulence.

The one area that the above mentioned works did not however seem to address, was the effect of introducing stator blades inside the duct. Although, there has been a proposal submitted by Patrick [14] to pursue the effect of stator blades in the overall noise levels emitted from the duct, there has been no actual research examining a ducted propeller with stator blades. It would seem than, that this could be another application for this apparatus besides the ANC research application.

1.3.2 ANC in Ducts

The origins of ANC date back to Paul Lueg, who in 1934 applied for a patent for a system which would use an upstream microphone to detect a plane wave traveling down a duct and use a loudspeaker downstream of the microphone to introduce an anti-wave. The anti-wave would then cancel the primary planewave through destructive interference thus creating the first ANC system [15]. After Lueg's initial flirt with ANC, not much was performed in the field until the 50's and 60's, at which time, names like Harry Olson, Evert May, and William Conover, started taking an active role in developing practical applications of ANC, such as "quiet headsets" and silenced transformers [16]. Still, during those times, with only analog systems available, ANC advancement was very slow. The analog systems did not have the speed or capability needed to adjust to acoustical systems. With the inventions of digital systems though, came the true birth of ANC as known today.

With the advent of digital controllers, ANC in ducts could finally proceed beyond simple cancellation of a one dimensional plane wave using a microphone to detect the wave upstream and a loudspeaker to cancel the noise downstream. One of the first advancements in the early eighties was the use of frequency measuring devices, such as a tachometer or accelerometer, to cancel noise of a constant repetitive nature. In 1980, Barrie Chaplin demonstrated this idea by showing a 20 dB reduction was possible in engine exhaust noise through replacement of the microphone with a tachometer [9]. His setup shown in Figure 12 was based on the Essex model seen in Section 1.2.1, and like

that setup, still employed the use of feedback control through use of a residual microphone placed downstream.

More recently, there has been a strong emphasis on trying to reduce levels of higher order mode acoustical waves. In 1989, Erickson, et al, used a two speaker setup to drive a (1,0) mode down by 20-25 dB [17]. He accomplished this by using one error transducer per speaker to provide independent inputs for each speaker, which allowed one
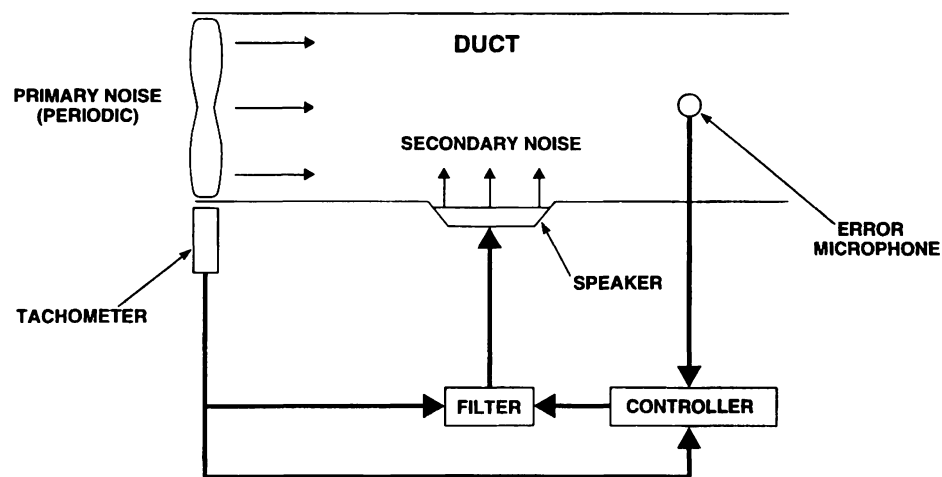
Figure 12. Essex System Using Tachometer for Upstream Signal

speaker to adjust to the negative crest in the pressure distribution, while the other was adjusting for the positive crest. Some reduction of higher order modes have since been accomplished in commercial systems [18].

While the previously mentioned works are pertinent to active noise control of a propeller, of particular interest to the work provided herein, is the research performed by

Sutliff and Nagel, presented in Sutliff's doctoral thesis in 1993 [4]. Sutliff and Nagel

developed an ANC system that successfully lowered the noise emitted from a propeller

located in a long duct. Reductions of 23 dB in the plane wave and 17 dB in the (1,0)

mode were noticed. Their experimental setup consisted of an eleven inch diameter

propeller driven by an electric motor, placed in a duct that was just under 8 feet long. The

ANC system consisted of a feedforward system with no feedback control. Two input

signals were used: a tachometer that measured rotational frequency of the propeller, and a

position detector that was used to determine the appropriate phase shift. The algorithm

was designed to first develop a high-resolution sinusoidal waveform a-priori to its

operation. With the waveform precalculated, the controller, a PC computer, read the

frequency from the tachometer and adjusted the waveform to the proper frequency.

Finally, phase shift was accounted for through use of a once-per-rev signal which provided

the algorithm with an indication of when to send the output signal to the loudspeaker.

The advantage to this system is that while there is some setup involved, once initialization

has been taken care of, processing time is kept minimal. Certainly, with even faster

technologies today, the "deadtimes" that Sutliff and Nagel experienced while operating

due to lack of parallel processing capabilities when they performed their work would be

eliminated, and their results would only be improved upon.

1.4 PURPOSE OF THE PROJECT

Based on previous work, there is a definite potential for significant noise reductions, however, there have not been any studies which fully examine the feasibility of applying ANC to a shrouded propeller. It is the purpose of this report to take the initial steps to merging these two fields of study in such a way that an ANC system can be used in conjunction with a shrouded propeller to create a quieter propulsion system for light aircraft. Certainly, there are many variables. What are the possible implications of the engine exhaust/intake noise? Will supporting struts influence the noise as predicted by classical rotor-stator interaction? What are the physical consequences of trying to apply ANC in a short duct? Through design and construction of an experimental shrouded propeller and subsequent acoustical testing, answers to these questions will be provided. With the initial evaluation and noise surveys completed, the feasibility of applying ANC to the apparatus will be reevaluated and suggestions for future work will be provided.

CHAPTER 2

APPARATUS, PROCEDURE, AND INITIAL DATA

2.1 APPARATUS

The apparatus used for testing consisted of a gasoline engine, a four bladed propeller, and a shroud that was approximately half it's diameter in length. An overview of the apparatus tested is provided in the following section, proceeded by more detailed descriptions of the major components in the next couple of sections. A photograph of the complete test setup is shown in Figure 13.

2.1.1 Overview

The design for the propeller/shroud test apparatus was driven by one long range goal: to demonstrate that this type of technology could have a useful application to general aviation aircraft currently flying. In order to accomplish this goal, ANC technology first has to be proven under actual flight conditions. With this goal in mind, the apparatus was designed to simulate a setup that could be used in flight, but was built such that it served only as a static test stand.

One scenario for flight testing a propeller/shroud apparatus in the future, would be
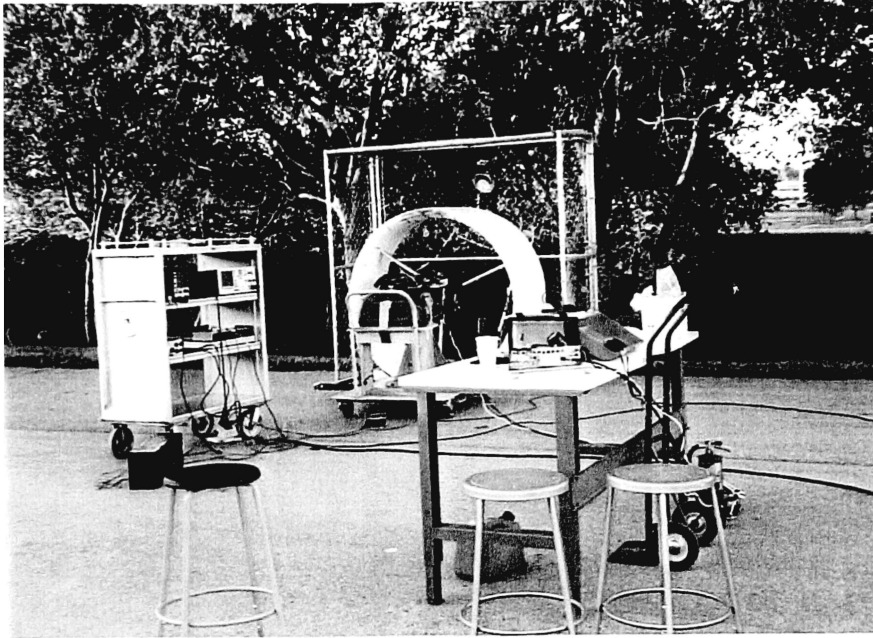
Figure 13. Complete Setup Ready to Run

to use a twin engine light aircraft such as the Air Cam by Lockwood Aviation, Sebring,

Florida, shown in Figure 14. As can be seen, the Air Cam has the unique feature of having

two engines. By affixing the shroud to only one engine, differences in fly-over noise could

be measured by operating only on the engine of interest. This would avoid errors due to

changes in outside variables, such as wind direction, temperature, extraneous noise, etc.

that could arise during the time spent to changeover the configuration on a single engine

aircraft. Further, the second engine would provide back-up in the event of an engine

failure during testing. Finally, for initial in-flight evaluation, this aircraft makes a lot of
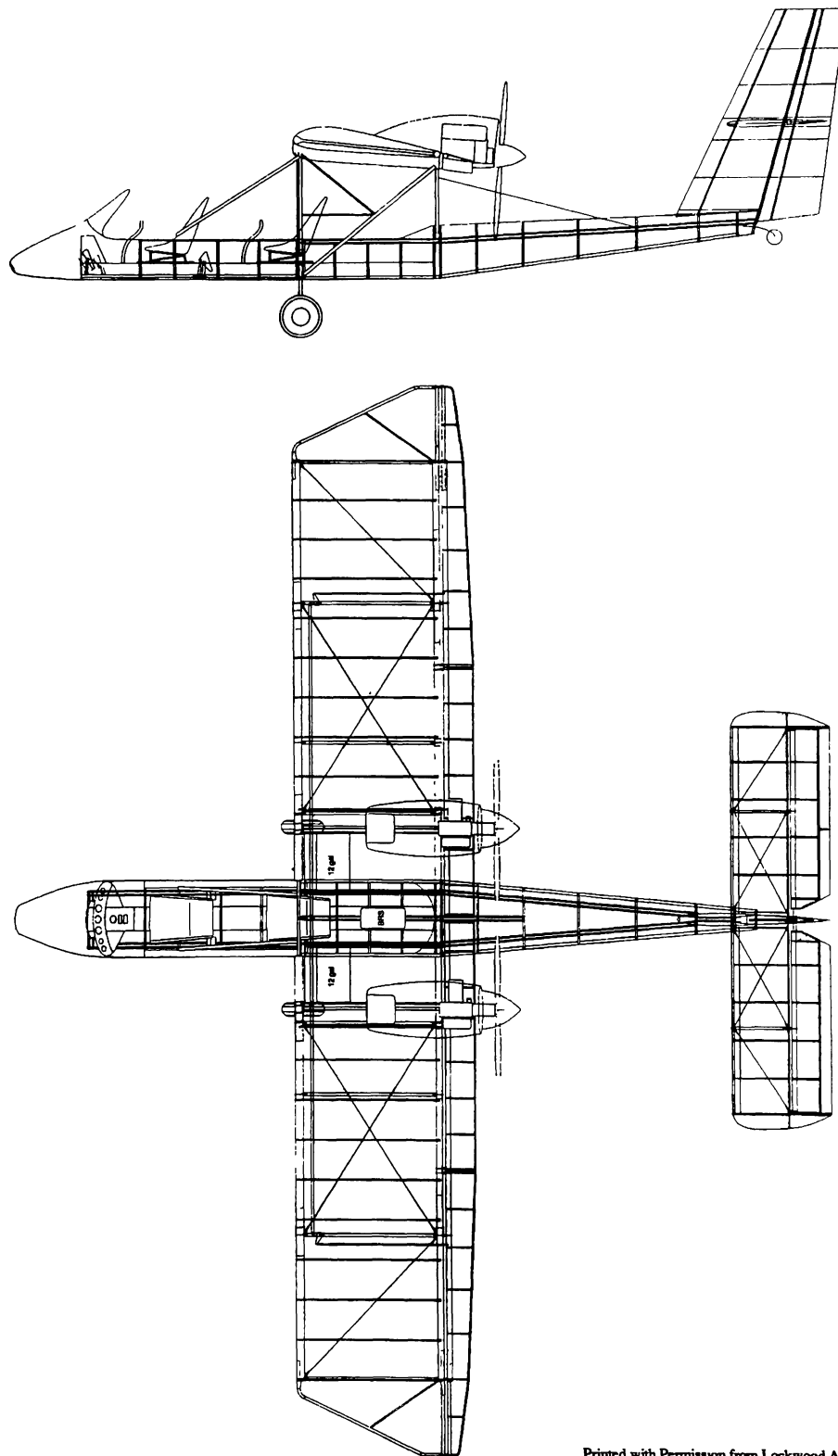
Figure 14. Lockwood Aviation's Air Cam Aircraft

sense due to its simplicity, docile handling characteristics, and slow flying speeds.

With this possible scenario in mind, the decision was made to design the apparatus around an ultralight engine and propeller, similar to the ones that were in the Air Cam, which would help to provide the realistic operating conditions desired. The engine and propeller were supplied by Lockwood Aviation, and a test stand was built to mount the engine in a similar fashion to how it might be attached to an ultralight. The entire test stand was mounted on a cart with four castored wheels. This allowed for easy transport of the apparatus which was important since no anechoic chamber was available and the entire unit had to repeatedly be rolled outside for testing purposes.

Another consideration when designing the apparatus was the ease of configuration changes. In other words, it was desirable to design the apparatus such that various propeller/stator combinations could be run with and without the shroud in place. This allowed for the opportunity to test the effects of number of blades and number of stators, as well as compare the unit with and without the shroud. While testing was only performed with a four bladed propeller and three stators, future configuration changes remain flexible by using an ultralight propeller which can be run in a two, three, or four bladed configuration, and at variable pitch angles. It is also possible to add more stator blades, although, they would have to be added in multiples of three.

Since the test apparatus was developed with the eventual goal of actual flight in mind, the design of the shroud could not be based strictly on the criteria for static conditions. Optimally, for static conditions, a large bellmouth intake would have provided the best conditions for unseparated flow into the shroud, however, since this would not be

realistic for flight conditions due to the additional drag that would be imposed, a compromise was made. Efforts were made to keep the weight down, but still maintain enough strength and rigidity to resist the aerodynamic and vibrational loads exerted on it. Finally, in order for the design to be transferred to an actual aircraft readily, the shroud had to be able to support itself with little or no outside structure. This was achieved by connecting the shroud directly to the engine using the three stators as struts. Figure 15 shows a drawing of the ducted propeller portion of the test apparatus.
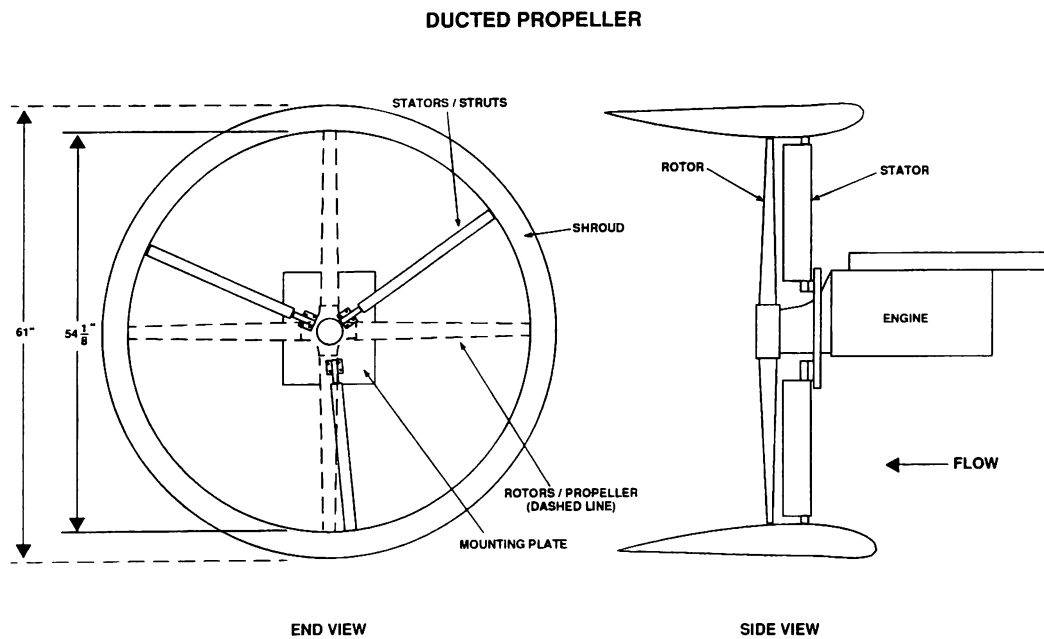
DUCTED PROPELLER

Figure 15. The Ducted Propeller

2.1.2 Engine and Propeller

The engine used for the test rig was a Rotax 377, 35 horsepower, two cylinder, two stroke, air-cooled, ultralight engine. This type of engine is currently in use in ultralights today. The specifications are listed in Appendix A.

Due to the nature of a two stroke engine to run very rough at low operating speeds, the engine was bolted directly to the engine stand using four bolts which screwed into the bottom of the crankcase. This helped reduce the "shaking" of the engine at low RPM settings and was in response to a concern that there might not be enough stiffness in the struts between the engine and the shroud to dampen out the low frequency vibrations which could result in a propeller rubbing along the inside wall of the shroud. Long term vibrational fatigue was not a major factor due to the relatively low amount of time the engine was run for testing purposes. In the future, however, a more suitable means of vibration isolation between the engine and test stand should be developed if the test apparatus is going to see long term continued use.

The engine speed was controlled using a simple quadrant type throttle, which was connected to the engine using 25 ft of push/pull cable. In addition, there was an "on/off" switch which could be used to ground out the spark plugs, shutting the engine completely off. Two engine gauges were used to monitor the operation of the engine: an engine tachometer and a cylinder head temperature gauge which provided temperatures for both cylinder heads. All controls and gauges were mounted to a remote base which could be carried anywhere within the limits of the cables. This allowed for operation of the engine

from a safe distance, and provided the mobility to retain control while moving around for purposes of data gathering. The engine was started via a recoil type pull starter, connected to the back of the engine.

Overall engine noise was reduced as much as possible through additional mufflers both on the exhaust and intake sides of the engine. On the exhaust side, a small second muffler, or after-muffler, was installed behind the main exhaust muffler and on the intake side, a specially designed intake muffler was installed onto the carburetor. Both of these additional installations were designed to fit specifically onto Rotax engines and were readily available through the engine distributor. Overall noise of the engine and the effectiveness of these additional noise suppression devices will be addressed further in the results section.

The engine RPM was reduced through means of a 2.58:1 ratio gearbox. This provided engine speeds of just over 6,000 RPM, while providing propeller testing speeds around the desired setting of 2,400 RPM. Acoustically speaking, this odd ratio of engine RPM to propeller RPM is very helpful in distinguishing between the engine operating tones and the propeller tones which are functions of their respective RPM's.

The propeller used was a standard ultralight, four bladed, adjustable pitch composite blade propeller. The blades were clamped at the hub, using mounting blocks sandwiched between two metal face plates. When the bolts were drawn tight, the blades were secured in position. The pitch of the blades was set to 10 degrees, measured at the 4/5 radius location, which provided the desired RPM at full power setting. The diameter of the propeller, which was adjustable within about half an inch was set to match the inside

diameter of the shroud, while allowing for tip clearance. The final propeller diameter

setting was 53 5/8 inches. The blades had a constant taper ratio with square tips and 13

degrees of twist from root to tip. The shape of the tips did not make them ideal for

operating under the small clearances inside the duct since a constant clearance was not

provided. While no testing of two or three bladed propellers was performed as part of this

work, the propeller could be easily modified to either of these configurations for further

testing.

2.1.3 Shroud

The shroud used in the testing of the apparatus was designed and built for this

particular application. It had a 54 1/8 inch inside diameter at the propeller plane of

rotation and a chord of 28.8 inches. The cross section of the shroud was based on a

modified NACA 4312 airfoil and was identical to one used by H. Hubbard [11] for his
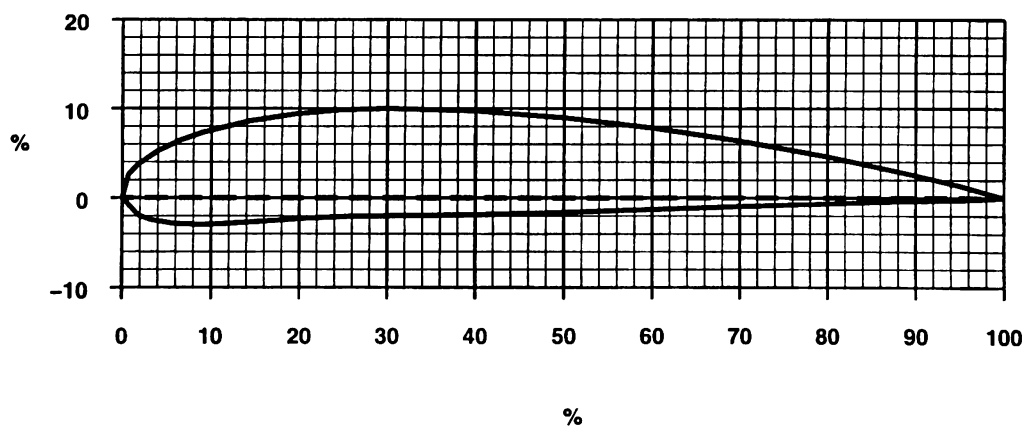
Figure 16. NACA 4312 (Modified) Airfoil

acoustical testing of shrouds. From the 30-percent-chord station back to the trailing edge,

the dimensions were identical to a NACA 4312 airfoil, but from the 30-percent-chord

station ahead, the modified airfoil had a leading-edge radius that was 50 percent greater

than the original. Under static conditions, if the leading-edge radius was too sharp, the

shroud would likely exhibit separated flow. On the other hand, if the leading-edge radius

was too large, excessive amounts of drag would be exerted under dynamic conditions.

With a maximum thickness of only 12 percent of the chord and a leading-edge radius

increase of 50 percent, the modified NACA 4312 made for a good compromise. A table

of the exact ordinates are provided in Appendix B.

Due to it's large shape, and complex curves along the inside surface, construction

of the shroud was a challenge. Two design concepts were evaluated: one consisted of a

Table 2. Comparison of construction techniques for shroud

	Advantages	Disadvantages
Wooden Skeleton	• Easier to shape the airfoil contour by cutting identical ribs	• Hard to maintain perfect circular shape while at the same time preventing chordwise twisting • More weight • Harder to modify once glassed over
Foam Core	• Circular shape could be easily maintained using the lathe • Similar procedure had been used successfully in the past • Followed a more modern method of construction	• Harder to sand foam to final shape • Due to construction of lathe, overall construction time took longer

wooden skeleton covered with a combination wood and fiberglass composite skin, and the other was made up of a foam core that would have a fiberglass skin. The advantages and disadvantages to both are listed in Table 2. After preliminary evaluations, the foam core looked to be the best option.

The shroud was constructed using the same basic procedures that are used in the construction of modern composite homebuilt aircraft. The foam core was shaped on a specially built lathe which provided the circular shape. Final shaping to the airfoil dimensions was done by hand, using a combination of hot-wire cutters and sanding tools. After the strut mounts were attached into the foam, the entire structure was covered with fiberglass. This is what provided the stiffness to the shroud. The final step included sanding and painting of the shroud. A detailed description of the construction procedure can be found in Appendix C.

The shroud was bolted directly to the engine gearbox, using three struts. The struts, were aerodynamically shaped to help reduce drag and acoustically were treated as three stator vanes. All three struts tied into a mounting plate, which attached to the gearbox, using the same studs that held the gearbox halves together. A cradle was built to provide a means for the shroud to support itself when not attached to the engine, as well as, to reduce some of the additional weight and moment exerted on the engine and test stand when secured to the engine with bolts. The cradle remained in place for all testing due to safety concerns.

Initial evaluation of the shroud consisted of attaching yarn tell tales around the leading edge and other key points on the shroud to determine the amount of unseparated

flow. Attempts to reduce the separation through reshaping of the leading edge in certain

areas proved somewhat successful. It was noted that the condition of the inflow was

easily disturbed due to crosswinds and for this reason, testing was attempted only when

the there was very little interference from outside wind. Also, as the inflow velocity

increased, the flow tended to separate from the leading edge more, which was expected.

Overall, the shroud displayed good separation characteristics, as the majority of the time,

the flow remained attached to the airfoil surface as can be observed in Figure 17.
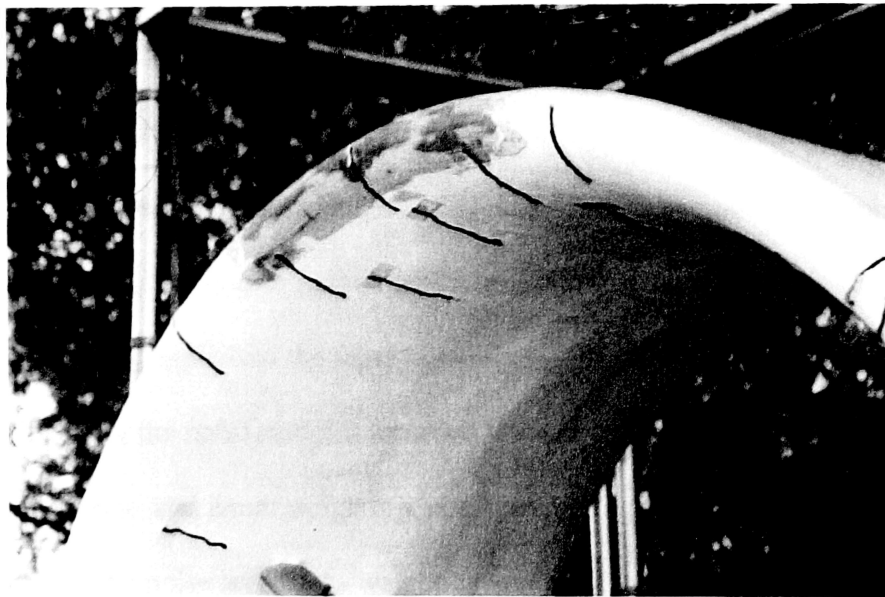
Figure 17. Yarn Telltales Showing Attached Flow Over Leading Edge Region of Shroud

2.2 DATA ACQUISITION

2.2.1 Instrumentation

Primary instrumentation for recording and analysis of the data consisted of a precision microphone and sound pressure meter level, a FM reel to reel type tape recorder, a frequency analyzer, and an analog to digital board with PC computer used to store the final plots on disk. The data of interest consisted of overall-sound-pressure-levels (OASPL's) measured in the farfield, as well as, frequency spectrum plots which were used to determine levels of noise at discrete frequencies.

All farfield measurements of noise were taken using a Brüel and Kjaer type 4155 precision microphone, affixed to a type 4230 Brüel and Kjaer sound level meter. Although the unit had built-in functions to adjust the weighting, filtering, time response and type of output applied to the input noise signal, efforts were taken to adjust these settings such that the noise samples recorded were as pure as possible. This meant using a fast time response and linear weighting, not A-weighting which is often applied when measuring overall noise levels. A- weighting was not used for this work since, if an ANC system was employed, a linear input signal would most likely be used for input. For this reason, all results presented are expressed in unweighted decibels (dB). In any case, the type of weighting was found to only make about a 2 dB difference in OASPL. One plot was generated with A-weighting applied, just for comparison purposes and can be found in Appendix D.

The noise signal was recorded onto tape using a RACAL FM reel to reel type tape recorder. The tape recorder had a four channel recording capability, but only three channels were used. The Brüel and Kjaer occupied one channel, with the other two signals coming from small condenser microphones set along the inside walls of the shroud. These microphones, while not as precise as the farfield microphone, proved to be useful when examining the acoustics inside the duct. The final tape recording speed was 7.5 in/s, which provided a recording bandwidth of 0 - 2500 Hz. Further discussion of the recording bandwidth and the analysis bandwidth is provided in Section 2.2.3.

After the noise samples were recorded on tape, the signals were played back through a HP 3582-A frequency analyzer which performed power spectral analyses on the recorded data. With the spectral analyses plotted on the screen, the plots were transferred to diskettes through use of an A to D board which converted the output signal voltages from the wave analyzer to binary points, which were saved as text files. Hard copies of the plots were then generated from the text files. An alternate method for plotting the curves was to use a HP 7046-A XY recorder which would draw the curves out on paper. The primary advantage of this method was it provided an immediate hardcopy, without all the manipulation required for digitizing and printing out the plots. Unfortunately, the XY recorder had no capabilities to draw any axes or scales, which made it hard to interpret the data once the original curve was cleared from the screen.

A complete listing of the equipment identification numbers, parts, and settings used on the equipment is contained in Appendix E.

2.2.2 Procedures

Since no anechoic chamber was available for testing, all the acoustical recordings

were performed outdoors which provided the best freefield conditions over a hard surface.

To assure that the surrounding building was not close enough to cause significant

reflections of noise, initial noise level measurements, shown in Table 3, were performed

for both the shroud-on and shroud-off configurations. Since sound power is inversely

proportional to the square of the distance from a noise source, doubling the distance from

the noise source should decrease the OASPL 6 dB for a spherical wave (monopole

source). From the results in Table 3, differences close to 6 dB were measured for each

configuration as the distance from the apparatus was doubled, thus it was concluded that

the location of the apparatus during testing was sufficiently far enough from the walls of

the nearest building to avoid interference due to reflections of noise.

Table 3. OASPL measurements taken to assure adequate acoustical separation between
apparatus and building (all measurements are in dB, re: 20 µPa)

Distance from Apparatus	Without Shroud		With Shroud	
	In-Line with Propeller	In-Plane with Propeller	In-Line with Propeller	In-Plane with Propeller
12.5 ft	107.3	105.5	112.4	111.7
Δ dB (should be ~6dB)	5	5.9	5.7	4.2
25 ft	102.3	99.6	106.7	107.5
Δ dB (should be ~6dB)	5.8	5.7	4.6	4.0
50 ft	96.5	93.9	102.1	103.5

All testing was attempted during conditions of minimal wind and low levels of surrounding noise. This generally meant testing during the early hours of the morning. It was found that minimal crosswinds would cause the flow traveling over the leading edge of the shroud to become separated. Although never verified in these tests, it has been shown from past results of shrouds that separated flow around the leading edge can reduce the thrust from the shroud by as much as 50%. Acoustically speaking, separated flow can cause significant increases in noise due to the propeller blades interacting with the vortices which are shed off the leading edge. This was observed in Hubbard's results [11] when he experienced a 6 dB OASPL increase with separated flow.

Generally, the levels of noise generated from the apparatus were high enough to sufficiently cover up noise from other outside sources. One exception to this rule was the commercial jets that would depart from the nearby airport. All testing was suspended when one of these planes departed until it was far enough away, not to effect the noise results. It was found that during the hours of recording, the background noise level was typically about 63 dB.

Sound recordings were taken around a 25 ft radius from the test stand, at 15 degrees intervals. The positions started at a theta of -90° and proceeded to a theta of 150°, allowing for a total of 17 locations as shown in Figure 18. Twenty-five feet proved to be in the farfield, which was verified by first taking the lowest frequency of interest which was defined by the BPF, 160 Hz, and determining the wave number, k,

$$k = \frac{2\pi f}{c} = \frac{2\pi (160\ \text{Hz})}{1116\ \dfrac{\text{ft}}{\text{sec}}} = 0.900\,/\,\text{ft} \qquad \text{Eq. 7}$$

where c is the speed of sound and f is the critical frequency. Since the farfield is defined

as the distance beyond which kr ≥ 10, [8] where r is the minimum distance,

$$r \ge \frac{10}{k} = \frac{10}{0.900\big/_{\text{ft}}} \Rightarrow r \ge 11.1\ \text{ft} \qquad \text{Eq. 8}$$

r needed to only be greater than about 11 feet.
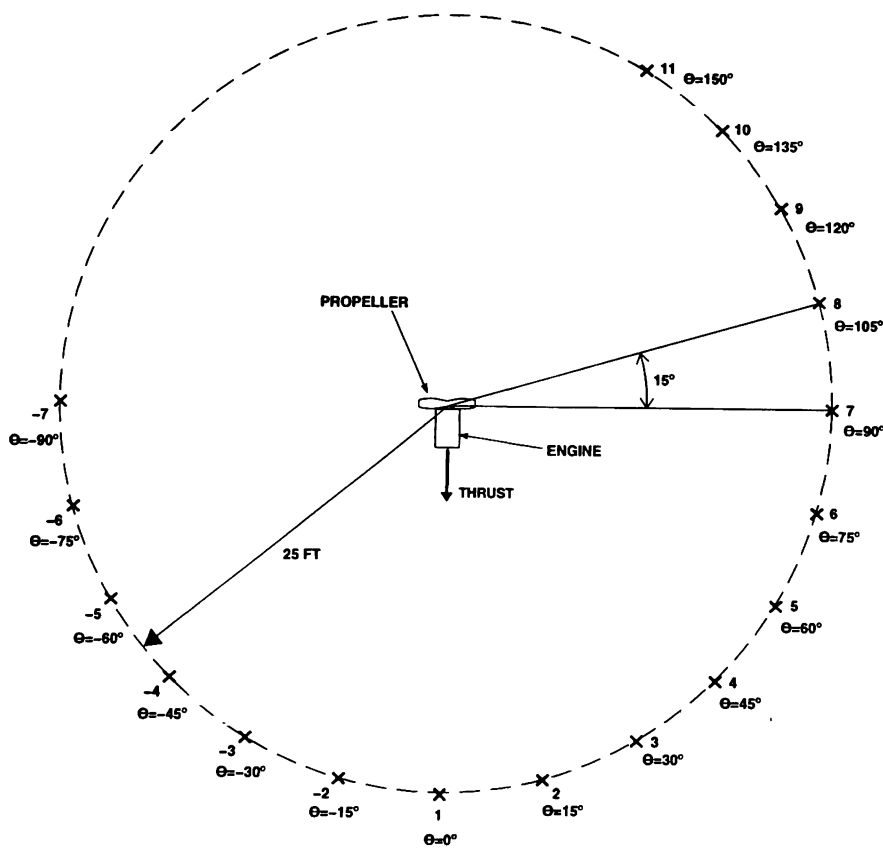
Figure 18. Sound Measurement Locations As a Function of Azimuthal Angle at 25 Feet

Theoretically, sound emissions from a propeller will be symmetrical from side to side so only measurements on one side need to be taken in order to map the directivity of the noise 360° around the propeller. However, given the asymmetry of noise radiated from the engine, due to differences between the intake and exhaust, as well as asymmetries in the propeller noise due to imperfections, measurements were taken around the entire front end of the apparatus. Measurements continued on further around to a theta position of 150°, beyond which further measurements were impractical due to interference by prop wash as well as limitations in the physical surroundings.

In addition to taking sound recordings at the different locations, sound recordings were also taken under varying operating conditions, to try to provide a rough idea of how various factors can affect the overall noise. For these particular tests, all sound measurements were taken at $\theta = 45°$. This is where both engine noise and propeller noise appeared to be very prominent. Recordings were performed while varying the RPM, for both shroud in place and shroud removed conditions. In an attempt to compare engine intake noise and exhaust noise levels, recordings were made with various silencer configurations on the engine. These were performed without the shroud in place. Finally, a recording was taken with the A-weighting turned on, to see the effects on the recorded noise levels.

2.2.3 Verification of Recorded Bandwidth

The frequency range of 20 Hz - 20 kHz is audible to the typical human ear. The overall-sound-pressure-level provides a measure of the level of noise present, and takes into account noise at all frequencies. This measurement is important, because it is a measure of the total noise. A narrow-band frequency spectrum (power-spectrum, autospectral density function) provides a breakdown of the noise into its individual frequencies. Performing a power spectrum analysis results in a curve where levels of individual components of noise such as propeller noise or engine noise can be determined.

Presented in Figure 19 is the power spectrum of the noise measured at $\theta = 45°$ and 25 feet where the sound-pressure-level (SPL) in decibels referenced to 2×10^{-5} pascals is plotted as a function of frequency. The analysis was performed up to a frequency of 5 kHz with an analysis bandwidth (BW) of 30 Hz to determine the highest frequency of significant noise. Inspection of these noise curves for the shrouded propeller reveals that noise at 2.5 kHz and higher is at least 17 dB lower than the highest tone of 100 dB at slightly less than 1 kHz. At frequencies greater than 2.5 kHz the tonal character of the noise has disappeared and the levels are insignificant to the OASPL. It was concluded, therefore, that all significant spectral information was at less than 2.5 kHz and all future spectral analyses were performed over a frequency range of 0 - 2.5 kHz resulting in a BW of 15 Hz.
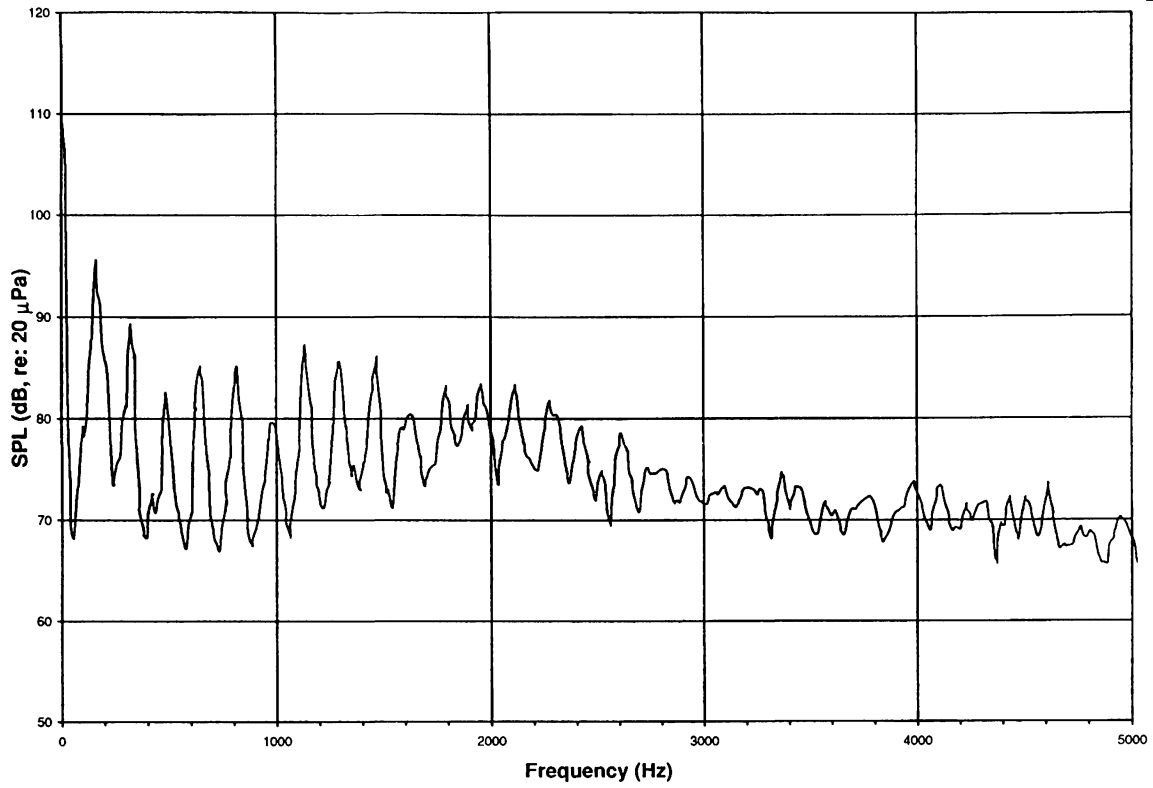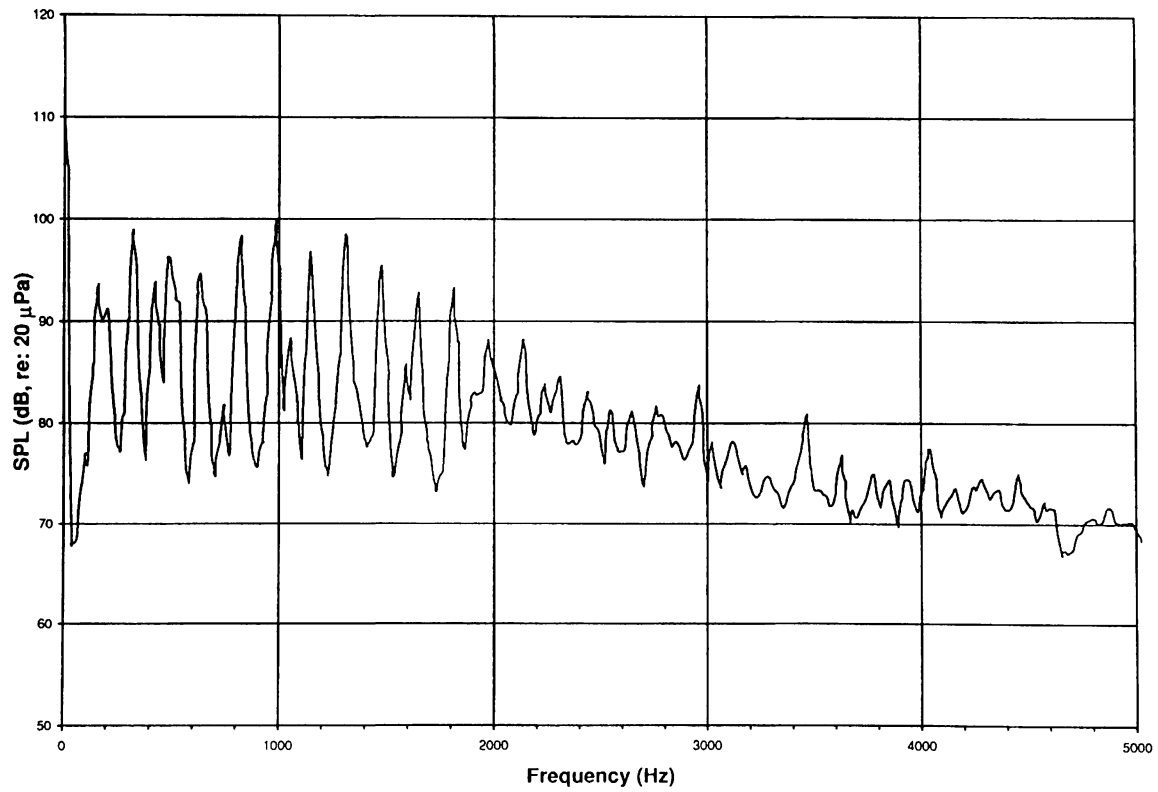
Figure 19. Power Spectrum of Noise up to 5000 HZ, With and Without the Shroud
θ = 45°, 25 feet, BW = 30 Hz

2.3 INITIAL DATA ANALYSIS

In this section, both performance and acoustical data is reviewed. The performance data compared the effective thrust versus propeller RPM, with and without the shroud to determine any significant effects the shroud had on overall performance of the propeller/engine combination. Following the performance review, examples of the power-spectral plots used for the acoustical analysis of the data are provided and reviewed to help setup further data analysis in Chapter 3.

2.3.1 Performance Data

The performance of the apparatus was measured in terms of overall thrust. Torque was not measured. Thrust measurements (in pounds) were taken at various RPM settings for both configurations and plots were developed. The procedure for measuring the thrust was very crude, and was designed to only demonstrate any significant effects (in excess of 15% differences in thrust) the shroud might have.

To measure the thrust, the cart on which the engine and propeller was bolted to was tied to a 1000 lb. deadweight scale. With the cart on wheels, the thrust from the propeller caused the entire apparatus to roll forward until equilibrium was reached, at which point all thrust (neglecting the friction) was transmitted through the scale and displayed. A correction factor of 10 pounds was added to the measurements taken with the shroud in place, to correct for the additional drag of having the shroud resting on the

ground. The results are plotted in Figure 20. From these curves, the shrouded

configuration demonstrated slightly higher thrusts at lower RPM's, while both

configurations demonstrated approximately equivalent thrusts at the higher RPM's. Data

scatter at low RPM was mostly due to measurement inaccuracies at low RPM.
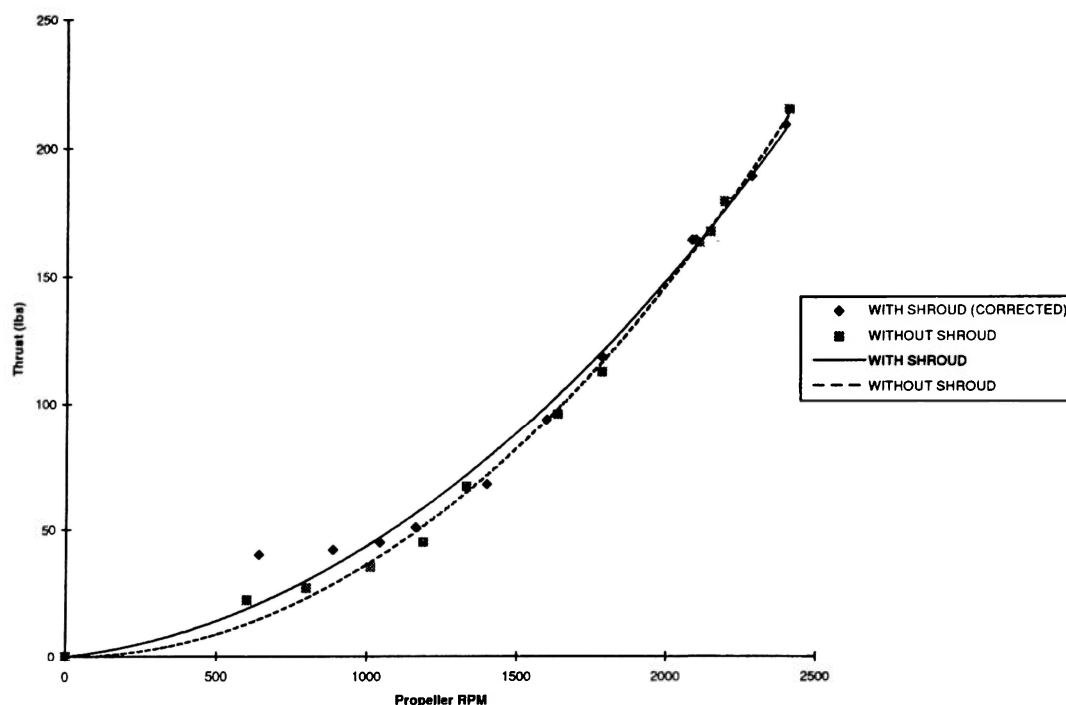
Figure 20. Thrust vs. Propeller RPM Curves, With and Without the Shroud

Given the conditions under which the thrust measurements were performed, the

only conclusion that was drawn was that no significant effect of the shroud was seen on

overall thrust performance. Considering the primary purpose of the apparatus revolves

around acoustical testing, this conclusion seemed adequate. Certainly, it has been proven

in past work, that under static conditions, a ducted propeller can produce more thrust than

an unducted propeller of equivalent dimensions and input power although the propellers

and shrouds that are used for those thrust versus drag measurements incorporate blade

tips specially designed for very small tip clearances. That is not the case with this

apparatus. Further, the increased skin friction drag tends to negate much of the extra

thrust.

2.3.2 Power-Spectrum Plots

As mentioned earlier, plots of the power-spectral (autospectral density function)

analysis of the noise were used to determine the individual components of the noise for the

final data analysis. Each power-spectrum plot.used in the analysis for this report provides

an analysis of the noise measured at one position averaged over a 10 second time span

with a sampling rate of approximately 2 Hz and through a frequency range of 0 - 2.5 kHz

providing for a BW of 15 Hz. Using the plot of the power-spectrum, individual tones,

shown as large spikes in the data were analyzed. In most cases, the frequencies at each

spike were attributed to a frequency common to either the rotational frequency of the

propeller, or the firing frequency of the engine. As an example, at an RPM of 2,400, a

four bladed propeller will have a blade-passing-frequency (BPF) of 160 Hz. Recalling

Equation 2, and inserting the given conditions yields the following:

$$\left(\frac{2400 \text{ revs}}{1 \text{ min}}\right)\left(\frac{1 \text{ min}}{60 \text{ sec}}\right) \times 4 \text{ blades} = 160 \text{ Hz} \qquad \text{Eq. 9}$$

These tones associated with BPF and harmonics can be clearly identified on the majority

of the plots. The engine firing tones was determined to be 200 Hz. This engine firing

tone was determined by,

$$(2 \text{ cylinders} \times 1 \text{ rev per firing} \times 6192 \text{ RPM}) / 60 \text{ sec} \approx 200 \text{ Hz} \qquad \text{Eq. 10}$$

where engine RPM for this apparatus was 2.58 times the propeller RPM due to the

reducing gearbox. Again, this engine firing tone and harmonics routinely showed up on

the plots as one of the more significant tones.

Table 4. Components of measured noise

Tone	Frequency (Hz)
Engine half tone	100
Primary propeller tone	160
Primary engine tone	200
First propeller harmonic	320
First engine harmonic	400
Second propeller harmonic	480
Second engine harmonic	600
Third propeller harmonic	640
Fourth propeller harmonic	800
Fifth propeller harmonic	960
Sixth propeller harmonic	1120
Seventh propeller harmonic	1280

Higher harmonics of these primary frequencies were also identified from the plots,

however, at some of the higher frequencies, the harmonics from the engine and the

propeller were close enough so that they tended to overlap, making it hard to distinguish the engine noise from the propeller noise. The table on the previous page lists some of the tonal frequencies which were prominent in the majority of noise recordings, and lists their corresponding source. The small differences in the values listed in Table 4 and the actual values that the associated tones occurred at, were due to slight variances in the engine rotational speed during testing. The values listed in Table 4 are based on an exact propeller RPM of 2,400, but since precise throttle control was difficult on the Rotax engine, exact settings were not always achievable.

Since engine intake noise and exhaust noise both occurred at the engine frequency, the farfield plots did not distinguish between the two. An attempt was made to differentiate between the two by placing one microphone near the exhaust and one microphone near the intake, and then taking recordings using different arrangements of silencers. These runs were only performed without the shroud in place since the shroud theoretically should not affect the levels of engine noise. Results are discussed in the following chapter.

CHAPTER 3

RESULTS

Results from the data are reviewed in the following chapter. The first two sections review the data recorded in the unshrouded configuration and the shrouded configuration, respectively. The third section contains results from data gathered to compare various exhaust / intake configurations on the engine. Complete listings of all the data recorded can be found in Appendix F.

3.1 WITHOUT SHROUD

In the unshrouded configuration, there are two primary sources of noise: the engine noise and the propeller noise. The engine has two monopole sources, one at the intake and one at the exhaust. However, since the distance between the two sources is very small when considered to the distance at which measurements are being made (1 ft compared to 25 ft), the engine noise is actually going to be considered as one monopole source. Propeller noise under static conditions is made up of two components. The first is the loading noise, which is a dipole source. The strength of the dipole source thus is based on the amount of thrust the propeller is creating. The second component is the thickness noise, which is a monopole source, and is caused be the propeller displacing the

air. When these two propeller noise components are added together the resulting

directivity pattern will look something like is shown in Figure 21 [5].

The overall noise emitted from this setup is modeled as the sum of the two primary

sources, also shown in Figure 21. This assumes, however, that the two sources are

emitting noise completely independent of one another and does not take into consideration

the additional noise due to interactions between the sources as well as phase effects

between tones of identical frequencies. Certainly, the sources are not completely

independent of one another, so the actual results can not be expected to look exactly like

the theoretical solution. Still, similarities are found between the theoretical solution and

the measured data which confirm that the assumption made is not completely unjustifiable.
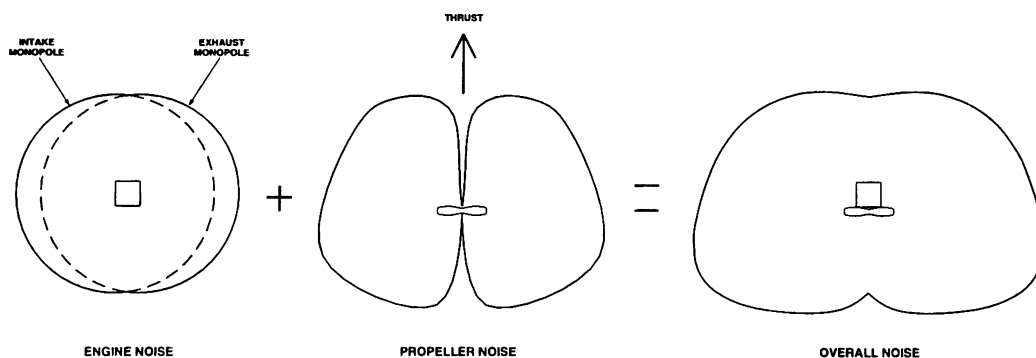

Figure 21. Predicted Directivity Pattern From Apparatus

OASPL measurements consisted of all noise evident, and thus all factors such as

outside noise, structural borne noise, and engine - propeller interactions due to turbulence

ingested by the propeller caused by the engine, affected the levels of overall noise. The frequency scans provided a means to break the noise down into its individual components and examine the sources of noise on an individual basis.

3.1.1 OASPL Tones

The OASPL's ranged between 98.5 and 104.6 dB. It will be seen in the next section, that for most of the angular (θ) positions recorded, the most significant tone is due to propeller noise, indicating that for these positions, the largest contributor to the level of OASPL is propeller noise. Certainly though, the engine noise is not low enough to be negligible and actually does appear as the dominant tone at some of the angular positions around the exhaust side of the engine.

Shown in Figure 22 is the measured OASPL directivity pattern for the unshrouded propeller. Upon examination of this curve, it is evident that noise levels were lowest at the positions inline with the propeller plane with levels of 98.5 dB on the exhaust side ($\theta = -90°$) and 99.0 dB on the intake side ($\theta = 90°$). This corresponds to a slight reduction in propeller noise at these locations. The highest noise level is noted at $\theta = 45°$, where the OASPL is 104.6 dB. Interestingly, this does not appear to be symmetrical as at $\theta = -45°$, the OASPL is only 101.4 dB and shows no significant increase in noise anywhere in this region.

Other than the 45° positions, the acoustical noise field appears to be fairly symmetrical from the $\theta = -90°$ position, around the front of the apparatus to the $\theta = 90°$

OASPL (dB, re: 20 μPa)
w/o shroud

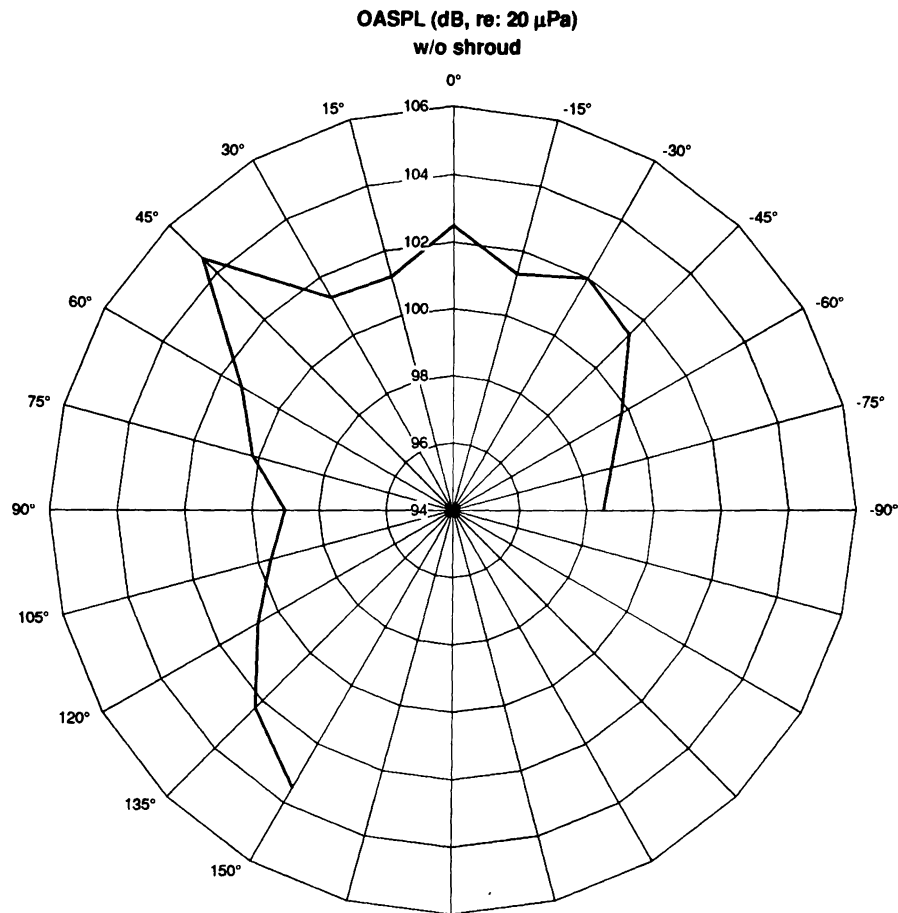Figure 22. Measured Directivity Pattern Without Shroud

position. From $\theta = 90°$ around to $\theta = 150°$, the OASPL is on the rise which follows the

lobe pattern behind the plane of rotation predicted by the theoretical solution.

Unfortunately, due to physical limitations, measurements beyond $150°$ were not able to be

taken, so it could not be determined if $150°$ was the high point of this lobe or not.

3.1.2 Frequency Spectra

Frequency spectra analyses were performed on the data at every angular position measured. From the individual spectrum plots, levels of noise due to the propeller and engine were able to be individually examined one at a time. The following contains the results from an examination of each noise source.

3.1.2.1 Propeller Tones

Based upon the power spectrum analysis, an attempt is made to plot the directionality field of just the propeller BPF which appears as a tone located at approximately 160 Hz. This tone can be seen clearly on the power spectrum curves for all positions, and in all but a couple positions, is the dominate tone. An example of the power spectrum is provided in Figure 23 in which the tone at 160 Hz can be seen to be 5 dB greater than any of the other tones (peaks).

By plotting only the BPF, the effect of the fundamental propeller tone on the OASPL field is shown in Figure 24. From this plot, the directivity field tends to appear somewhat lopsided. The propeller noise looks to be more significant on the intake side of the engine than on the exhaust side. Normally, for an ideal case, propeller noise is expected to be symmetrical along the centerline. Most likely, this asymmetry is a result of turbulence which is shed off the engine. With the engine and propeller setup in a pusher configuration, the resulting inflow into the propeller is not an even distribution, and as a result, the pressure distribution over the disk area was not symmetrical, leading to
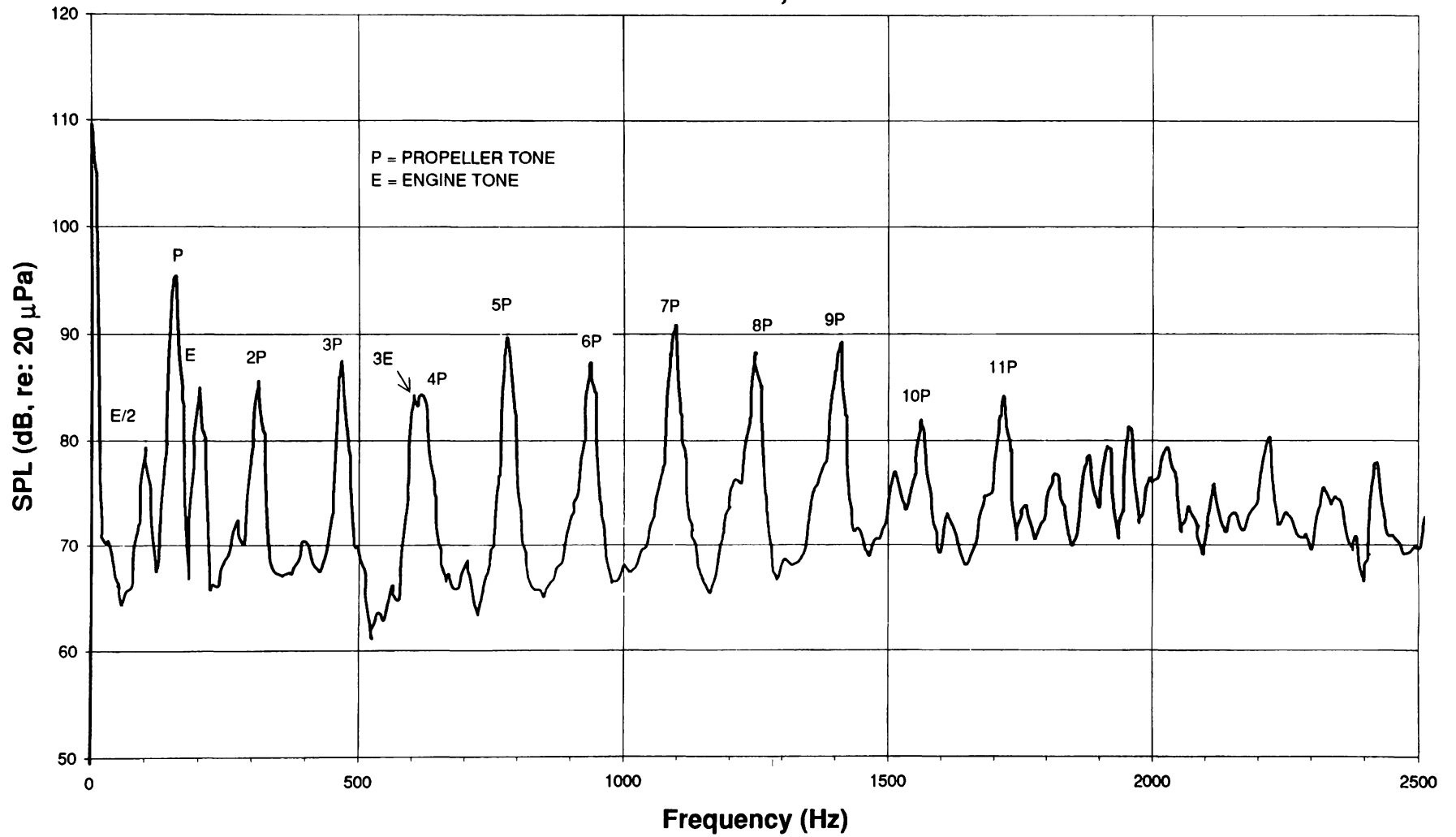
Figure 23. Spectrum Plot Without Shroud

BPF (dB, re: 20 μPa)
w/o shroud
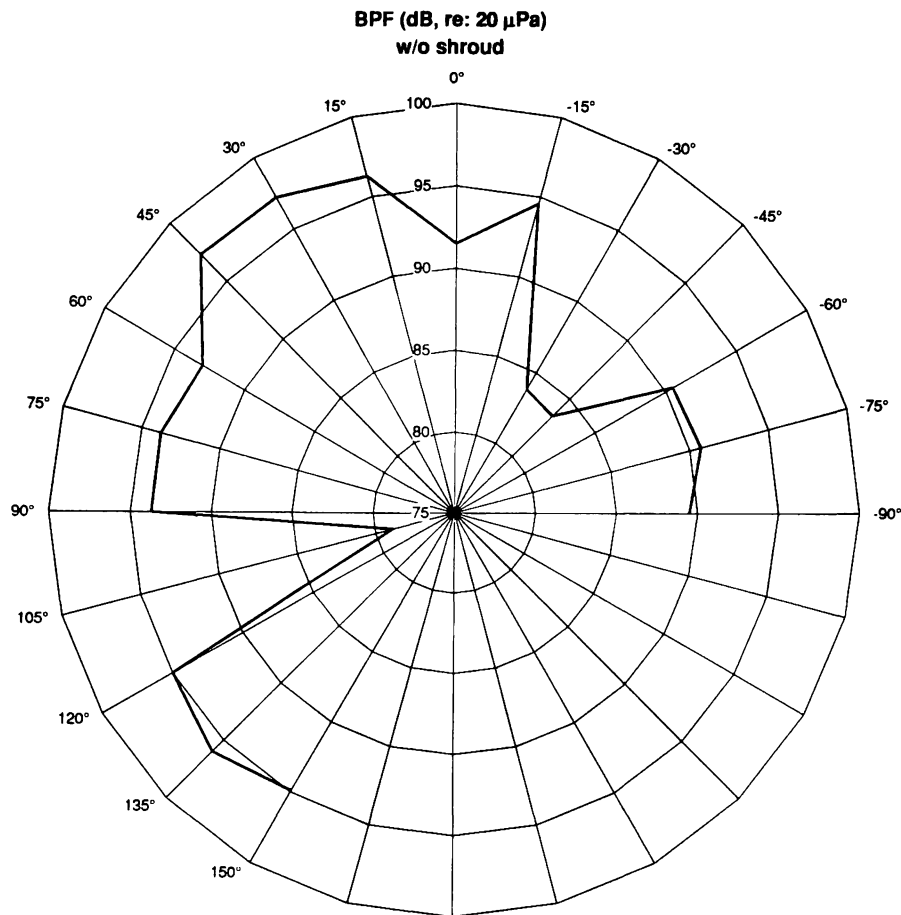
Figure 24. Directivity Pattern of BPF Tone at 160 Hz Without Shroud

asymmetrical acoustic emissions [20].

When examining the spectrum of noise emitted from a propeller, the BPF will

usually be the most significant tone and for this reason, it acts as a good representation of

the level of overall propeller noise [21]. Overall noise due to the propeller, though,

actually includes all propeller harmonics in addition to the fundamental BPF, which for the

case of the ultralight propeller used, are seen to be significant up till a frequency of about

1,500 Hz, or approximately the 11th harmonic, at which point they start to decay very

rapidly. Generally, propeller harmonics are seen to decay at a rate such that they can be

considered insignificant (more than 10 dB below the highest level) by about the fifth

harmonic [22]. The reason this particular propeller has significant harmonics up to the

eleventh one is in large part due to the blade airfoil shape and ingested turbulence inherent

in pusher propeller propulsion systems. The strength of the higher harmonics is

determined by the uniformity of the pressure distribution across the airfoil. Generally, a

more uniform distribution will lead to weaker harmonics. The fact that this ultralight

propeller used has strong harmonics up through the eleventh, is an indication that the

pressure distribution across the airfoil blade is not very uniform.

It should be noted in Figure 24, the drop seen in the frequency scan at $\theta = 105°$,

where the tone at 160 Hz drops by about 15 dB is not representative of the entire

spectrum of propeller noise. While this decrease is a real phenomenon, (i.e., the BPF tone

at 160 Hz does drop 15 dB) it does not show up as a reduction in all the propeller

harmonics. Most likely, the reduction in BPF at this location is a resultant of particular

characteristics of this propeller. No significant reduction in OASPL was noted at this

position.

3.1.2.2 Engine Tones

The fundamental engine tone occurs at 200 Hz. When plotted out in a similar

fashion to the BPF and presented in Figure 25, two separate monopole sources are clearly

depicted, one due to exhaust noise and one due to intake noise. It appears as though the

monopole sources are close enough to actually cancel out parts of one another, giving the

directivity pattern the look of a dipole as shown in Figure 25. This is noted because of the

significant drops in levels of noise in the region between θ = 0° and θ = 60° where the two

monopole sources overlap one another. Overall, the exhaust noise levels are

approximately four to five dB higher than the intake noise levels.

Higher harmonics of engine noise seem to be limited to only the third harmonic at

Engine Noise (dB, re: 20 μPa)
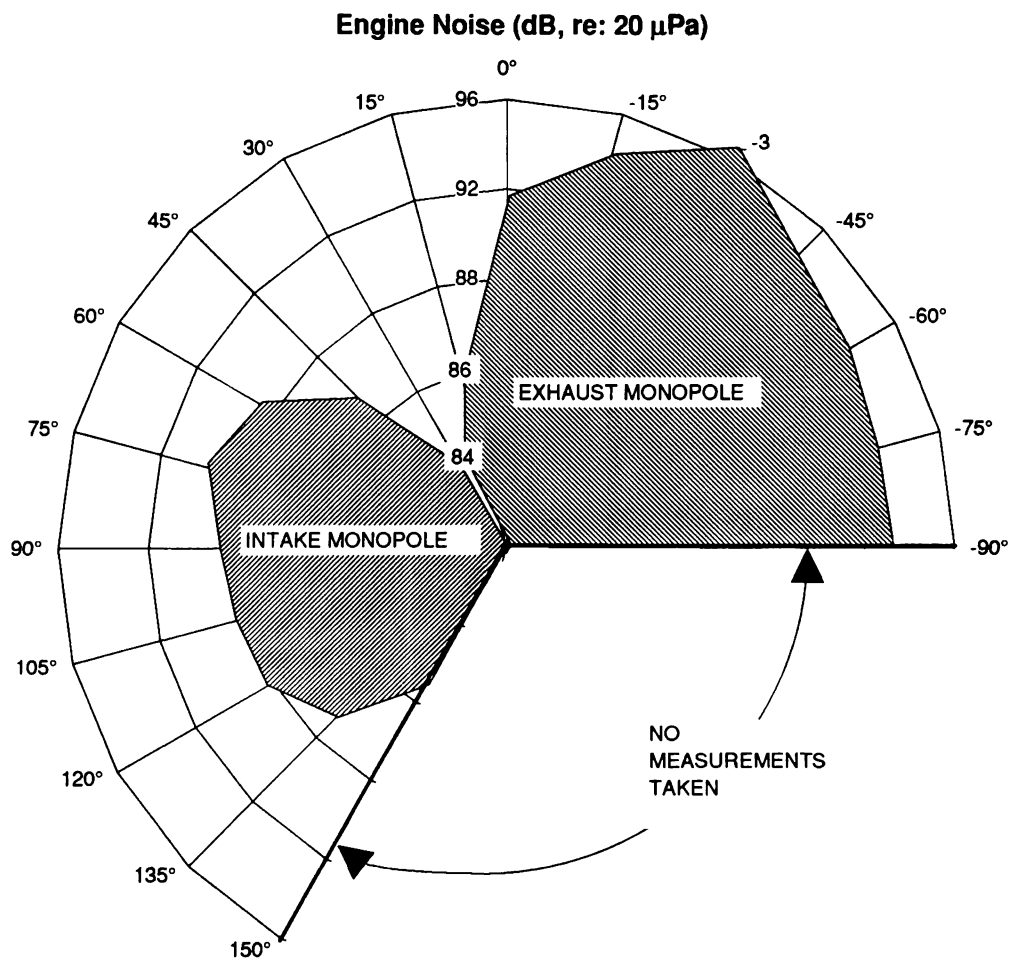
Figure 25. Directivity Pattern of Engine Tone at 200 Hz

most azimuthal positions. The second harmonic appears almost non - existent as does the

harmonics above the third.

3.1.3 Nearfield Noise

A clear picture of the propeller BPF and its harmonics is provided by the spectral analysis of the nearfield measurements as shown in Figure 26. Two microphones placed approximately six inches in front of the propeller tip path were used to record the nearfield noise. One mike was set on the exhaust side of the engine while the other was placed on the intake side. With the measurement microphones placed so close to the propeller plane of rotation, the effects of the engine noise are obscured by the strength of the acoustic pressure waves emitted by the propeller blades. This observation can be verified by inspecting the power spectrum curve in Figure 26, through the lack of any significant tones at the frequencies associated with engine tones such as 200, 400, or 600 Hz. However, the BPF and its harmonics are very clearly depicted as peaks at very regular intervals on the curve.

Unfortunately, these plots do not provide quantified data that can be applied to the farfield, since the relationships between nearfield noise and farfield noise are extremely difficult. However, these nearfield measurements do provide a means of confirming the domination of BPF tones which are caused by blade passage.
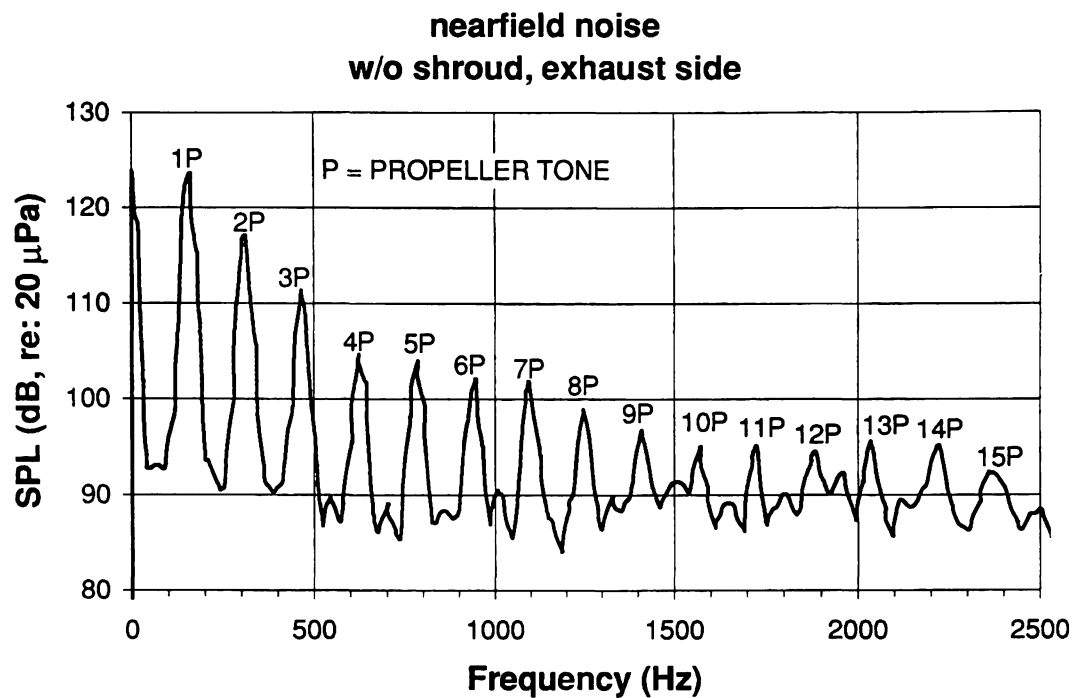
Figure 26. Spectrum Plots of Nearfield Noise Without Shroud
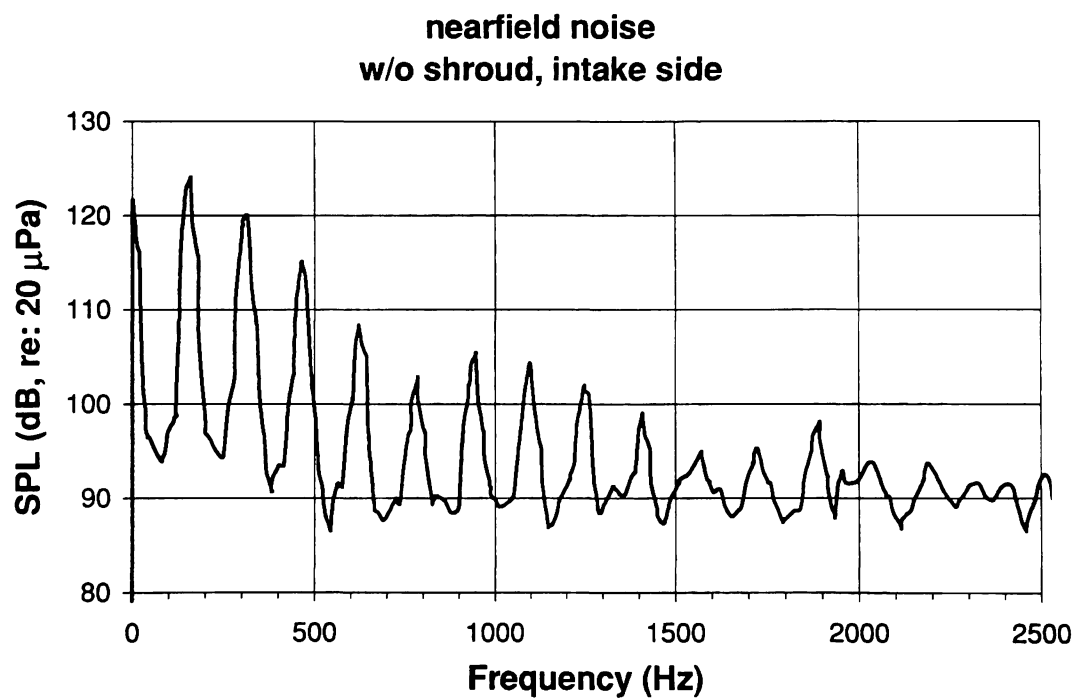
3.2 SHROUD IN PLACE

The same measurements previously discussed were taken with the shroud in place. Of primary interest was the OASPL measurements which provided a direct comparison to the unshrouded configuration. Also of importance were the power spectra, which proved to be most insightful when analyzing the propulsion system noise with the shroud in place. With the propeller blades passing within about half an inch behind the trailing edge of the stator vanes, it was assumed that strong interaction tones would be observed between the propeller and stators. In fact, this was the case. Other factors thought to influence the overall noise included shroud shielding, duct acoustical emissions, and an increase in propeller efficiency due to a reduction in tip vortices. Results of the measured data follow.

3.2.1 OASPL Measurements

The directivity pattern of the OASPL with the shroud follows the same trends as the unshrouded case, although an increase in levels is evident. Increases in higher harmonics amount to approximately a six decibel increase in the overall sound pressure level. Upon examination of the directionality field in Figure 27 maximum OASPL's are observed at both $\theta = 45°$ and $\theta = -45°$ with values of 110.1 dB and 111.3 dB, respectively. This varies only slightly from the pattern noted without the shroud, as a slightly higher increase is seen around $\theta = -45°$ with the shroud. Behind the plane of
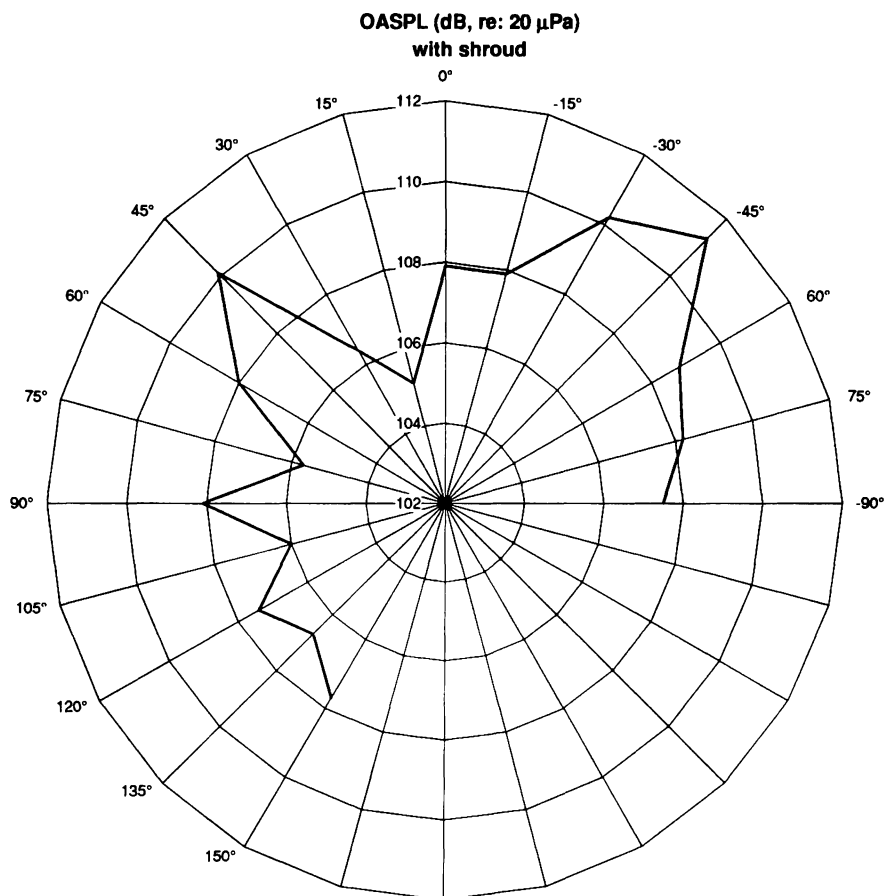
Figure 27. Measured Directivity Pattern With Shroud in Place

rotation, (90° < θ < 150°) the levels of noise appear fairly constant, (within 2 dB's) indicating no distinct lobe at this position. This is in contrast to the unshrouded propeller which appears to have a distinct lobe at this location as can be seen by comparing the curve in Figure 22. Measurements beyond 150° would help to determine if this is the case.

3.2.2 Frequency Spectra

Power-spectral analysis scans were performed in the same manner as for the unshrouded configuration. Again, all tones fall under one of two types: either rotor - stator interaction noise or engine noise, except for one unidentified tone at 520 Hz which appears in all the frequency scans with the shroud in place.

3.2.2.1 Rotor - Stator Tones

From examination of the power spectrum presented in Figure 28, the increase in OASPL can be attributed mostly to a set of distinct tones that occur at intervals of 160 Hz and higher. Notice that the tones appear at the same frequencies as the BPF and its corresponding harmonics, however, these tones are attributed more to rotor-stator interactions than the propeller harmonics.

Unlike the BPF and associated propeller harmonics, the fundamental rotor-stator interaction tone does not appear as the most significant tone. Instead, the highest level in the spectrum appears at around the 4th or 5th interval tone, and instead of the higher tones diminishing as they increase in frequency, they remain at fairly constant levels until a frequency of about 1,500 Hz, when they decay very rapidly. Further, a comparison of the BPF tone at 160 Hz between the unshrouded and shrouded configurations in Figure 29 shows differences in the directivity patterns. With the shroud in place, the directivity pattern of the 160 Hz tone does not exhibit the significant decreases on the engine exhaust side ($-75° < \theta < -15°$) as does the 160 Hz BPF tone without the shroud.
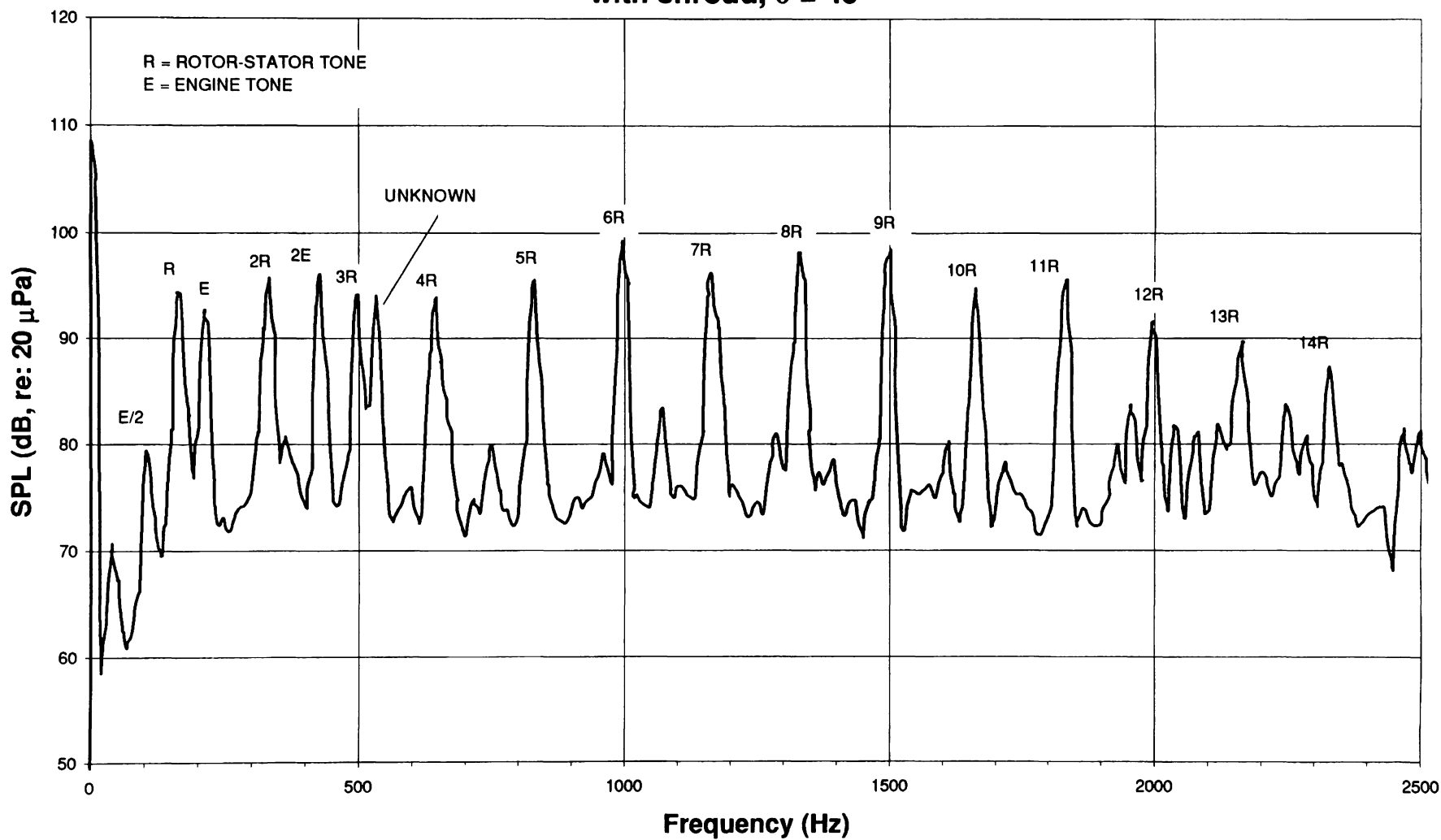
Figure 28. Spectrum Plot With Shroud

BPF (dB, re: 20 μPa)
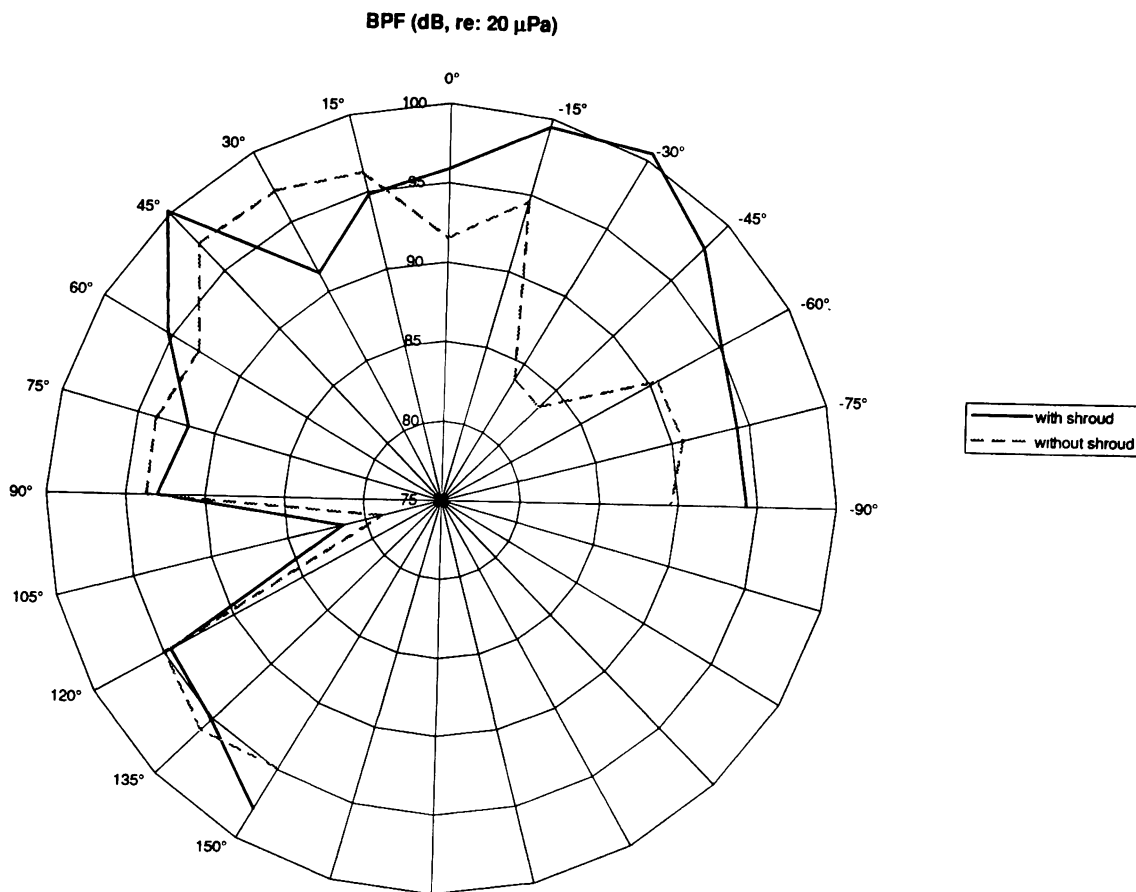
Figure 29. Comparison of Directivity Patterns at Blade Passing Frequency

Applying the rotor-stator interaction concepts from Chapter 1, the rotor-stator

interaction tones for this apparatus can be accounted for in the power spectrum. As an

example, lets look at the fundamental tone (s = 1). Using the same notation as in

Chapter 1,

$\Omega = 40\,\text{Hz}$ $B = 4$ $c = 1116\,\text{ft}/\text{s}$

$D = 54\,\text{in}$ $V = 3$ $k = (0, \pm1, \pm2...)$

and recalling for propagation of the tone to occur, Ω_m has to be greater than Ω, since Ω is subsonic, Equation 6 from Chapter 1 can be rewritten as

$$-8/3 < k < 0. \qquad\qquad \text{Eq. 11}$$

Integer values of k which satisfy Equation 11 are -1 and -2. Substituting these values of k into Equations 5 and 6, from Chapter 1,

$$m = sB + kV \qquad\qquad \text{Eq. 5}$$

$$\Omega_m = \Omega \Big/ (1 + \frac{kV}{sB}) \qquad\qquad \text{Eq. 6}$$

corresponding modes of 1 and -2 and Ω_m's of 160 and -80 Hz respectively, are found. This indicates that for the fundamental tone, the only modes that are rotating at a faster speed than the propeller are 1 and -2. To determine if either of these modes might propagate, their corresponding cutoff frequencies must be found. The cutoff frequencies for circumferential modes 1 through 8, found using Equation 3 and the corresponding Bessel functions for the modes, are presented in Table 5 for up to the eighth mode.

Table 5. Cutoff frequencies for mode m (hub to tip ratio = 0, radial mode = 0)

m	1	2	3	4	5	6	7	8
J_m	1.8412	3.0542	4.2012	5.3175	6.4156	7.5013	8.5778	9.6474
f^*_m (Hz)	145	242	332	420	507	592	677	762

$$f^*_m = J_m c / \pi D \qquad\qquad Eq. 3$$

Recalling that in order to have sound propagation in the duct or shroud, the frequency of the tone has to be greater than its corresponding cutoff frequency, propagation of the (1,0) mode can be seen to occur at 160 Hz, while decay of the (-2,0) mode will occur.

$(1,0)$: $f^*_{m=1} = 145\,Hz \; < \; \Omega_m = 160\,Hz \rightarrow$ Propagates

$(-2,0)$: $f^*_{m=2} = 242\,Hz \; > \; \Omega_m = \; 80\,Hz \rightarrow$ Doesn't Propagate

In Table 6, the results of similar type of analysis performed on harmonics through s = 6 are shown. From these, frequencies through 960 Hz are accounted for and further analysis of higher harmonics produce similar results for the higher frequencies examined in the power-spectrum scans. By the ninth harmonic or so, corresponding to a frequency of 1,420 Hz, the effects start to weaken significantly and the majority of remaining tones can be neglected.

It should be mentioned, that every third harmonic (s = 3, 6, 9,...) there is no rotating pattern due to interaction tones. Instead, a plane wave is set up. This occurs whenever the blade harmonics are divisible by the number of stator blades. When this situation is set up, the interactions between the blade harmonics and the stators occur such that each stator is acted upon at the same exact time. The result is a strong tone at the particular blade harmonic.

Table 6. Possible Propagating Modes For Shroud Aparatus

possible k's	-1	-2
m lobes	1	-2
omega$_m$ (Hz)	160	-80
propogation ?	Yes	No

s = 1
tone = 160 Hz

possible k's	-1	-2	-3	-4	-5
m lobes	5	2	-1	-4	-7
omega$_m$ (Hz)	64	160	-320	-80	-45.7
propogation ?	No	No	Yes	No	No

s = 2
tone = 320 Hz

possible k's	-1	-2	-3	-4	-5	-6	-7
m lobes	9	6	3	0	-3	-6	-9
omega$_m$ (Hz)	53.33	80	160	p.w.	-160	-80	-53.3
propogation ?	No	No	No	Yes	No	No	No

s = 3
tone = 480 Hz

possible k's	-1	-2	-3	-4	-5	-6	-7	-8	-9	-10
m lobes	13	10	7	4	1	-2	-5	-8	-11	-14
omega$_m$ (Hz)	49.23	64	91.43	160	640	-320	-128	-80	-58.2	-45.7
propogation ?	No	No	No	No	Yes	Yes	No	No	No	No

s = 4
tone = 640 Hz

possible k's	-1	-2	-3	-4	-5	-6	-7	-8	-9	-10	-11	-12	-13
m lobes	17	14	11	8	5	2	-1	-4	-7	-10	-13	-16	-19
omega$_m$ (Hz)	47.06	57.14	72.73	100	160	400	-800	-200	-114	-80	-61.5	-50	-42.1
propogation ?	No	No	No	No	No	Yes	Yes	No	No	No	No	No	No

s = 5
tone = 800 Hz

possible k's	-1	-2	-3	-4	-5	-6	-7	-8	-9	-10	-11	-12	-13	-14	-15
m lobes	21	18	15	12	9	6	3	0	-3	-6	-9	-12	-15	-18	-21
omega$_m$ (Hz)	45.71	53.33	64	80	106.7	160	320	p.w.	-320	-160	-107	-80	-64	-53.3	-45.7
propogation ?	No	No	No	No	No	No	No	Yes	No	No	No	No	No	No	No

s = 6
tone = 960 Hz

p.w. = plane wave

3.2.2.2 Engine Tones

The tones attributable to the engine with the shroud appear very similar to those without the shroud. Other than the shroud providing possible blockage effects at certain azimuthal angles, there is no further reasoning that the engine noise should differ due to the apparatus configuration. For a further description of the engine directionality pattern, see Section 3.1.2.2.

3.2.3 Nearfield Mikes

Nearfield placed microphones installed flush with the inside surface of the shroud were used to record the nearfield noise in the same fashion as the case without the shroud. Again, the microphones were located about six inches in front of the propeller tip plane path, with one on the exhaust side and one on the intake side. The power-spectrum plots generated from the measurements of these microphones are shown in Figure 30. A comparison between these curves, and those of Figure 26, without the shroud, reveals two important differences: the overall levels of the broadband noise are much higher with the shroud in place, and the individual tones are not nearly as organized and powerful with the shroud in place.

The first difference noted is rather easily accounted for. The high level of broadband noise with the shroud in place is due to air traveling along the inside walls flowing over the microphone. It is estimated that at the locations of the microphones, the velocity of the air is about 40 ft/s. With the shroud removed, the microphones are not as
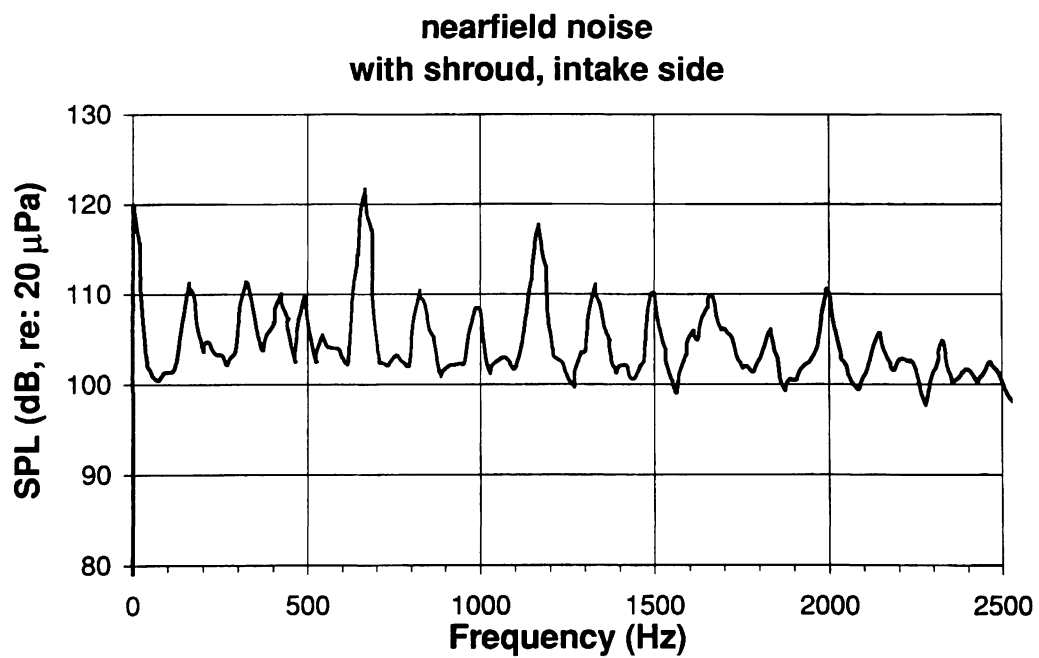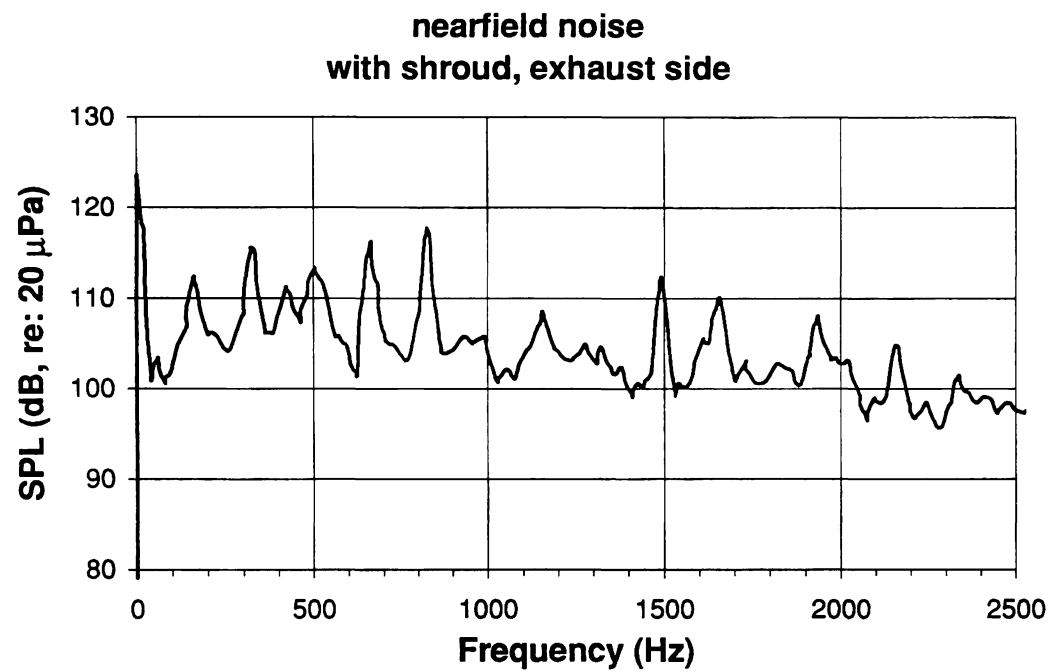
**nearfield noise
with shroud, exhaust side**

**nearfield noise
with shroud, intake side**

Figure 30. Spectrum Plots of Nearfield Noise With Shroud

exposed to the propeller stream inflow and thus do not pick up as much "wind noise".

The second difference mentioned earlier is caused by a reduction in strength of the tip vortices shed from the propeller blade tips. In an ideal propeller/shroud system, tip vortices are non-existent. Without the tip vortices, the nearfield microphones do not see the strong pressure pulses which are apparent every time a blade passes a mike without the shroud in place and as a result, no obvious pattern to the frequencies of the tones shows up in Figure 30. A matter of fact, the apparent tones which are seen as spikes in the power-spectrum plots do not appear to be very repeatable, either from one test to the next, or even from one mike location to another mike location. No further information from these measurements can be applied to farfield characteristics with any degree of reliability.

3.3 ENGINE NOISE

In the past two sections, the directivity patterns of the engine noise levels are plotted as a function of azimuthal angles. Results show the engine noise being generated by two monopole sources: one is the intake and the other is the exhaust. Since the engine noise is significant enough to affect the overall noise levels while testing, further investigation into the effectiveness of the silencers focusing on the intake and exhaust seems appropriate.

Recordings were taken at the azimuthal angle $\theta = 45°$, at the standard distance of 25 ft from the engine. All recordings taken for this comparison were performed with the shroud removed. The four operating configurations measured were:

1. intake silencer on, secondary exhaust muffler on

2. intake silencer off, secondary exhaust muffler on

3. intake silencer on, secondary exhaust muffler off

4. intake silencer off, secondary exhaust muffler off

"Intake silencer off" indicates the entire intake silencer and air filter were removed. Essentially noise was free to propagate out of the carburetor throat into the open atmosphere uninhibited. "Secondary exhaust muffler off" indicates removal of the additional muffler, or "after-muffler" which was placed in series with the main muffler. Due to the nature of a two - stroke engine, testing with the main exhaust muffler removed was not feasible since it was needed for the engine to run properly. For a listing of the specifications for these parts, see Appendix A.

Based on initial testing of the apparatus without the intake silencer in place, it is felt that the impact of the intake silencer on the engine noise levels is greater than the impact of the after-muffler. Results presented in Figure 31 prove this conclusion where the power-spectrum of the farfield radiated noise for the different intake/exhaust mufflers are presented. The tone of interest is the fundamental engine tone at 200 Hz. From the two plots in Figure 31 with the intake muffler in place, the primary tone is not significant

exhaust on, intake on

PRIMARY ENGINE TONE

exhaust off, intake on

PRIMARY ENGINE TONE

exhaust on, intake off

PRIMARY ENGINE TONE
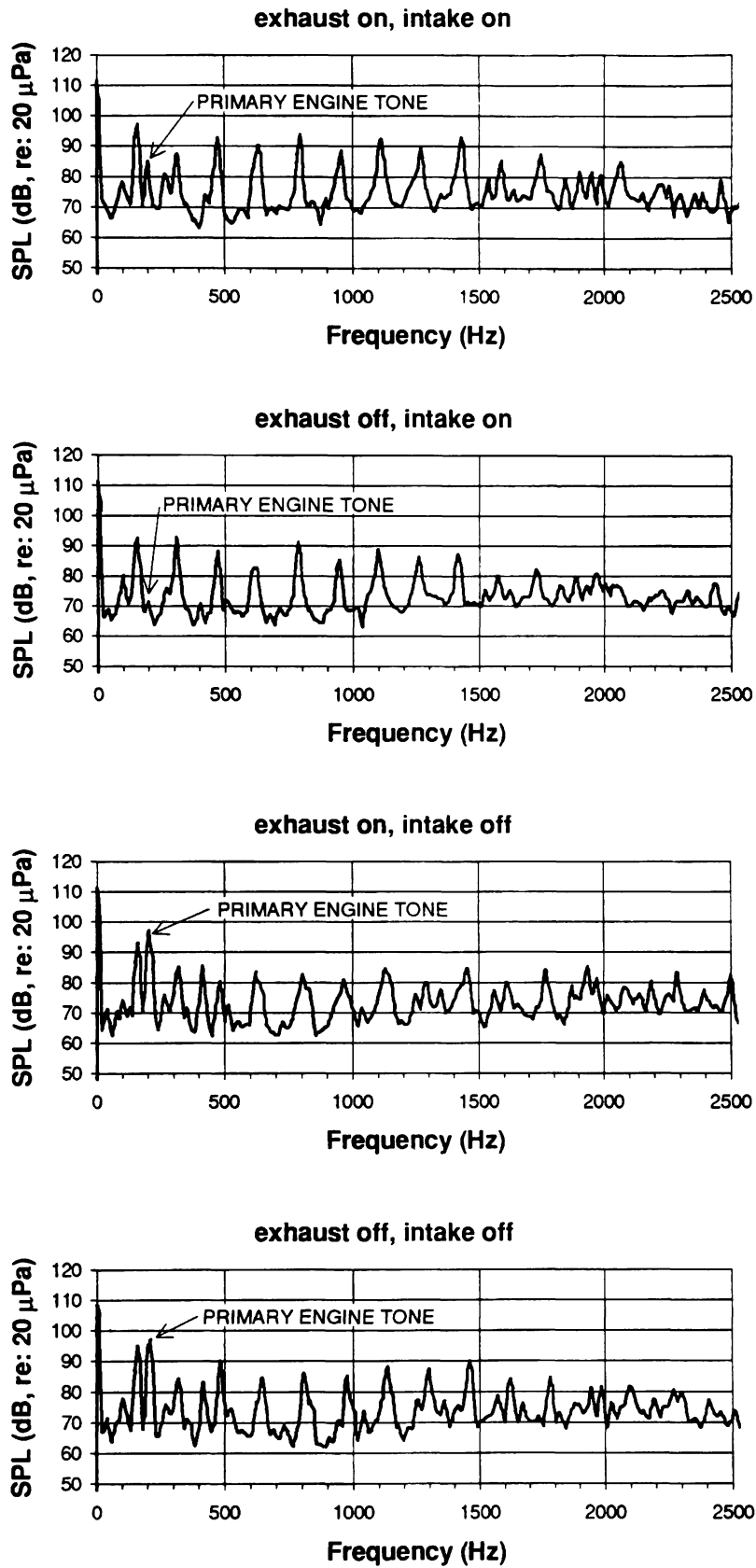
exhaust off, intake off

PRIMARY ENGINE TONE

Figure 31. Spectrum Plots of Engine Noise Using Four
Different Exhaust/Intake Configurations

when compared to the overall levels of noise. Also, the second engine harmonic levels

both indicate levels in the low 70 decibels. When these configurations are compared to

those in which the intake silencer is removed in Figure 31, a large difference is noted in the

tone at 200 Hz. With the intake silencer removed, the engine noise jumps up to levels of

97 dB from an average of 78 dB with the intake silencer installed. Corresponding to the

increase in engine noise when the intake silencer is removed, is the OASPL which

increases by about 2 dB. Without the intake silencers in place, the engine noise becomes

the primary tone in the overall power-spectrum of noise.

A similar type comparison is attempted between the power-spectrum curves with

the exhaust muffler installed and comparing these two curves with the exhaust off as

shown, in Figure 31, indicates no significant differences between the various

configurations. There are two explanations for this result. First, as the secondary muffler,

the results will not be nearly as dramatic as they would have been had the primary exhaust

muffler been removed. Second, all recordings of exhaust / intake noise are taken on the

intake side of the engine, ($\theta = 45°$) so there tends to be much more bias in the results, due

to changes in the intake configuration than changes in the exhaust configuration. It is felt

that any differences in engine noise due to exhaust configuration are probably

overshadowed by the intake noise, so the only conclusion about the effectiveness of the

after-muffler is that it is not effective enough to be noticed from the intake side of the

engine.

Results do conclude the need for use of the intake silencer to avoid levels of engine

noise that will affect the OASPL on the intake side.

CHAPTER 4

IMPLICATIONS FROM THE RESULTS

This next chapter discusses some of the implications from the results, as they might

affect future work. First, the rotor-stator interaction tones are addressed, and the

theoretical effects of more stator vanes is examined. The second section discusses the

significance of the results as applied to an ANC system for the shroud.

4.1 ROTOR - STATOR INTERACTION INVESTIGATION

Strong rotor - stator interaction tones account for a 6 dB increase in the OASPL

with the shroud in place, compared to without the shroud as discussed in Section 3.2.1.

Certainly, this is not helping the effort to reduce the levels of noise emitted with the

shroud in place. However, it does help to confirm the validity of the rotor-stator

interaction theory, presented in Chapter 1. As mentioned earlier, to date, there has been

no published work performed which experimentally verifies that the rotor-stator

interaction theory is valid for a propeller operating in a short duct. The following takes a

look at what the predicted results would be if more stators were added to this apparatus,

as a means of reducing some of the lower frequency aerodynamic interaction tones.

Recalling from Chapter 1, that if the number of stators is at least twice the number of rotor blades, than theory predicts there to be no fundamental tones (s = 1) which will propagate. Using the same methodology used in Section 3.2.2.1, and assuming nine stators now, instead of the previous three, with a four bladed propeller, Equation 6 is rewritten as

$$-8/9 < k < 0. \hspace{4cm} \text{Eq. 12}$$

Immediately, it is seen that there are no values of k which satisfy the necessary condition. This implies that all fundamental modes have an Ω_m which is equal too, or smaller than the rotational velocity of the propeller. Since the propeller tip speed is subsonic, all fundamental tones are predicted to decay [10].

As the data recorded for this work indicated, the fundamental tone is only one tone out of many that show up in the power spectral analysis. In order to fully understand the impact of the additional stator blades, the tones that occur at the higher harmonics (s = 2, 3,...) have to also be examined. It is through examination of these tones, that some very interesting results become apparent.

Table 7 shows the predicted results based on an analysis of a nine stator, four bladed propeller setup for this apparatus, for harmonics through s = 6. The table is setup identically to Table 6, in Chapter 3. Notice the reduction in the values of k that will satisfy each given harmonic. As mentioned above, the BPF tone at 160 Hz should not propagate, since there are no possible values of k which will provide for an Ω_m greater than Ω. Next,

for s = 2, corresponding to the 2BPF tone at 320 Hz, there is a mode which will

propagate. For s = 3, all possible modes are below their respective cut-offs, so in theory,

Table 7. Possible propagating modes from shroud using 9 stators with a 4-bladed rotor

possible k's	none
m lobes	
omega$_m$ (Hz)	
propagation ?	

s = 1
tone =   160 Hz

possible k's	-1
m lobes	-1
omega$_m$ (Hz)	-320
propagation ?	Yes

s = 2
tone =   320 Hz

possible k's	-1	-2
m lobes	3	-6
omega$_m$ (Hz)	160	-80
propagation ?	No	No

s = 3
tone =   480 Hz

possible k's	-1	-2	-3
m lobes	7	-2	-11
omega$_m$ (Hz)	91.429	-320	-58.18
propagation ?	No	Yes	No

s = 4
tone =   640 Hz

possible k's	-1	-2	-3	-4
m lobes	11	2	-7	-16
omega$_m$ (Hz)	72.727	400	-114.3	-50
propagation ?	No	Yes	No	No

s = 5
tone =   800 Hz

possible k's	-1	-2	-3	-4	-5
m lobes	15	6	-3	-12	-21
omega$_m$ (Hz)	64	160	-320	-80	-45.71
propagation ?	No	No	No	No	No

s = 6
tone =   960 Hz

no 3BPF tone at 480 Hz should propagate. From the remaining harmonics listed in the

table, the 4BPF tone at 640 Hz and 5BPF tone at 800 Hz are both seen to have modes

which will propagate, while the 6BPF tone at 960 Hz does not appear to have any

propagating modes. In other words, from a quick analysis, it can be predicted that the additional stators will result in a reduction at some tones, while other tones will still be apparent.

Assuming that experimental results validate the theoretical predictions, the next question would be: how much effect does the reduction of some of the tones have on the overall levels of noise emitted, and the directionality patterns? This question is hard to answer, due to the many variables still present, one of which is the decay rate of the individual tones. The rate at which the tones decay is dependent in part on the how far below the cut-off frequency they are. For example, from Table 7 it was seen that no tone at 960 Hz is predicted to propagate, however, there is a mode which has a rotational speed of -320 Hz. This is not very far below the cut-off of 332 Hz. There is a good chance that in this case, this mode will not decay fully before exiting the shroud, resulting in some amount of residual 6BPF tone at 960 Hz.

4.2 FUTURE APPLICATION OF ANC

Many of the higher frequency tones induced from the rotor-stator interactions tended to be higher than the optimal range of operation for most active noise control systems. As described in Chapter 1, once the frequencies of cancellation exceed about 800 Hz, the effectiveness of active noise reduction will decrease rapidly. Since a majority of the tones generated by the rotor stator interaction are in excess of 800 Hz, effective noise cancellation of the lower frequencies might not be noticed with many of the higher frequencies being unaffected.

The cancellation of noise using active noise control is by nature a very unstable process, even when applied to simple plane waves. Active noise control of a (1,0) mode wave complicates the process, since two speakers are required to generate a (1,0) mode anti-phase tone. With two speakers, comes the increase in complexity of the system as well as a decrease in the amount of reduction noticed. Considering the majority of higher frequency tones which propagate into the farfield from this setup are of a (2,0) mode or higher, ANC quickly becomes a very impractical means of noise reduction.

Based on these conclusions, it would appear that this apparatus would be much better suited for active noise control tests if the stators were removed. With the stators removed, no higher interaction tones due to stator wake would occur. Barring additional wake interaction tones due to separation off the leading edge, the primary tone of concern would occur at BPF (neglecting engine tones). There still remains the concern, however, with such a short duct, propagation as a plane wave might not be noticed, in which case the acoustic pressure field exiting the shroud would have to be modeled as one with a four lobe pattern. This would require the use of an eight speaker ring place along the inside wall of the shroud.

With a duct that is as short as this one is, the chordwise speaker placement is somewhat limited. Acoustically, placement of the speakers for optimal effectiveness would depend on which end of the shroud optimal noise cancellation would be required, as well as the velocity of the air traveling through the shroud which of course would vary in actual flight. Other factors to keep in mind would include the CG shift of placing the speakers forward or aft of the airfoil CG, and the potential for one of the speakers being

damaged if placed in-line with the propeller plane of rotation. With these factors in mind, a speaker ring placement slightly aft of the propeller plane of rotation would seem to be most reasonable.

Due to the tight coupling associated between the speakers and the noise source under this type of setup, a feedback system would have many instabilities associated with it. It has been the intent of this project all along that should ANC be applied to this apparatus, the algorithm used would be an extension of the one developed by Sutliff and Nagel, in which the use of two feedforward signals were employed [4]. This type of algorithm would seem ideal for this setup as minimal processing time is needed by the controller once initialized. Further, it has been proven to reduce noise (under ideal situations) up to 25 dB for long ducts and no stators. With some modifications, this apparatus still has a lot of potential for ANC applications, from both a theoretical and practical view.

CHAPTER 5

CONCLUSIONS AND FUTURE RECOMMENDATIONS

5.1 CONCLUSIONS

Initial evaluation of the shrouded propeller apparatus is aimed at providing data which can be used to evaluate acoustical performance of the apparatus. Results are gathered for both the unshrouded, as well as the shrouded configuration. Further results are aimed at measuring engine intake versus exhaust noise.

For the unshrouded propeller, the OASPL is between 98.5 and 104.6 dB, with the highest levels exhibited at azimuthal angles of $\theta = 45°$ and $\theta = 150°$. The noise consists of propeller components and engine components which are separated using power-spectrum analysis. The propeller noise is greatest on the intake side of the apparatus. The lack of symmetry in the propeller noise between the intake side and the exhaust side is due primarily to effects of engine blockage. Propeller harmonics from the ultralight propeller are noticed up through the eleventh harmonic. The engine noise consists of two monopole sources as expected - the intake port and the exhaust port. Of these, the exhaust appears strongest, and at a few locations is measured to be greater than the propeller noise.

With the shroud installed, OASPL increases by about 6 dB above the unshrouded propeller. The increase is due to an increase in levels of higher frequency tones which are attributed to rotor-stator interaction. The directionality pattern of the OASPL with the shroud seems to be more symmetrical than without the shroud; however, there also appears to be higher levels of standard deviation in the measurements.

Testing of various silencer configurations on the two-cycle engine concludes the need for the intake silencer to be in place when measuring the OASPL's emitted by the propeller. With the intake silencer, engine noise levels drop anywhere between 15 - 25 dB and OASPL decreases by 2 dB. Without the intake silencer, engine tones dominate the overall noise spectrum, which throws off attempts to measure the overall levels of propeller noise. Similar conclusions can not be drawn about the effectiveness of the secondary exhaust muffler.

5.2 FUTURE RECOMMENDATIONS

Continued evaluation of this propeller - shroud setup is essential to eventually equipping the apparatus with an effective ANC system. Although the theories applicable to this apparatus are thought to be fairly well understood, small subtleties particular to this apparatus could have a significant effect on the performance of an ANC system. With the apparatus currently "ready to go", further evaluation can begin immediately. Looking at the long term plans for the apparatus, three stages of progression can be developed, based on complexity and importance:

1) Finish a complete survey of the current apparatus, including a complete analysis of the engine noise and propeller noise, under static and dynamic conditions.

2) Perform further rotor-stator interaction work to prove / disprove validity of the theories presented in Chapter 1.

3) Pursue application of ANC system.

Each of these steps is described further in the following sections.

5.2.1 Survey of Complete Apparatus

Although the data provided in this report covers the basic configurations for the apparatus, a more complete survey of all possible operating configurations and conditions is needed to fully understand the characteristics of this apparatus. Further, a continuation of the type of evaluation presented in this work, with the apparatus in its current configuration will provide one with the opportunity to become familiar with the apparatus and its operation before attempting more advanced research.

As an initial step, a three bladed and possibly a two bladed propeller should be installed instead of the current four bladed propeller to collect noise measurements and OASPL's similar to those performed with the four bladed propeller. As mentioned earlier, the propeller used is easily modified to run with three blades or possibly two blades. Testing under various blade configurations would help to show the effects of number of blades on propeller acoustics as well as on rotor - stator interaction.

A further engine noise evaluation is also needed, as only a small amount of data has currently been gathered on this subject. Since all engine data from this apparatus was taken at only one position, a more thorough investigation is needed, before any strong

conclusions can be drawn about the directionality of the engine noise and the effectiveness of the various engine silencer configurations.

Finally, testing the entire apparatus under dynamic conditions will provide invaluable data, as currently, the majority of past research performed using similar setups has been performed under static conditions only. Unfortunately, dynamic conditions were not available at the time this work was performed, and the size of the apparatus makes finding an anechoic wind tunnel difficult. There is currently an anechoic wind tunnel under construction at ERAU that will be able to handle up to a 24 inch diameter shroud.

5.2.2 Rotor-Stator Evaluation

This next stage involves some configuration changes to the apparatus itself. The purpose is to confirm that the rotor-stator theories presented in Chapter 1 are applicable to this apparatus, specifically, that an increase in the number of stator vanes will reduce the lower frequency components. With three stator vanes in its current configuration, an increase of six to bring the total to nine stator vanes will be needed in order for the number of stator vanes to be more than twice the number of propeller blades. The stator vanes will be spaced every 40°. Installation of the additional vanes should be relatively simple as they will not have to support any structural loads, other than the drag imposed on them due to air traveling over them.

5.2.3 ANC Installation

Once the previous two stages have been completed, development of an ANC system will proceed. For reasons discussed in Chapter 4, the implementation of an ANC system will most likely proceed without any stator vanes installed. Due to the construction and design of the apparatus, however, removal of the stators will require some sort of alternative method of securing the shroud to the engine. Currently, the stators act as structural struts, in addition to acoustical stators. With these struts removed, there would be nothing left keeping the shroud in line with the center of the engine and preventing the blades from contacting the inside walls of the shroud. Most likely, some sort of bracing that would be mounted to the exterior of the shroud and tie into the engine would be required. Finally, speakers could be mounted into the shroud walls and an active noise control system could be applied.

With careful planning and some modifications the apparatus can be used as an invaluable tool for further development and confirmation of acoustic principles and theories.

REFERENCES

[1]   Sutton, John W., <u>Aviation Noise: Problems...Solutions</u>, Embry-Riddle Aeronautical University, Graduate Project, 1994.

[2]   Eldred, Kenneth McK., "Airport Noise: Solving a World Class Problem", <u>Inter-Noise 92</u>, Proceedings of the 1992 International Conference on Noise Control Engineering, 1992: pp. 3-12.

[3]   <u>Federal Aviation Regulations, Part 36</u>, FAA, 1997.

[4]   Sutliff, D. L., and Nagel, R. T., <u>Active Noise Control of the Farfield Noise Radiated by a Ducted Fan</u>, North Carolina State University, Doctoral Thesis, 1993.

[5]   Beranek, Leo L., <u>Acoustics</u>, Published for the Acoustical Society of America by the American Istitue of Physics, 1986.

[6]   Elliott, S. J., and Nelson, P. A., "Active Noise Control", <u>Noise/News International</u>, June 1994: pp. 75-98.

[7]   Shifrin, Carole A., "Saab 340B's Get Active Antinoise System", <u>Aviation Week & Space Technology</u>, May 1994: pp. 55-58.

[8]   Bies, D. A., and Hansen, C. H., <u>Engineering Noise Control</u>, E & FN SPON, 1996.

[9]   Chaplin, Harrie, "The Cancellation of Repetitive Noise and Vibration", <u>Inter-Noise 80</u>, Proceedings of the 1980 International Conference on Noise Control Engineering, 1980: pp. 699-702.

[10]   Tyler, J. M., and Sofrin, T. G., "Axial Flow Compressor Noise Studies", <u>Trans. S.A.E.</u>, 1961: pp. 309-332.

[11]   Hubbard, H. H., "Sound Measurements for Five Shrouded Propellers at Static Conditions", NACA TN-2024, 1950.

[12]   McLemore, H. Clyde, and Pegg, Robert J., "Aeroacoustic Wind-Tunnel Tests of a Light Twin-Boom General-Aviation Airplane With Free- or Shrouded-Pusher Propellers", NASA TM-80203, 1980, NASA Langley Research Center.

[13]   Metzger, F. B., Menthe, R. W., and McColgan, C. J., Performance and Noise of a Low Pressure Ratio Variable Pitch Fan Designed for General Aviation Applications, prepared for NASA Langley Research Center under contract NAS1-13774, Hamilton Standard, January 1980.

[14]   Patrick, H. V. L., Proposed Wind Tunnel Evaluation of the Aerodynamic and Acoustic Characteristics of a Ducted-Propeller, University of Tennessee Research Proposal Submitted to NASA Langley Research Center, 1990.

[15]   Lueg, P., "Process of Silencing Sound Oscillations", U.S. Patent #2,043,416, 1936.

[16]   Olsen, H. F., and May, M.E., "Electronic Sound Absorbers", Journal of the Acoustical Society of America, Vol. 25, 1953.

[17]   Eriksson, L. J., Allie, M. C., Hoops, R. H., and Warner, J. V., "Higher Order Mode Cancellation in Ducts Using Active Noise Control", Inter-Noise 89, Proceedings of the 1989 International Conference on Noise Control Engineering, 1989: pp. 495-500.

[18]   Pelton, H. K., Wise, S., and Sims, W. S., "Active HVAC Noise Control Systems Provide Acoustical Comfort", Sound and Vibration, July 1994: pp. 14-18.

[19]   "Lockwood Aviation Supply Catalog", Lockwood Aviation Supply, Inc., 1995.

[20]   Hanson, D. B., and Parzych, D. J., "Theory for noise of Propellers in Angular Inflow with Parametric Studies and Experimental Verification", NASA Contractor Report 4499, March 1993.

[21]   Schulten, Joannes Bernardus Henricus Maria, Sound Generation by Ducted Fans and Propellers as a Lifting Surface Problem, Universiteit Twente, Doctoral Thesis, 1993.

[22]   Hanson, D. B., "Influence of Propeller Design Parameters on Far Field Harmonic Noise in Forward Flight" AIAA paper 79-06096R, May 1979.

APPENDIX A

ROTAX 377 ENGINE SPECIFICATIONS

AND ACCESSORIES

Rotax 377 Engine Specifications [19]

Description:	Two-cycle, two cylinder engine, oil-in-fuel lubrication, fan-cooled
Bore:	62.0mm (2.441 in)
Stroke:	61mm (2.401 in)
Displacement:	368.3 cc (22.475 in)
Compression Ratio:	Theoretical 11.6, effective 6.9

Power Output:	26.0 kW (35.0 HP) @ 6500 rpm
Torque Max:	37 Nm (27.3 ft lb) @ 6200 rpm
Max Recommended RPM:	6800 rpm
Direction of Rotation:	Counter-clockwise, viewed toward pto end w/out gear box

Cylinder:	2 light alloy cylinders w/cast iron sleeves
Piston:	Aluminum Cast piston w/2 piston rings
Piston/Cylinder Clearance:	.08 - .09mm (.00315 - .00354 in)
Ignition System:	Flywheel magneto generator SCP2 w/contact breakers

Generator output:	AC12V 110W +30W
Rectifier-Regulator:	a) 866 080 requires minimum load 12W (1A) to operate
	b) 264 870 no minimum load required
Ignition timing:	2.09mm = .0823 in (19 degrees) B.T.D.C.
Contact breaker points gap:	.3mm - .4mm (.012 - .016 in)

Break away gap:	13-17mm (.512 - .67 in)
Spark plug:	14mm, B8ES
Electrode gap:	.5mm (.02 in)
Radio Frequency interference suppression:	Optional for AC or DC

Carburetor:	1 Bing 36mm (1.417 in) hand lever or cable choke
Fuel Pump:	Pneumatic fuel pump DF44
Lubrication of engine:	Automotive gasoline, not below MON83 or RON90
Mixing Ratio:	50:1 (2%)
Starter:	Rewind starter optional a) rewind starter w/electric starter for pto side (for engine w/gearbox)
	b) electric starter, magneto side without rewind starter (gearbox is possible)

Reduction gear box:	With torsional shock absorber, ratios available: 2, 2.24, 2.58, 3:1 (3:1 supplied only installed on engine)
Lubrication of gear box:	Gear oil SAE 140, APIGL5-GL6

Direction of propshaft rotation:	Clockwise, viewed towards prop flange
Cooling:	Air cooled by axial fan

Weights:	Engine without carb, intake silencer, fuel pump, or exhaust	26.8 kg (59.1 lb)
	carb assembly	.9 kg (2.0 lb)
	exhaust	4.9 kg (10.8 lb)
	intake silencer	.84 kg (1.9 lb)
	electric start, pto	3.42 kg (7.5 lb)
	electric start, mag	3.5 kg (7.7 lb)
	reduction gearbox	4.5 kg (9.9 lb)

Engine Accessories

Rotax After Muffler Kit for 377

SISK Intake Silencer with OCM300 Air Filter

Westberg CHT/CHT Gauge:	Part #K2DC8

Westberg Tach:	Part #2CT8A2/6

APPENDIX B

COORDINATES FOR MODIFIED

NACA 4312 AIRFOIL

NACA 4312 AIRFOIL (MODIFIED) [7]

Airfoil section .... NACA 4312 (modified)

Maximum thickness .... 12 percent of chord

Leading-ege radius .... 0.685 inch

Slope of leading-edge radius 0.267

Chord .... 28.8 inches

Inner surface				Outer surface			
Station		Ordinate		Station		Ordinate	
Percent chord	Inches	Percent thickness	Inches	Percent chord	Inches	Percent thickness	Inches
0.671	0.193	2.590	0.746	1.829	0.527	-1.938	-0.558
1.748	0.503	3.714	1.07	3.252	0.937	-2.436	-0.702
4.093	1.179	5.305	1.528	5.907	1.701	-2.861	-0.824
6.559	1.889	6.457	1.86	8.441	2.431	-2.957	-0.852
9.089	2.618	7.348	2.116	10.911	3.142	-2.904	-0.836
14.253	4.105	8.601	2.477	15.747	4.535	-2.601	-0.749
19.481	5.611	9.389	2.704	20.519	5.909	-2.279	-0.656
24.735	7.124	9.849	2.837	25.265	7.276	-2.071	-0.596
30.000	8.64	10.000	2.88	30.000	8.64	-2.000	-0.576
40.095	11.547	9.724	2.801	39.905	11.493	-1.886	-0.543
50.173	14.45	8.967	2.582	49.827	14.350	-1.621	-0.467
60.223	17.344	7.826	2.254	59.777	17.216	-1.296	-0.373
70.239	20.229	6.349	1.829	69.761	20.091	-0.961	-0.277
80.213	23.101	4.573	1.317	79.787	22.979	-0.655	-0.189
90.141	24.961	2.500	0.72	88.554	25.504	-0.378	-0.109
95.085	27.384	1.353	0.39	94.915	27.336	-0.251	-0.072
100.000	28.8	0	----------	100.000	28.8	0	----------

APPENDIX C

PROCEDURE FOR CONSTRUCTION

OF SHROUD

1) Start with at least two sheets of 3" thick, 4' x 8' blue Styrofoam®.

2) Cut sheets lengthwise into eight inch wide slices. Cut these slices every 24".

3) There should now be 40 rectangular pieces that measure 24" x 8" x 3".

4) Cut these pieces into a trapazoidal shape, with the long edge remaining at 24", and the short edge cut to aproximatly 18".

5) The trapazoidal pieces should now fit together, such that eight pieces fit end-to-end should complete a ring.

6) Using an epoxy resin, glue the first "ring" to the backing plate for the lathe.

7) Continue layering the rings, until a stack of 5 rings protrude off the backing plate. The stack of rings should now extend about 15" from the backing plate. When laying a ring on top off the next, be sure to offset the joints, so they don't lay on top of one another.

8) Attach the backing plate to the lathe, so that the entire foam ring can rotate.

9) Make initial cuts using hot wire. Be sure to use a template of the airfoil shape so as to avoid cutting off too much foam.

10) Final shaping of the airfoil should be done using a sanding block and sanding template while the shroud is rotating on the lathe.

11) Cut the first half of the shroud from the backing plate.

12) Repeat steps (1) through (10) to form other half of shroud.

13) Cut holes for stator/strut mounting blocks.

14) Glue two halves of foam shroud together.

15) Attach strut attachment link into strut mounting block. Then glue entire mounting block assembly into foam core.

16) To help distribute the load of the mounting blocks over a large area on the shroud, 1/16" aluminum sheeting can be screwed into the back end of the mounting blocks, so that the aluminum sheeting will lay flush on the outside surface of the shroud.

17) Cover entire shroud with fiberglass and epoxy resin. A light cloth (6 oz) should be used to avoid excess creasing and bubbling of the cloth during the layup procedure. Two layers of fiberglass cloth should be sufficient. If possible, layup a Kevlar patch around the inside surface of the strut attachments for extra strength.

18) Use a combination of Bondo and sanding to help form final airfoil shape.

19) When surface is sanded smooth, paint shroud.

APPENDIX D

COMPARISON OF A-WEIGHTED DATA

TO LINEAR WEIGHTED DATA

linear weighting
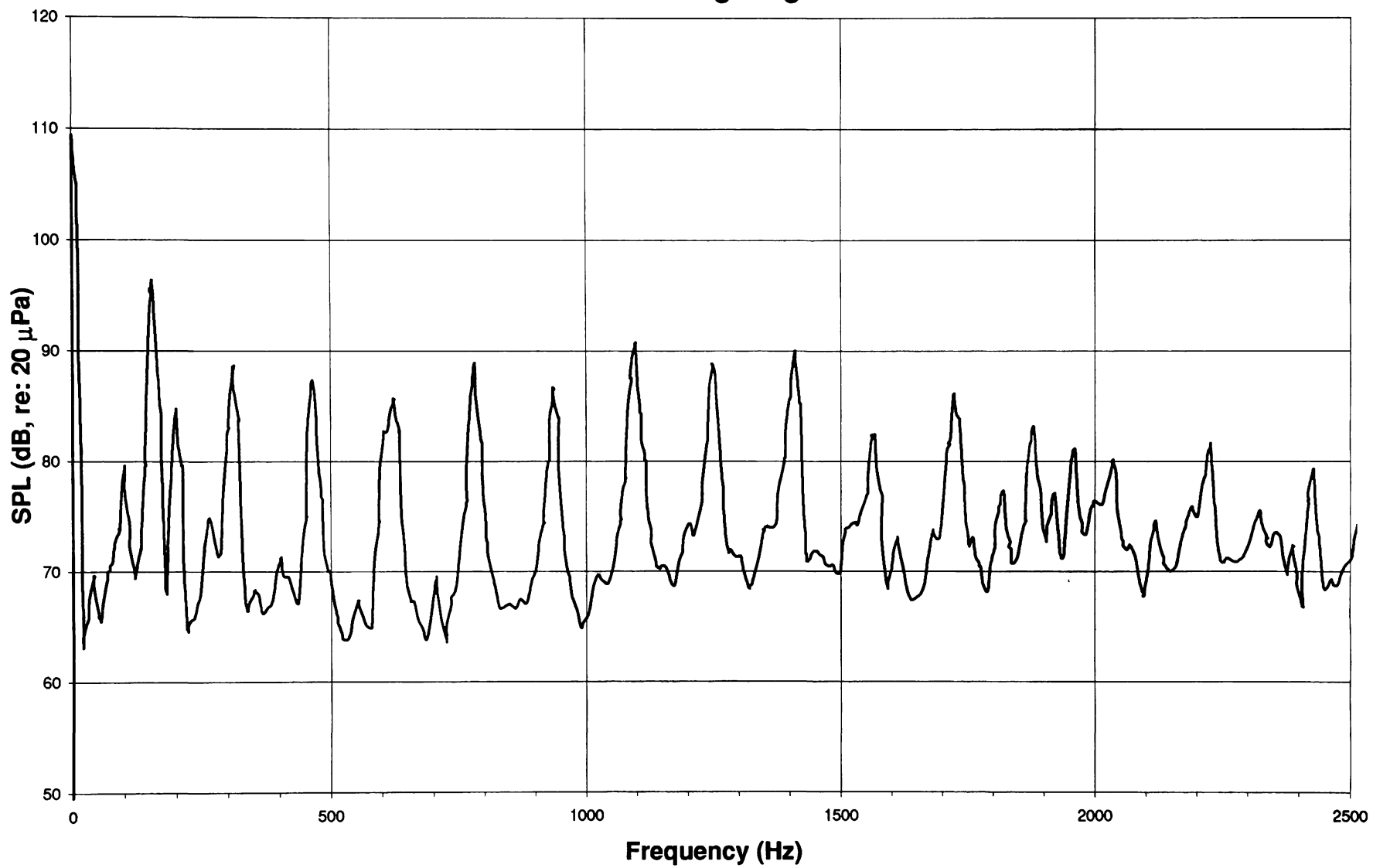
a - weighting
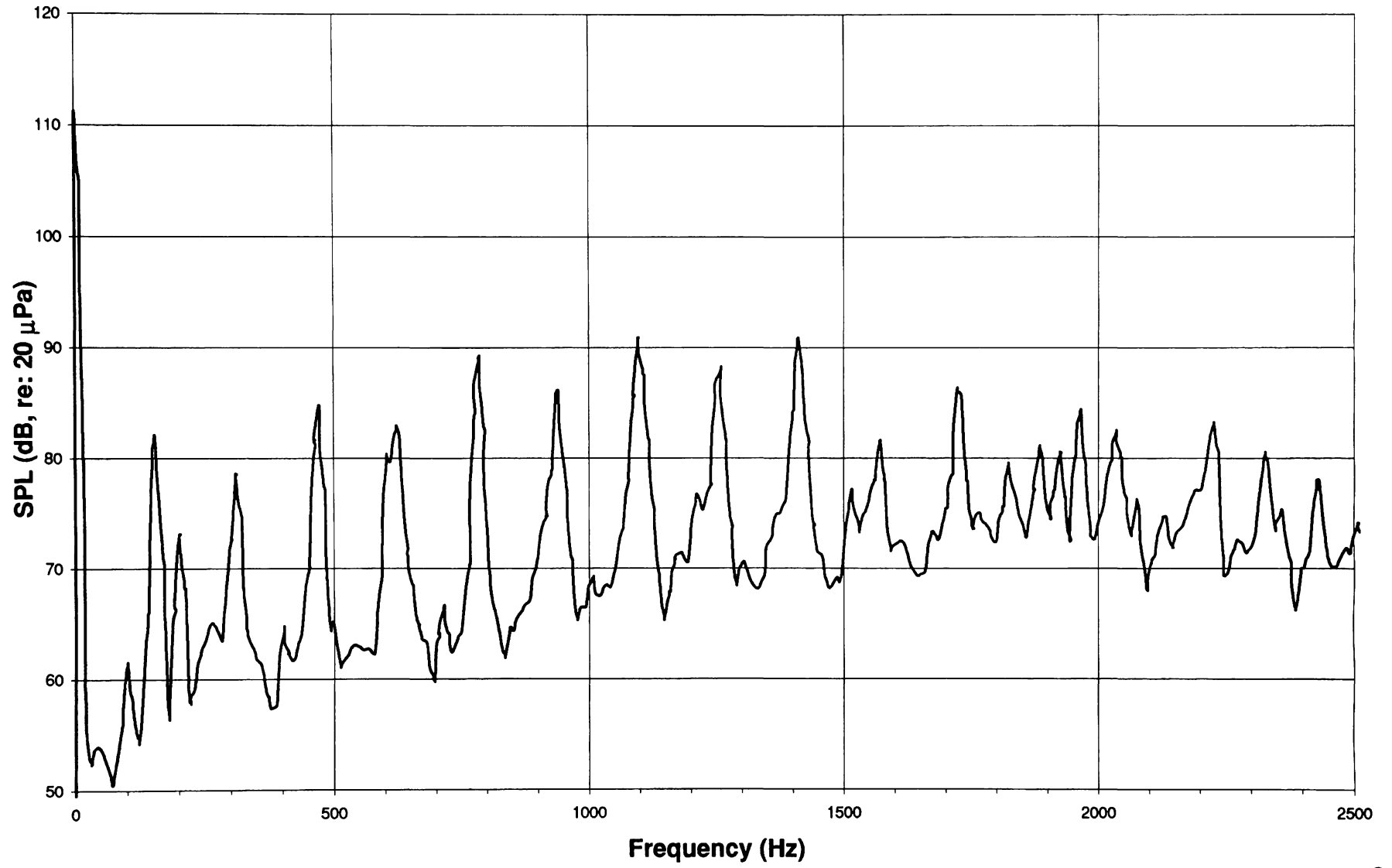
APPENDIX E

TEST INSTRUMENTATION AND

EQUIPMENT PART NUMBERS

Equipment List

- Racal Magnetic Tape Recorder (Serial #1461, ERAU #14968)
  Tape Speed: 7.5 in / s (Tape/Tach switch ==> Tach)

  Channel 1 (Exhaust noise):   Gain = 1 V
  Channel 2 (Intake noise):   Gain = 1 V
  Channel 3 (SPL meter):   Gain = 2 V
  Channel 4 (unused)

- Sony Techtronix T912 Oscilloscope (Serial #310060, ERAU #18433)

- Brüel and Kjaer Precision Integrating Sound Level Meter, Type 4230
  (Serial #1033458, ERAU #17833)
  Settings: Linear Weighting
                  Fast Response
                  110 dB scale

- Brüel and Kjaer Sound Level Calibrator, Type 2230
  (Serial #1026795)

- Hewlatt Packard Spectrum Analyzer, Type 3582 A
  (Serial #1809A03084, ERAU #13269)

APPENDIX F

SPECTRAL PLOTS OF

ACOUSTICAL DATA

without shroud, θ = -90°
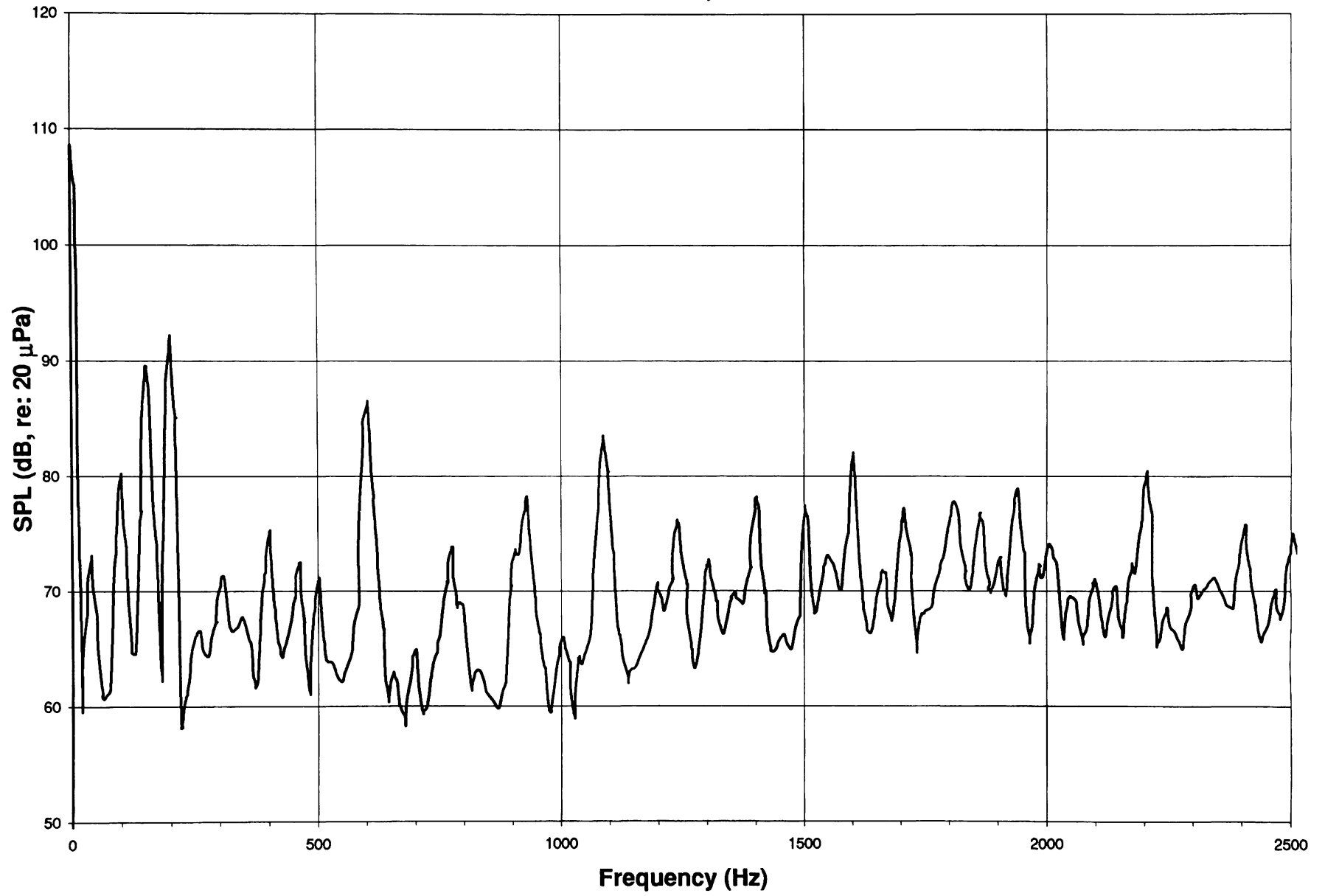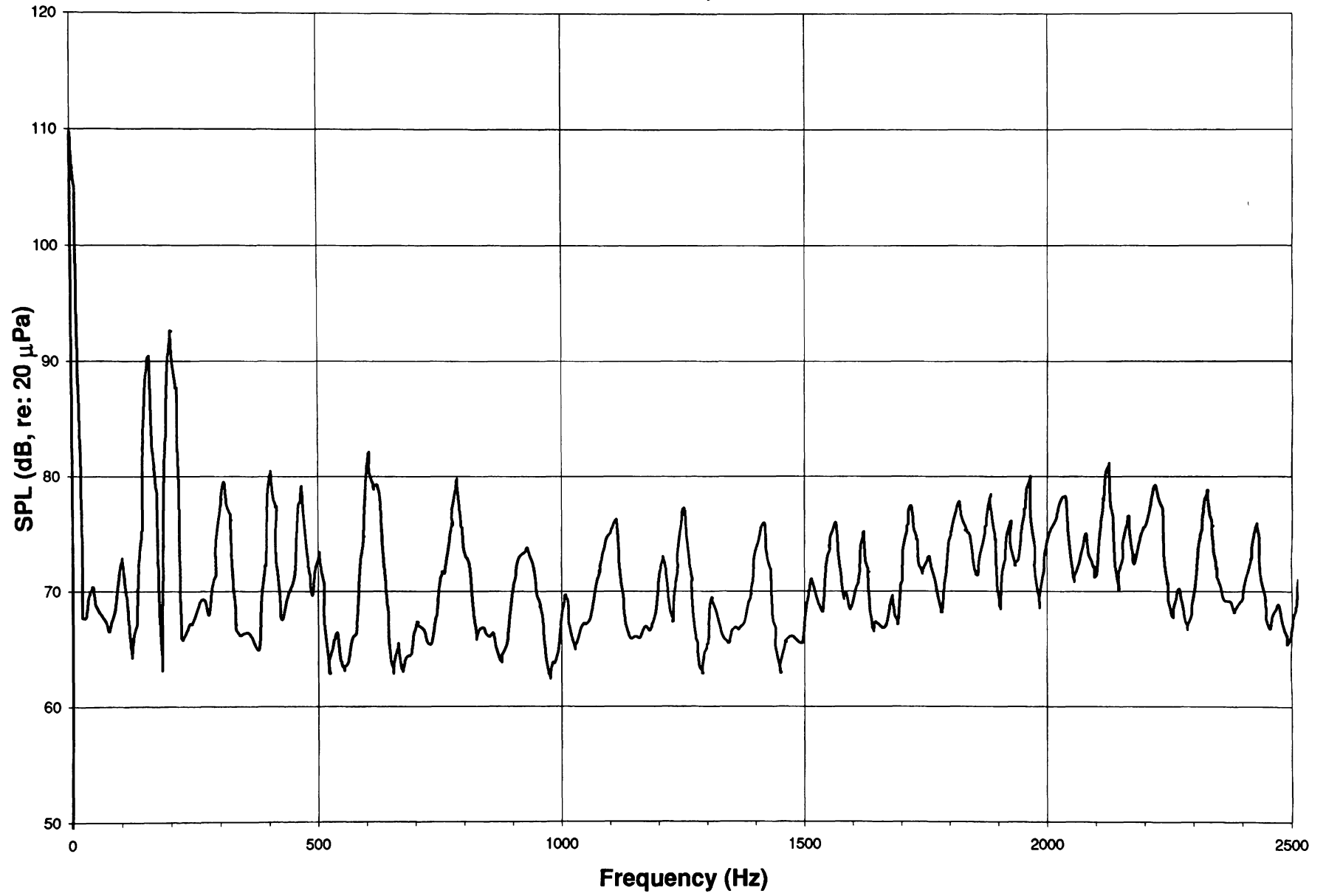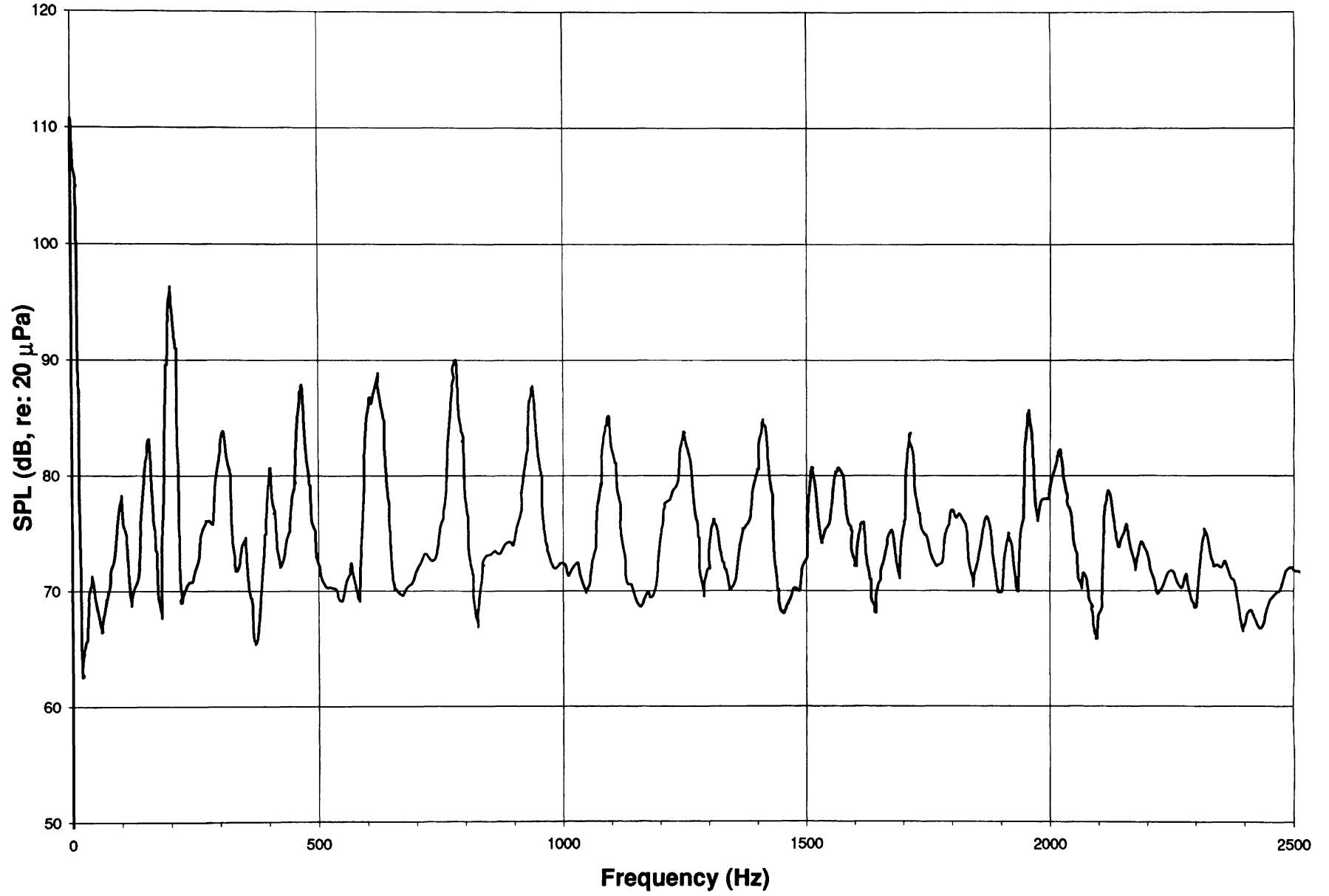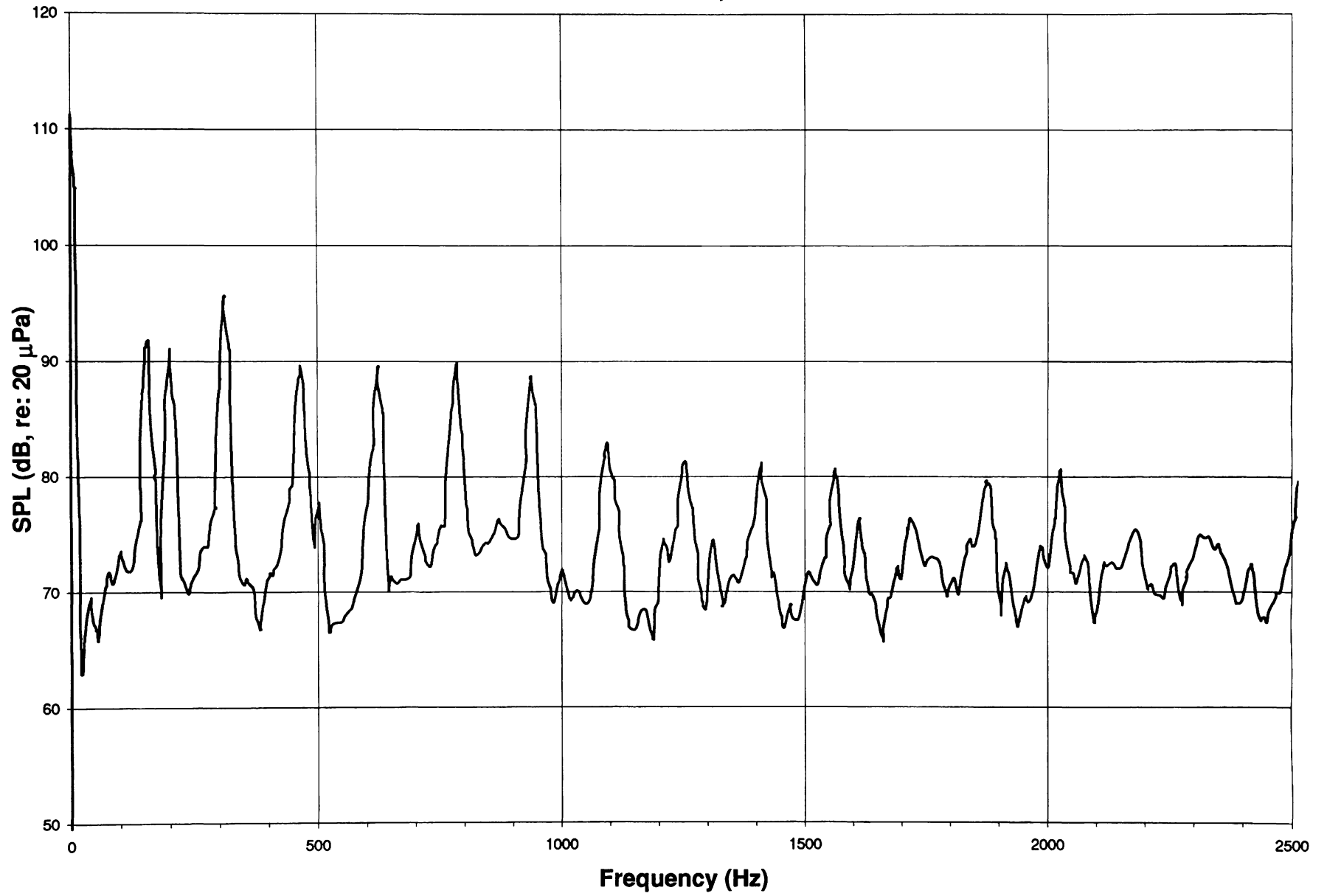
Frequency (Hz)

SPL (dB, re: 20 μPa)

without shroud, θ = -60°

without shroud, θ = -30°

SPL (dB, re: 20 μPa)

Frequency (Hz)

without shroud, θ = 0°

without shroud, θ = 30°

Y-axis: SPL (dB, re: 20 μPa)

X-axis: Frequency (Hz)

without shroud, θ = 60°

Frequency (Hz)

SPL (dB, re: 20 μPa)

without shroud, $\theta = 90°$

Y-axis: SPL (dB, re: 20 μPa)

X-axis: Frequency (Hz)

without shroud, θ = 120°

SPL (dB, re: 20 μPa) vs Frequency (Hz)
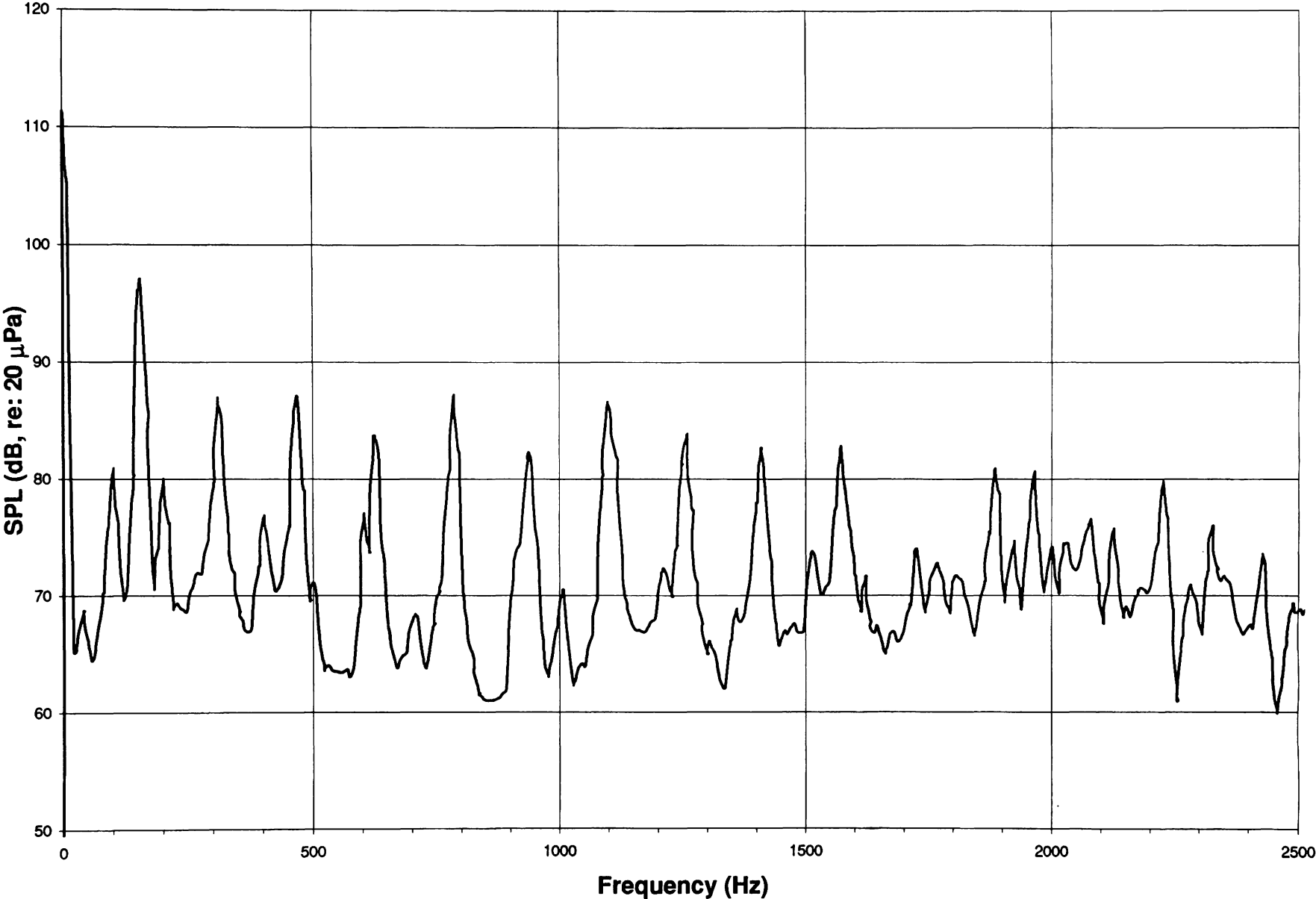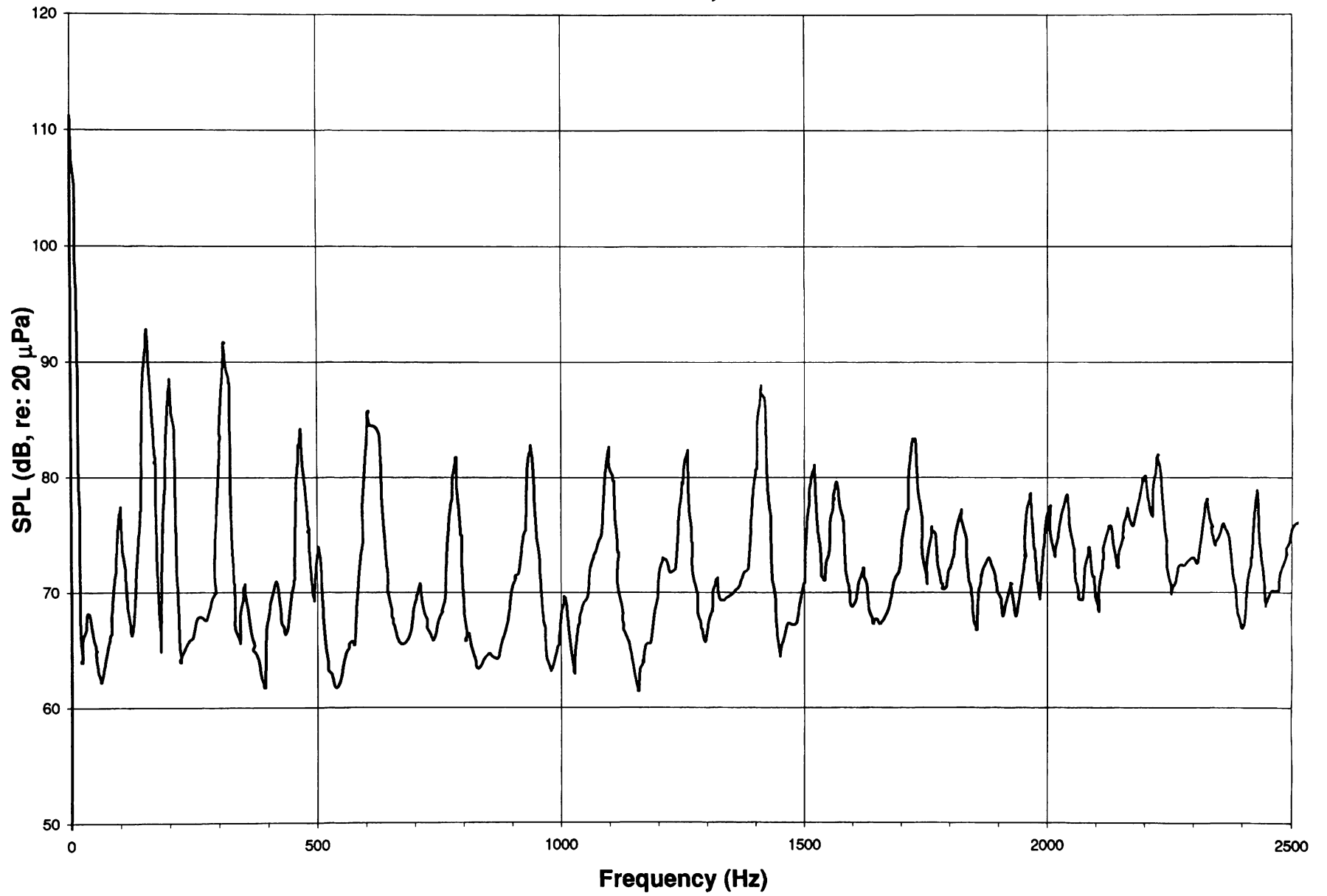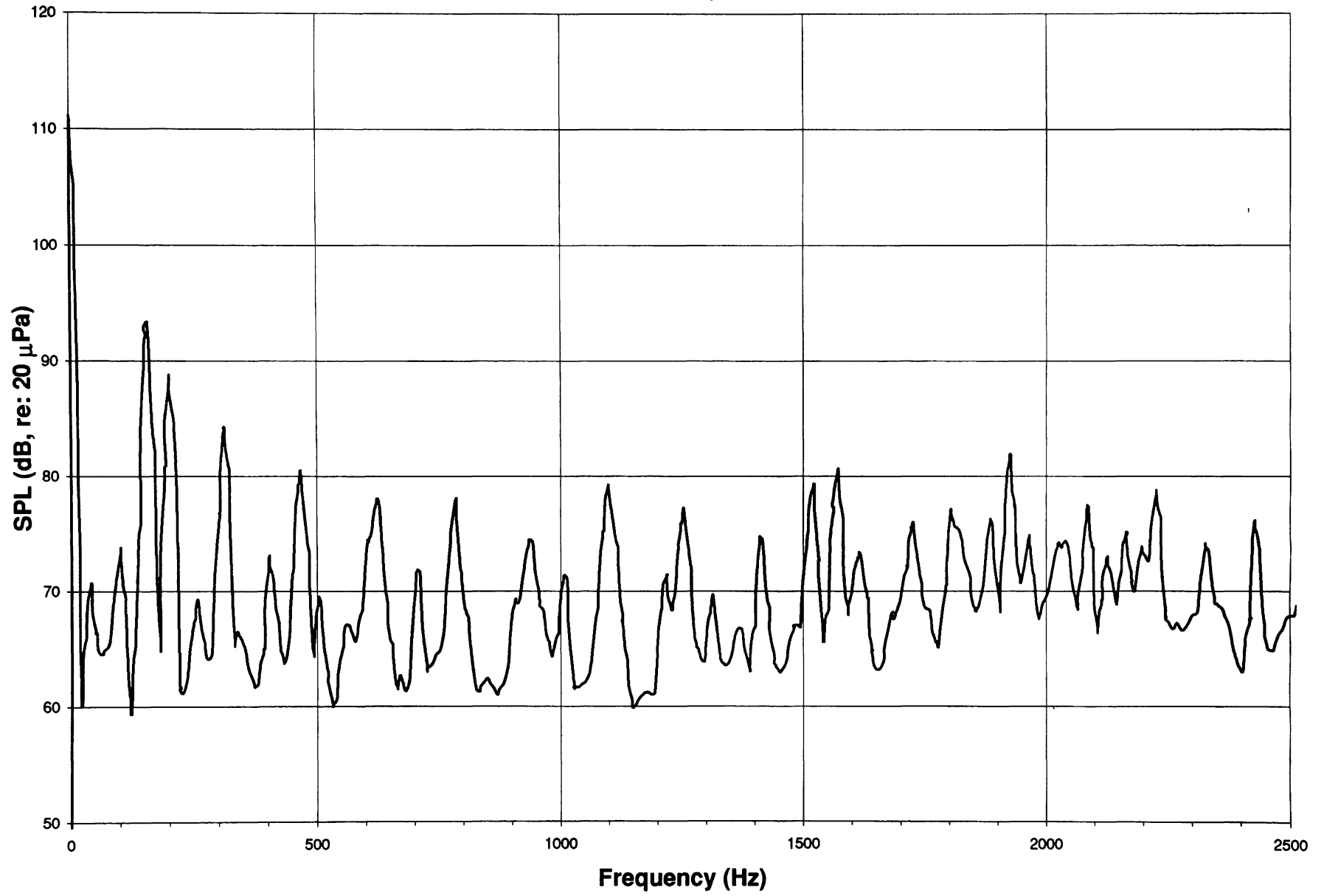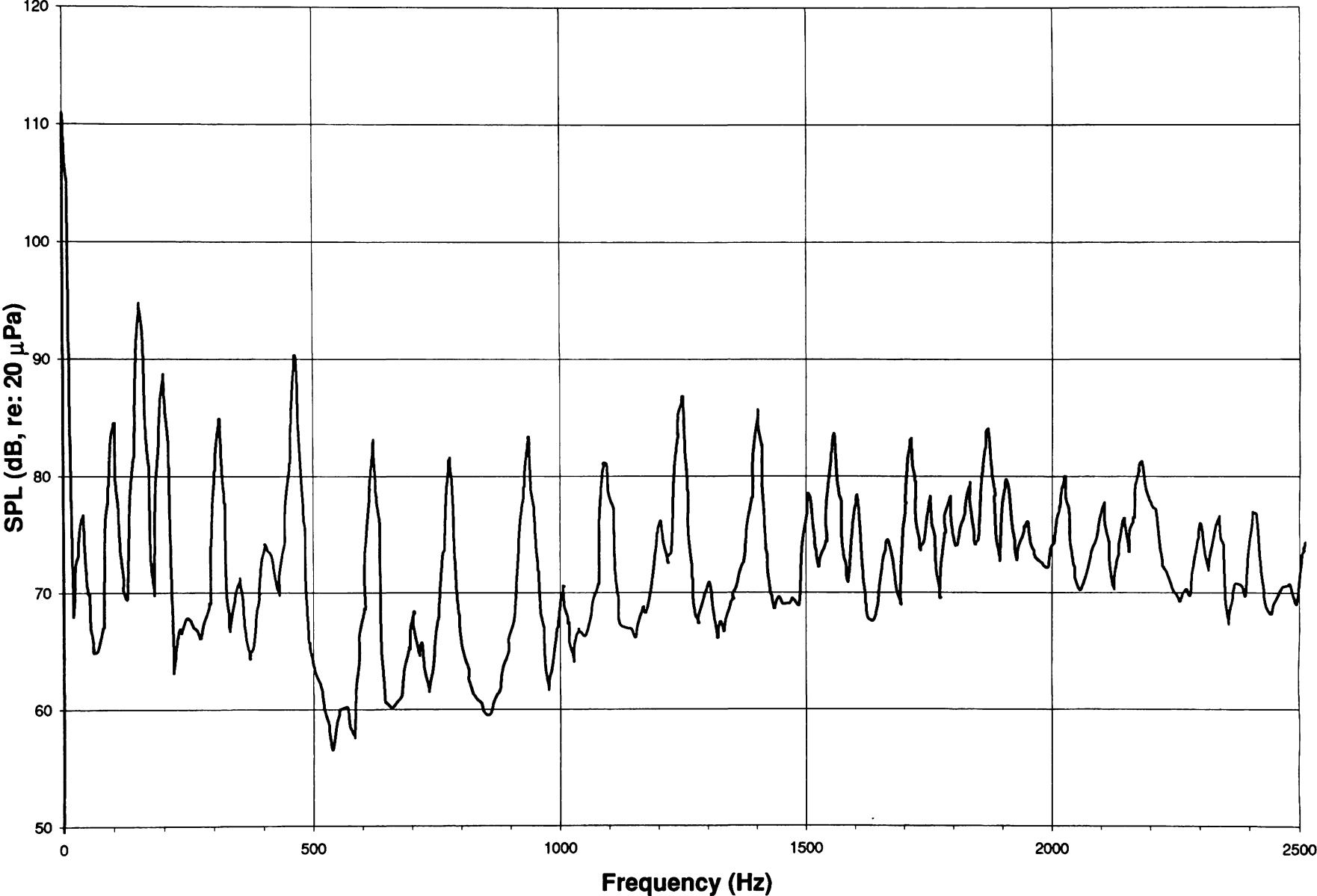
without shroud, $\theta = 150°$

with shroud, θ = -90°

Frequency (Hz)

SPL (dB, re: 20 μPa)

with shroud, θ = -60°

SPL (dB, re: 20 μPa)

Frequency (Hz)

113

with shroud, θ = -30°

Frequency (Hz)

SPL (dB, re: 20 μPa)

with shroud, θ = 0°

with shroud, θ = 30°

Frequency (Hz)

SPL (dB, re: 20 μPa)
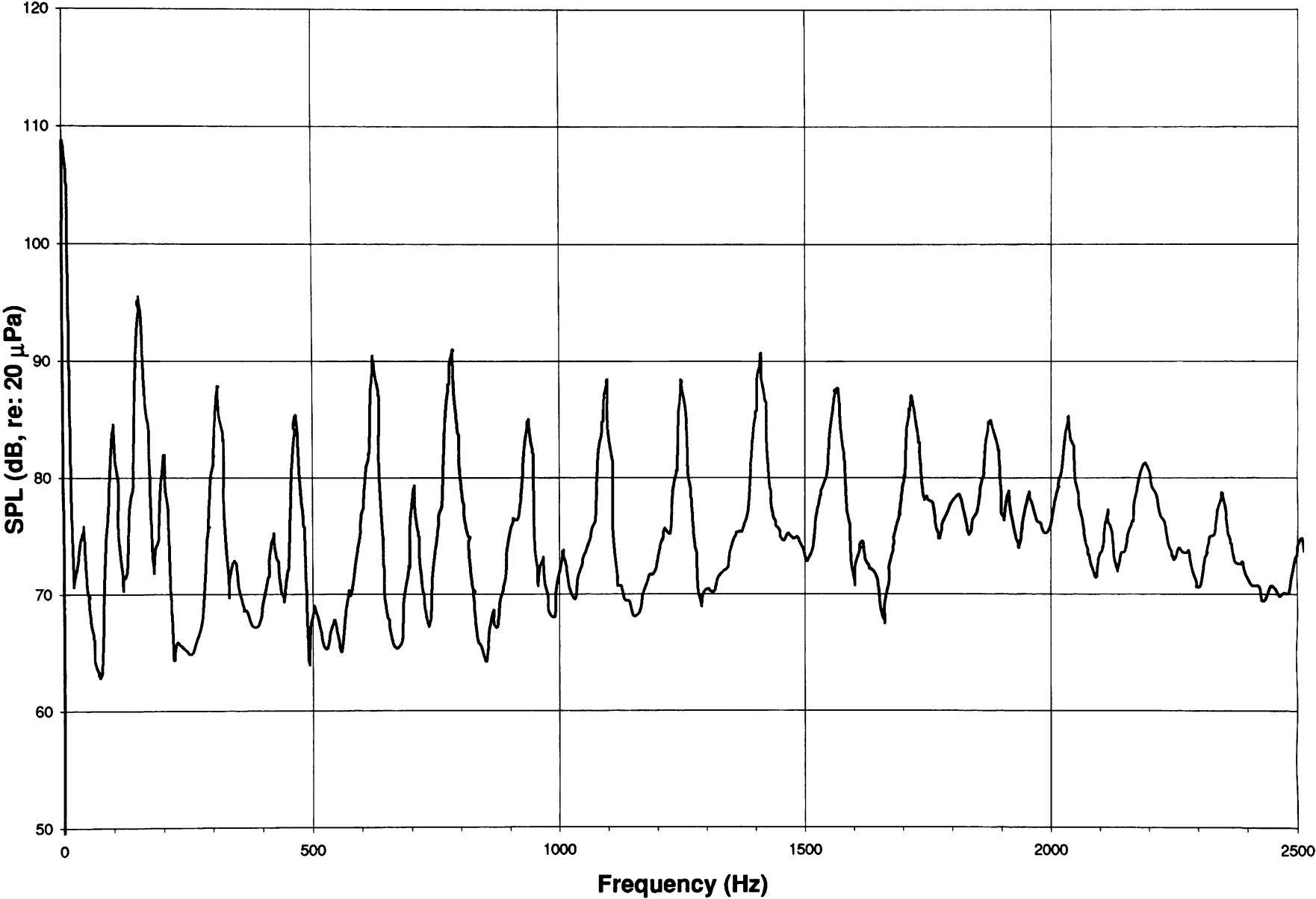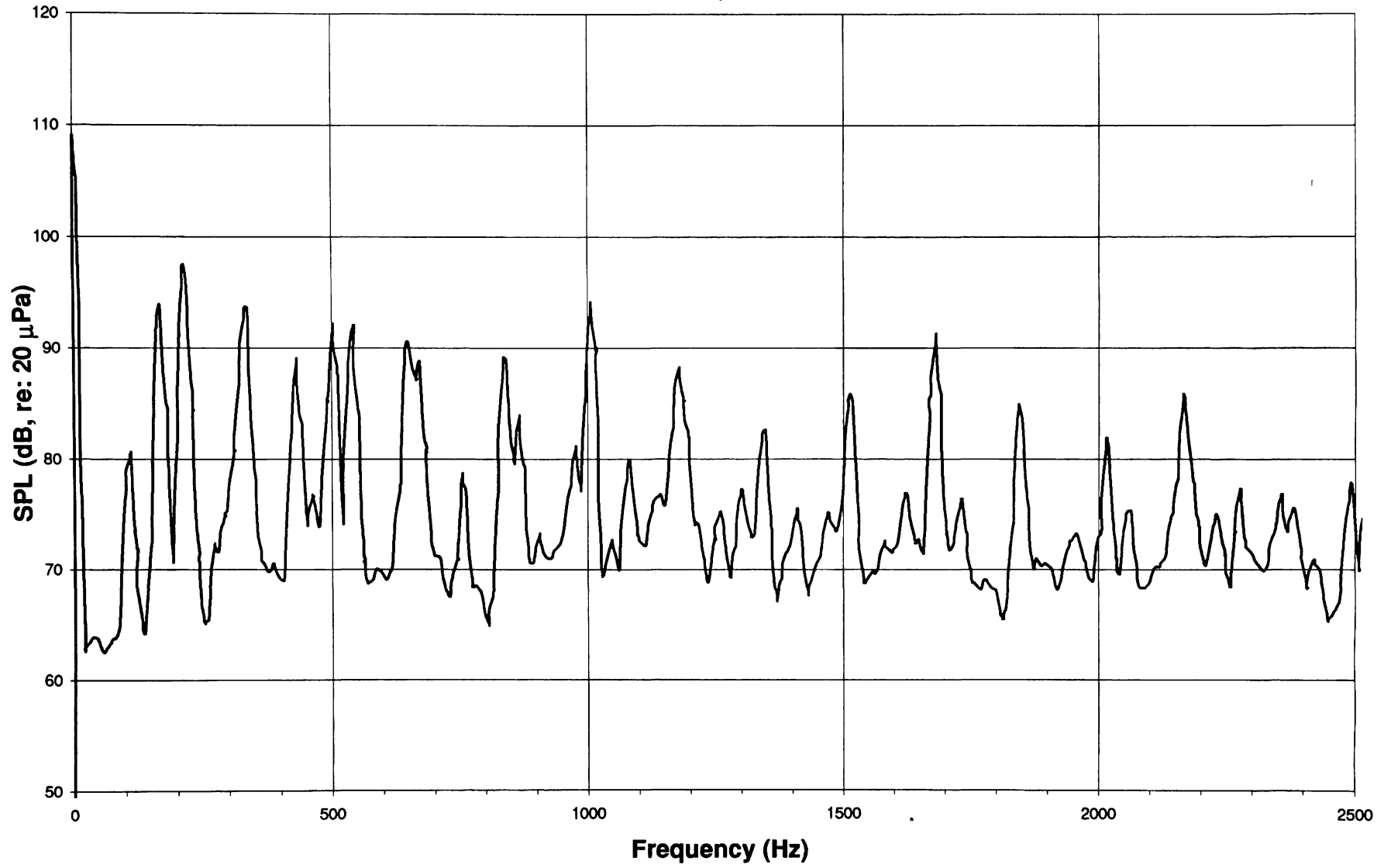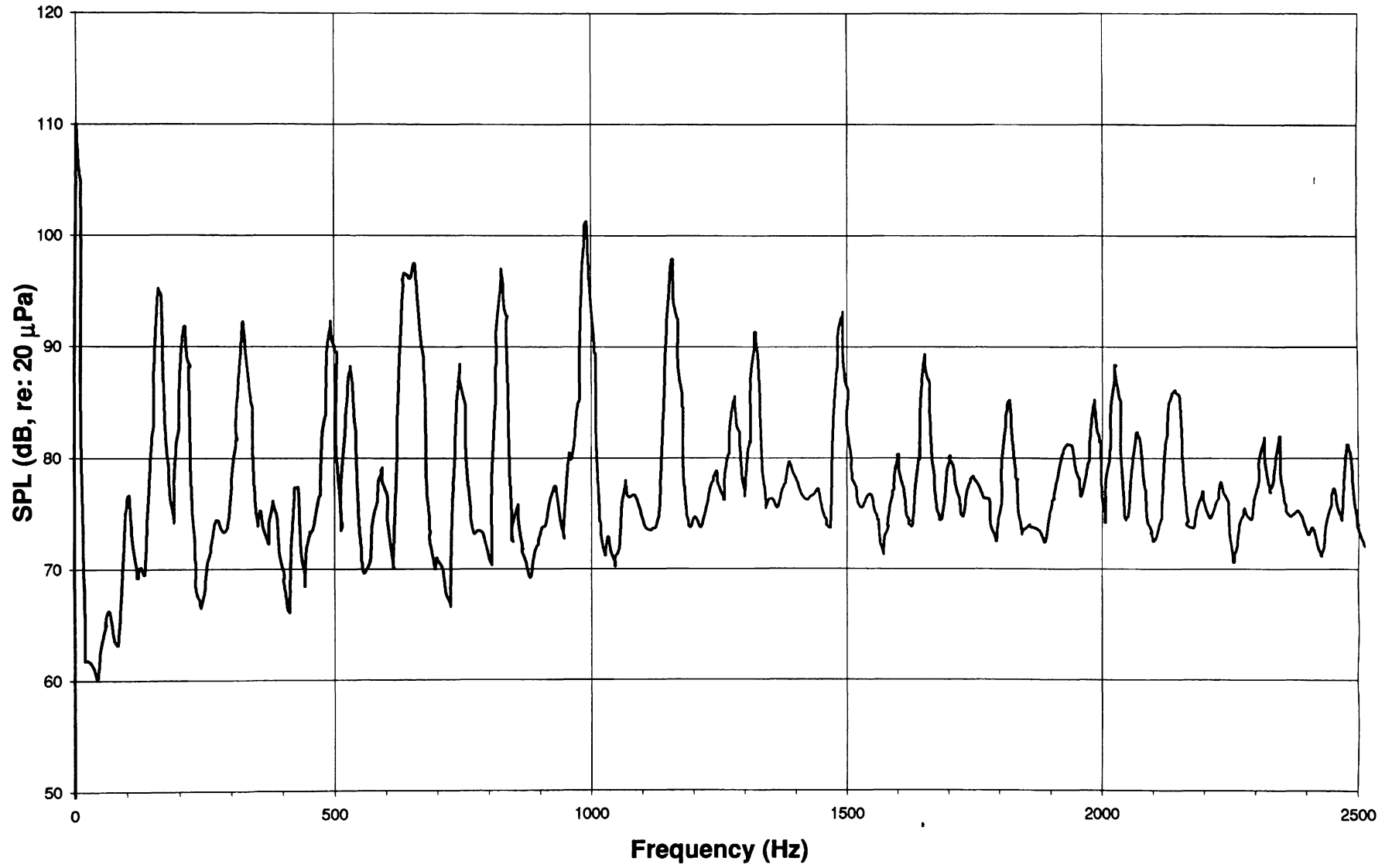
with shroud, $\theta = 60°$

with shroud, θ = 90°

with shroud, θ = 120°

Frequency (Hz)

SPL (dB, re: 20 μPa)

with shroud, θ = 150°

y-axis: SPL (dB, re: 20 μPa)

x-axis: Frequency (Hz)
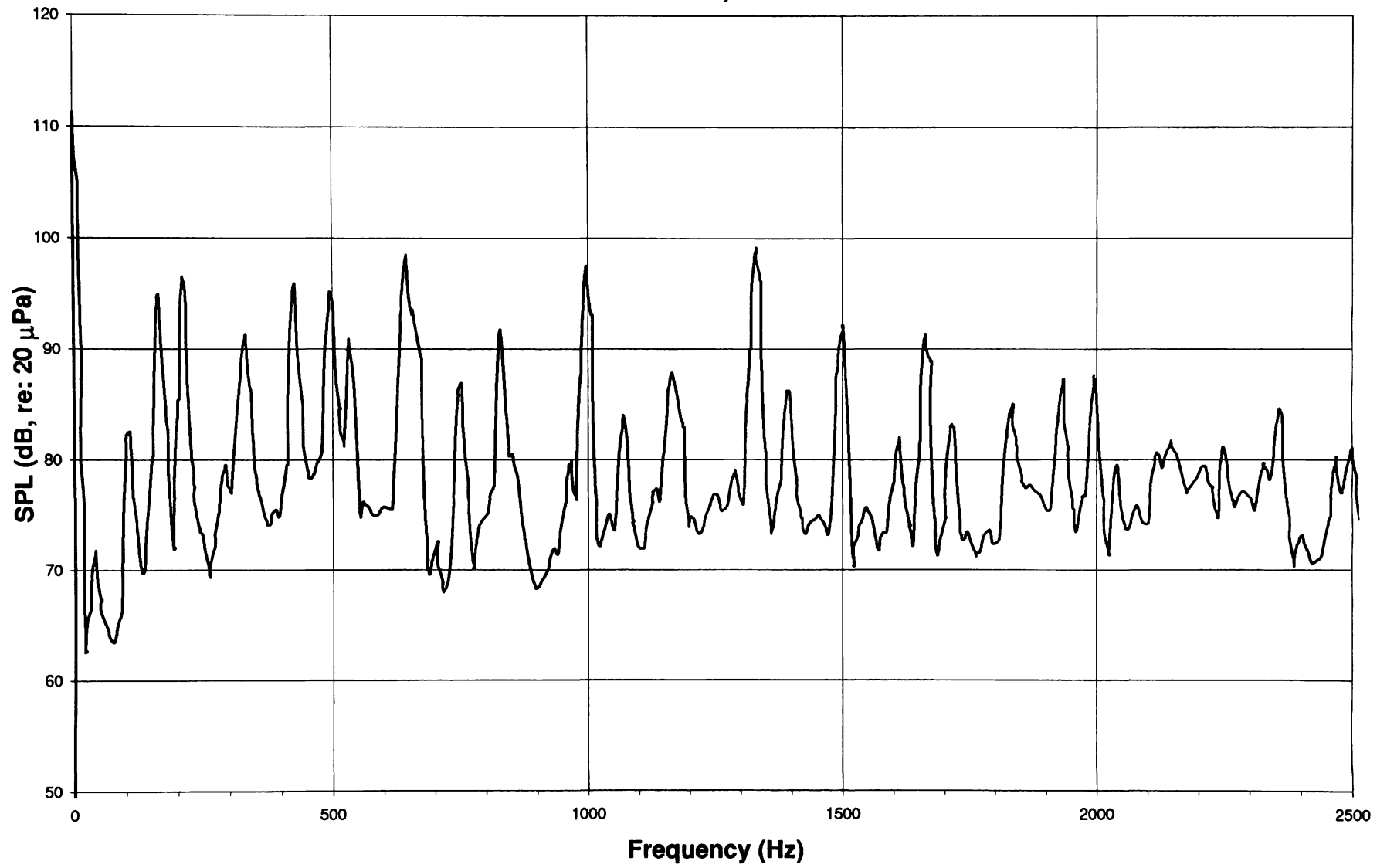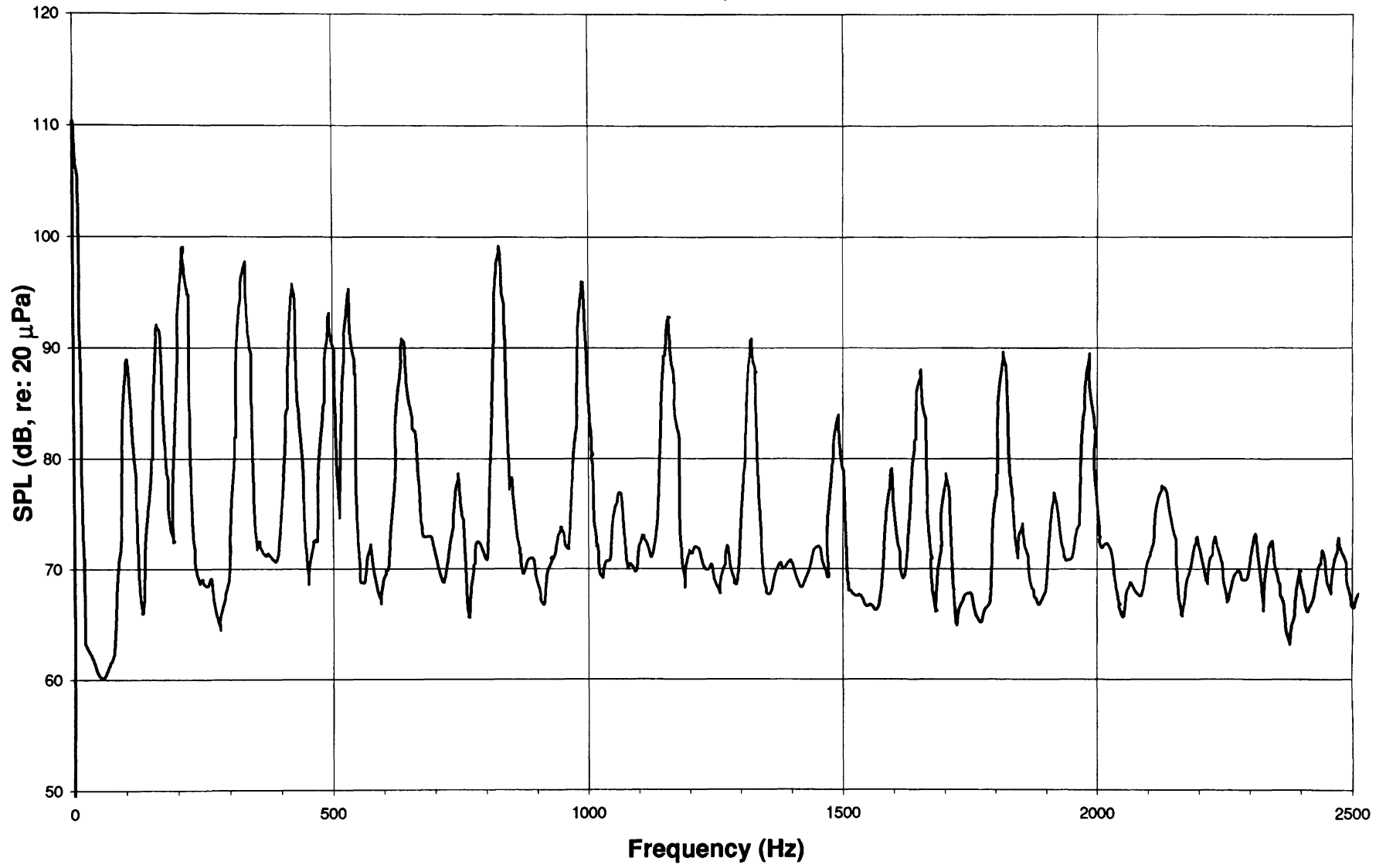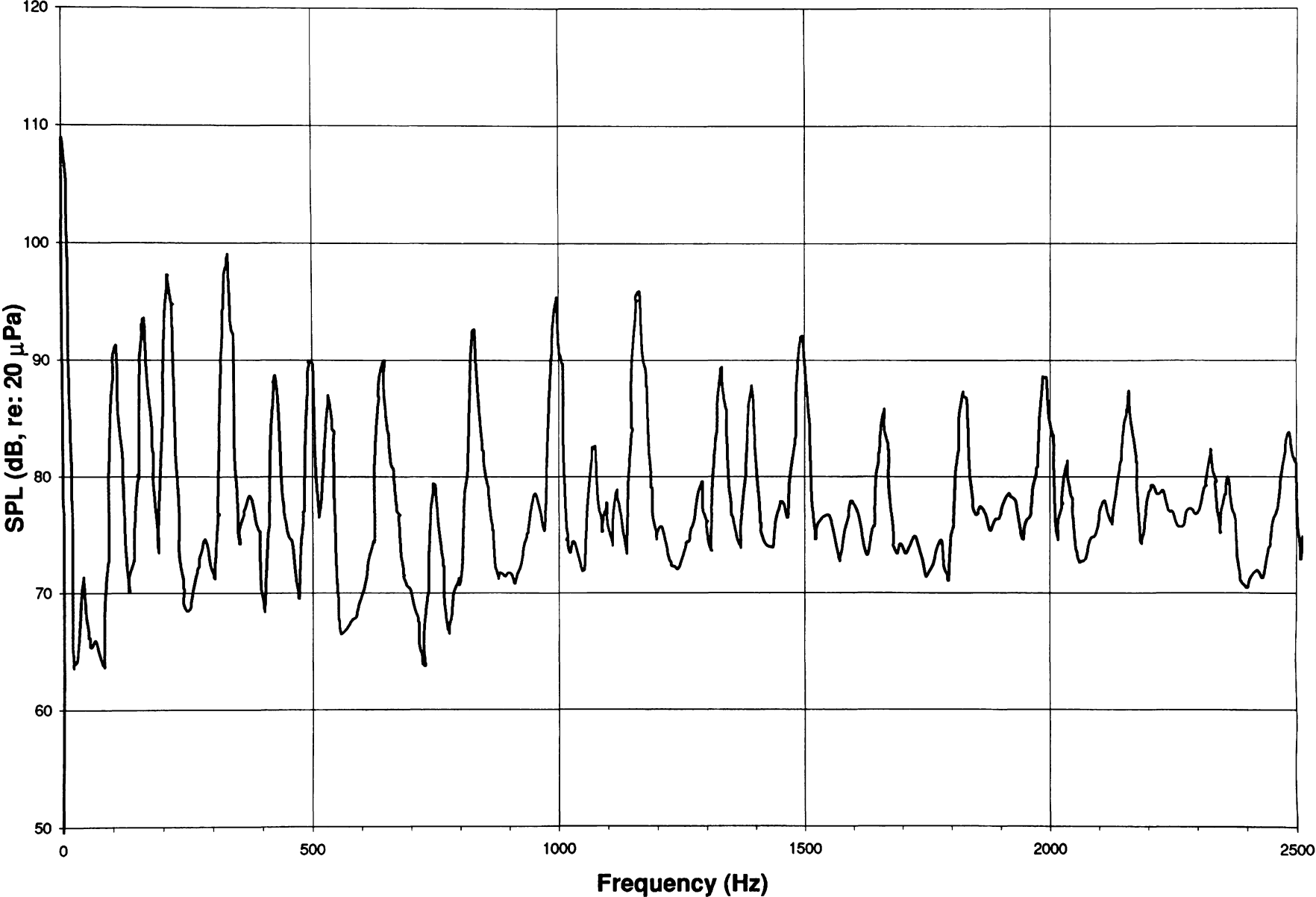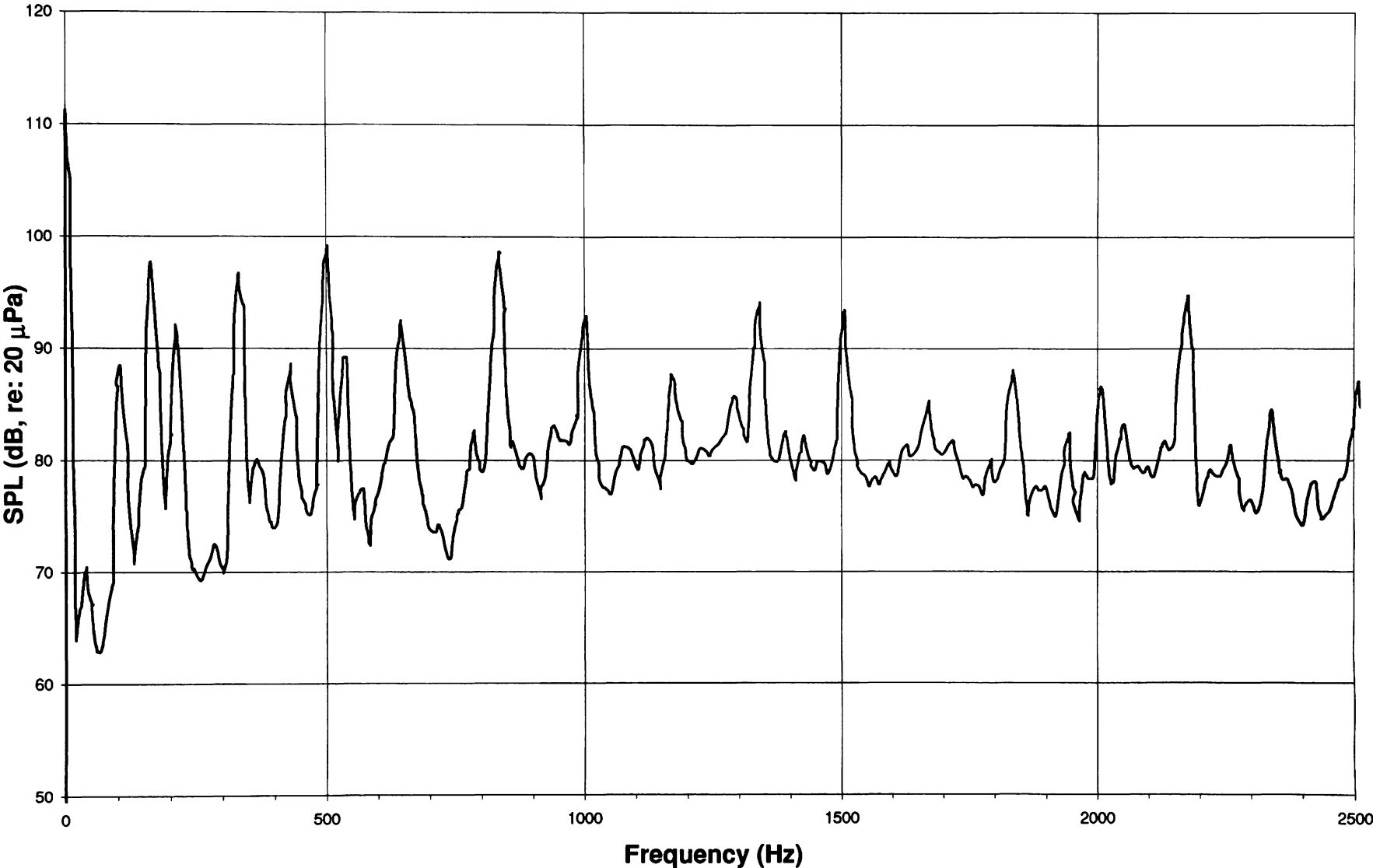
without shroud, RPM = 9600
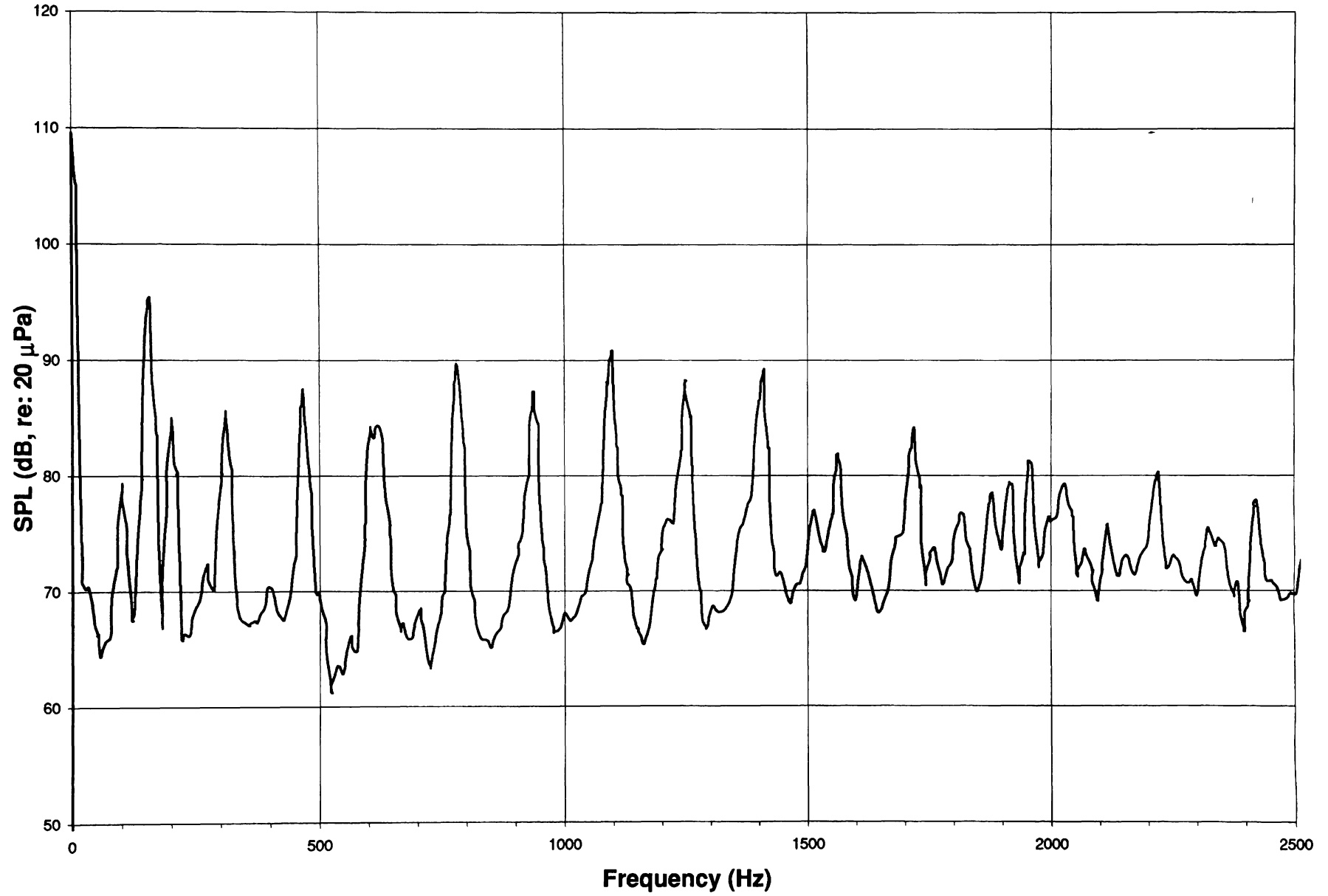
without shroud, RPM = 8200
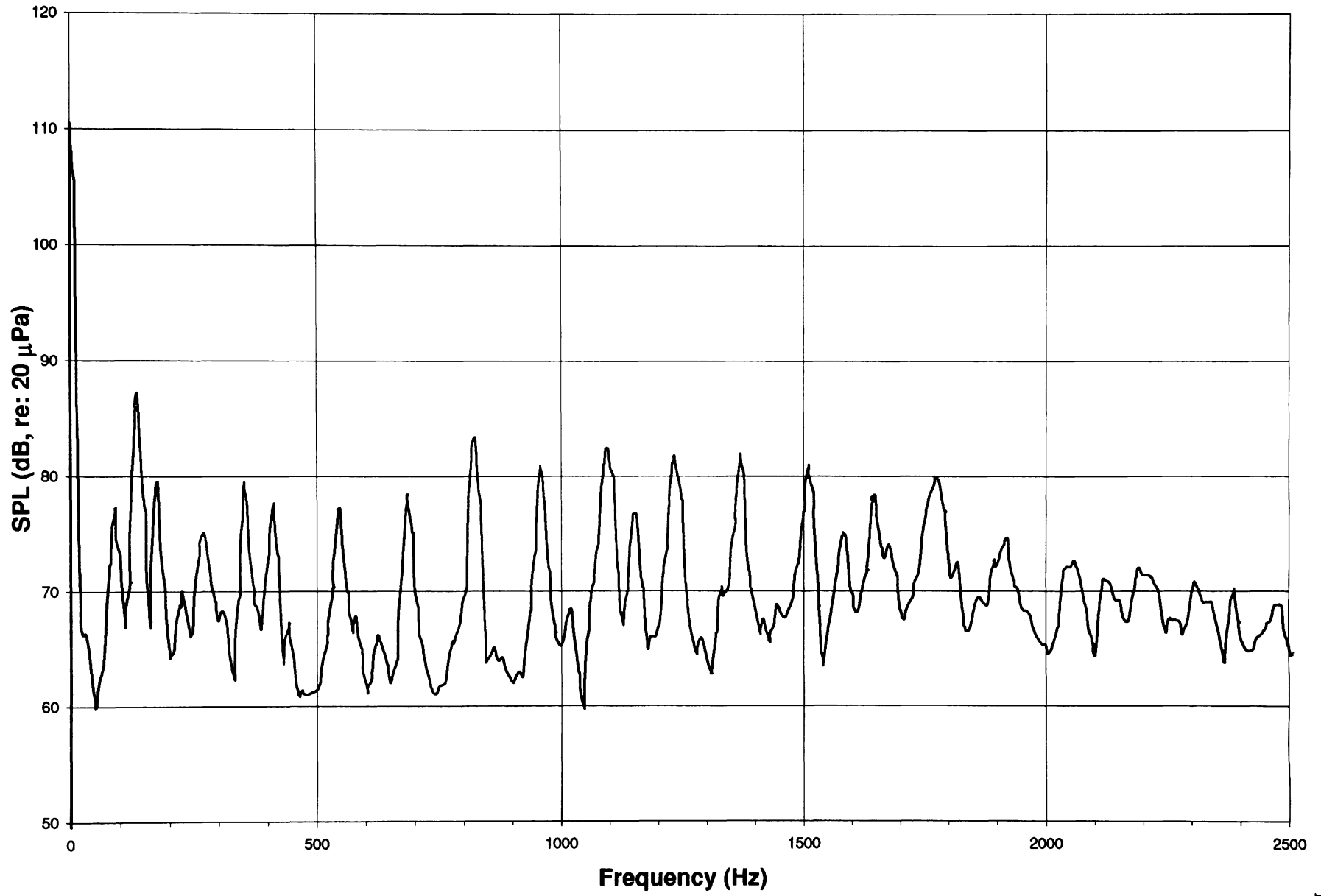
without shroud, RPM = 6500

without shroud, RPM = 5500

SPL (dB, re: 20 μPa) vs Frequency (Hz)
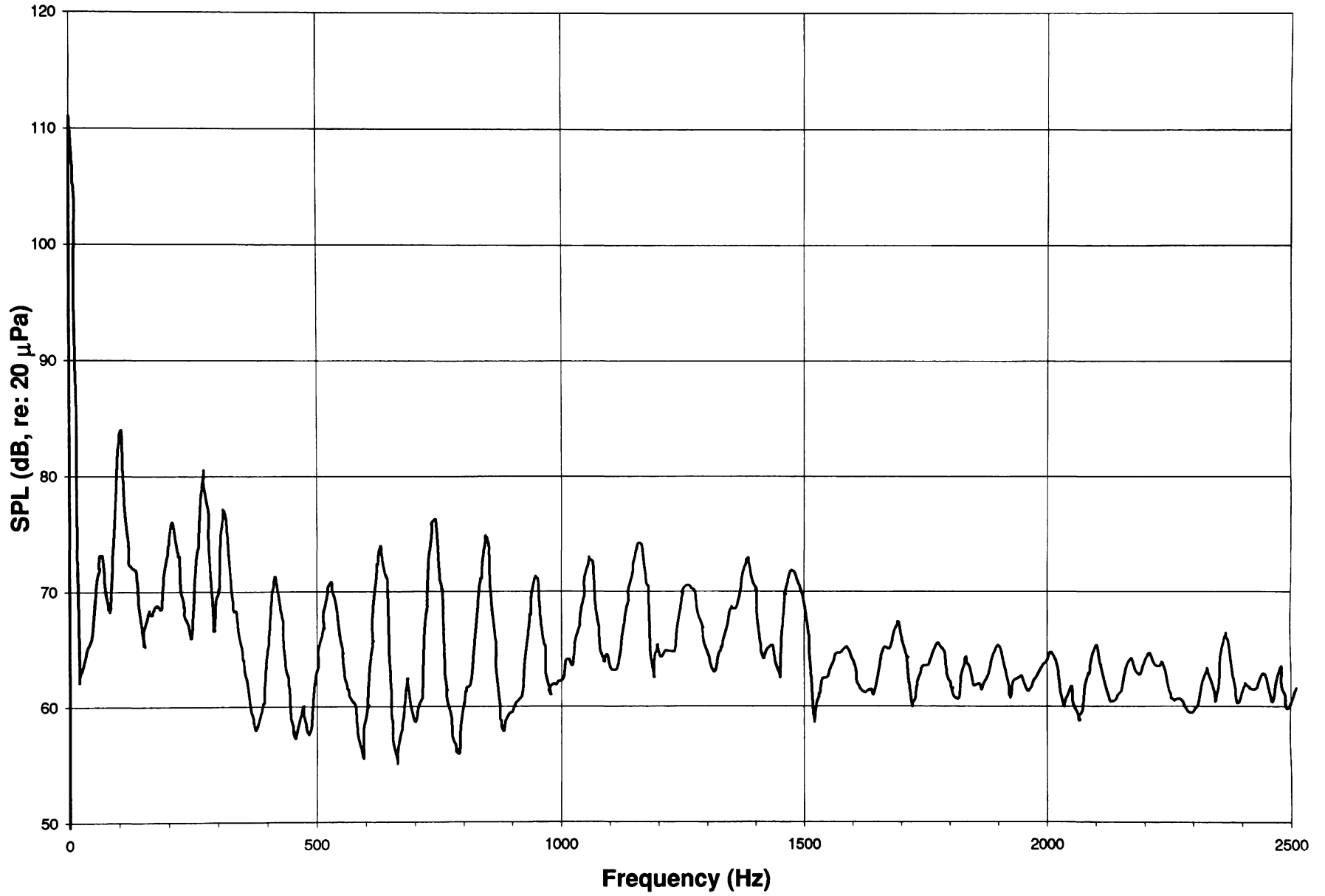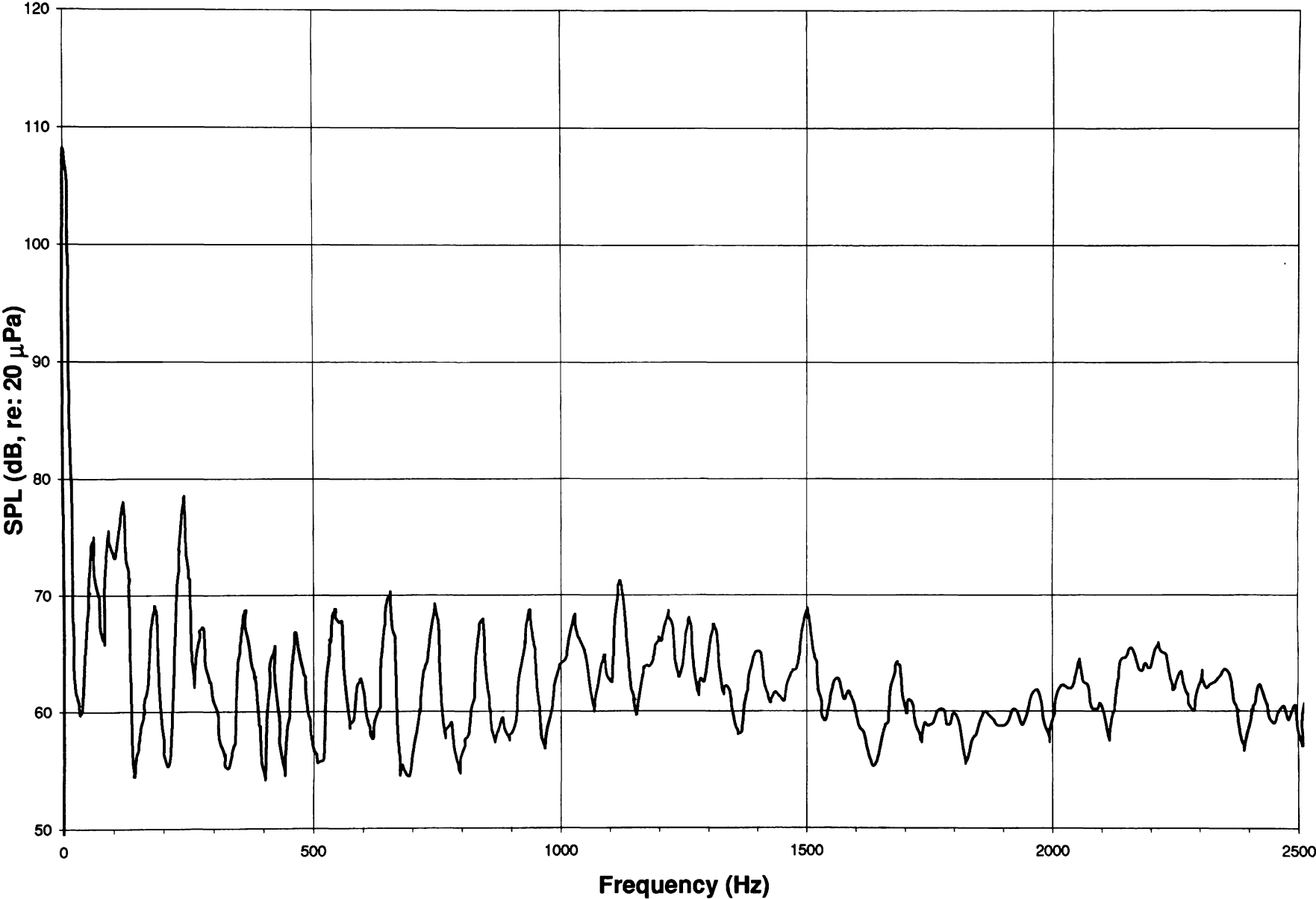
with shroud, RPM = 9600
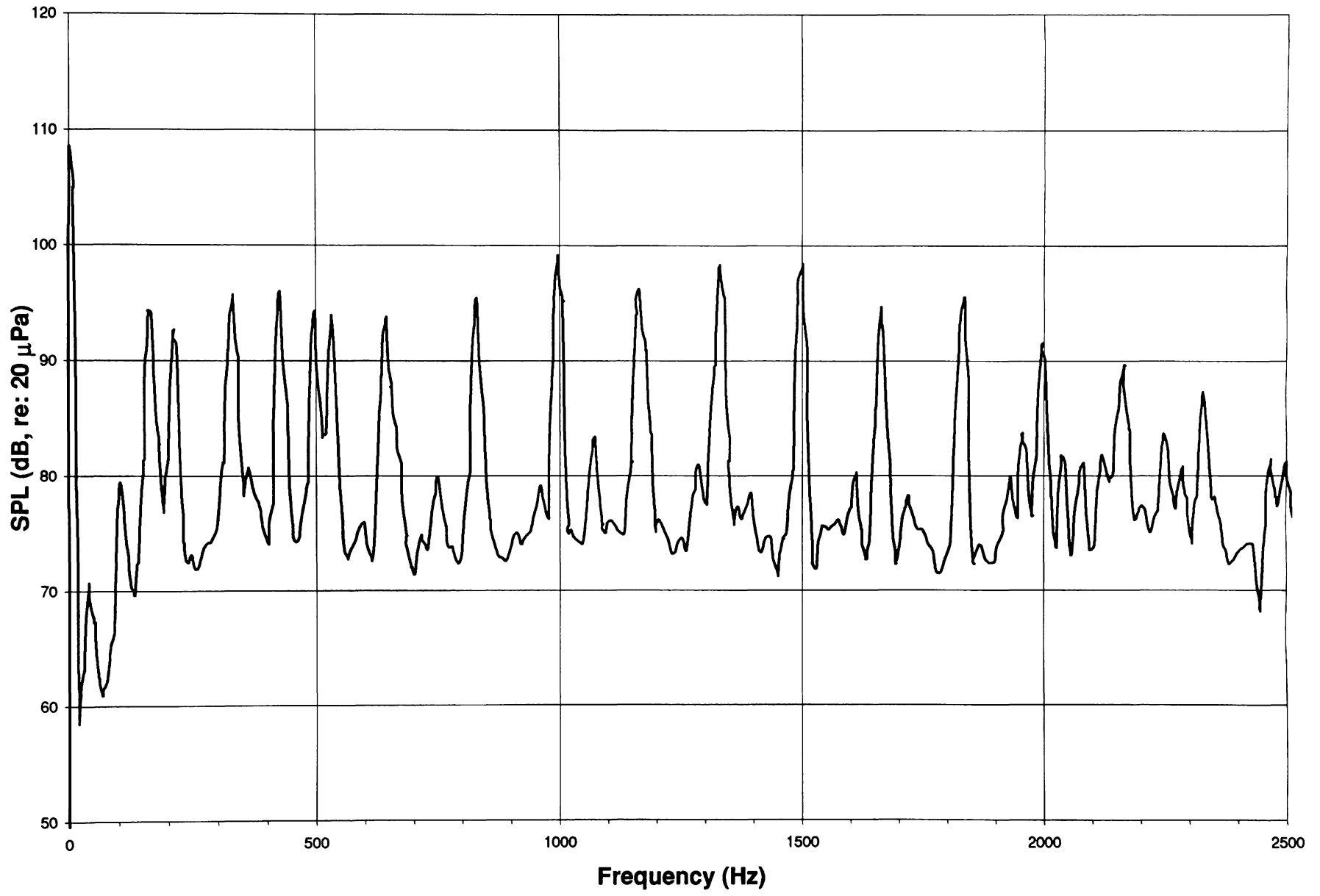
with shroud, RPM = 7300
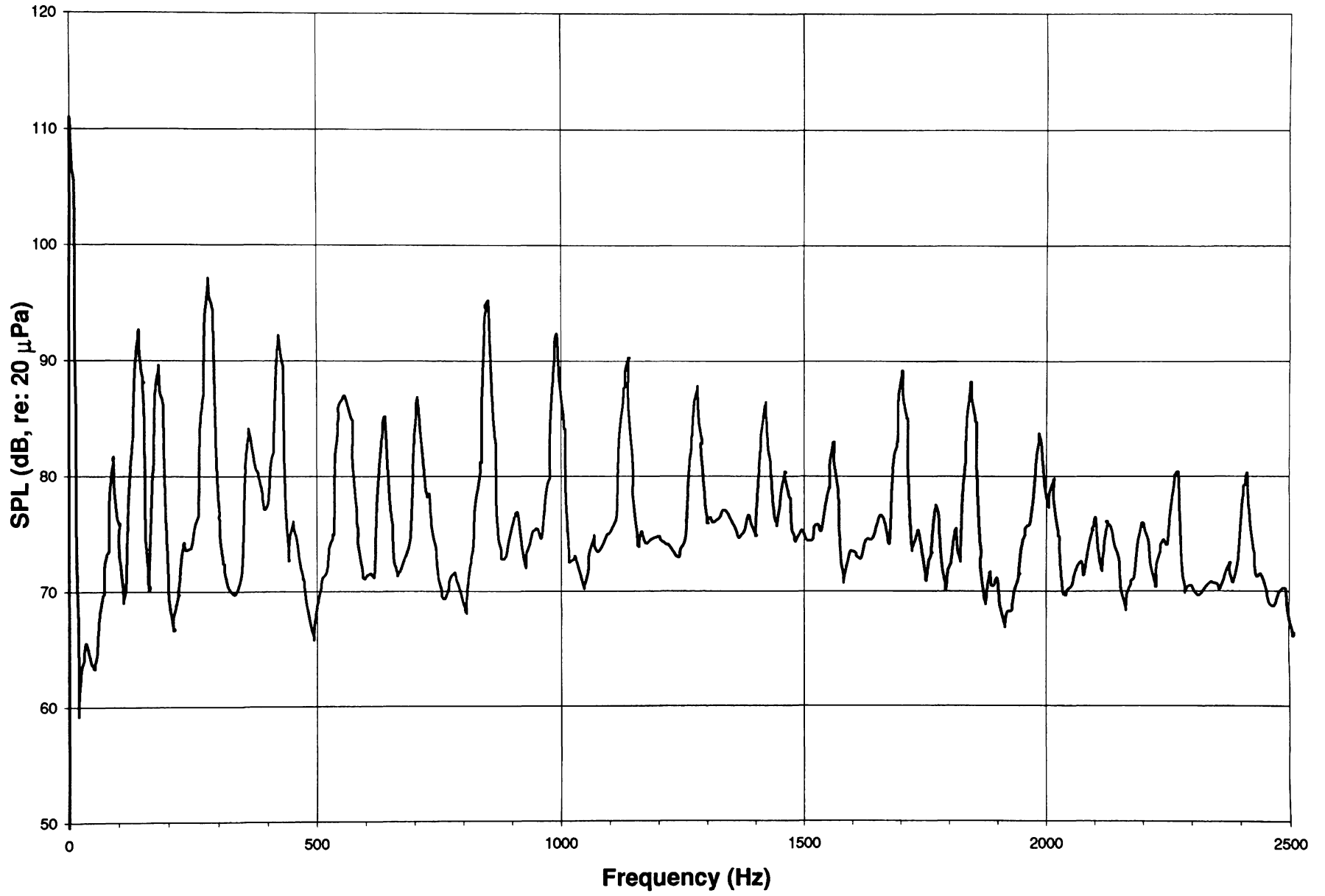
with shroud, RPM = 6400
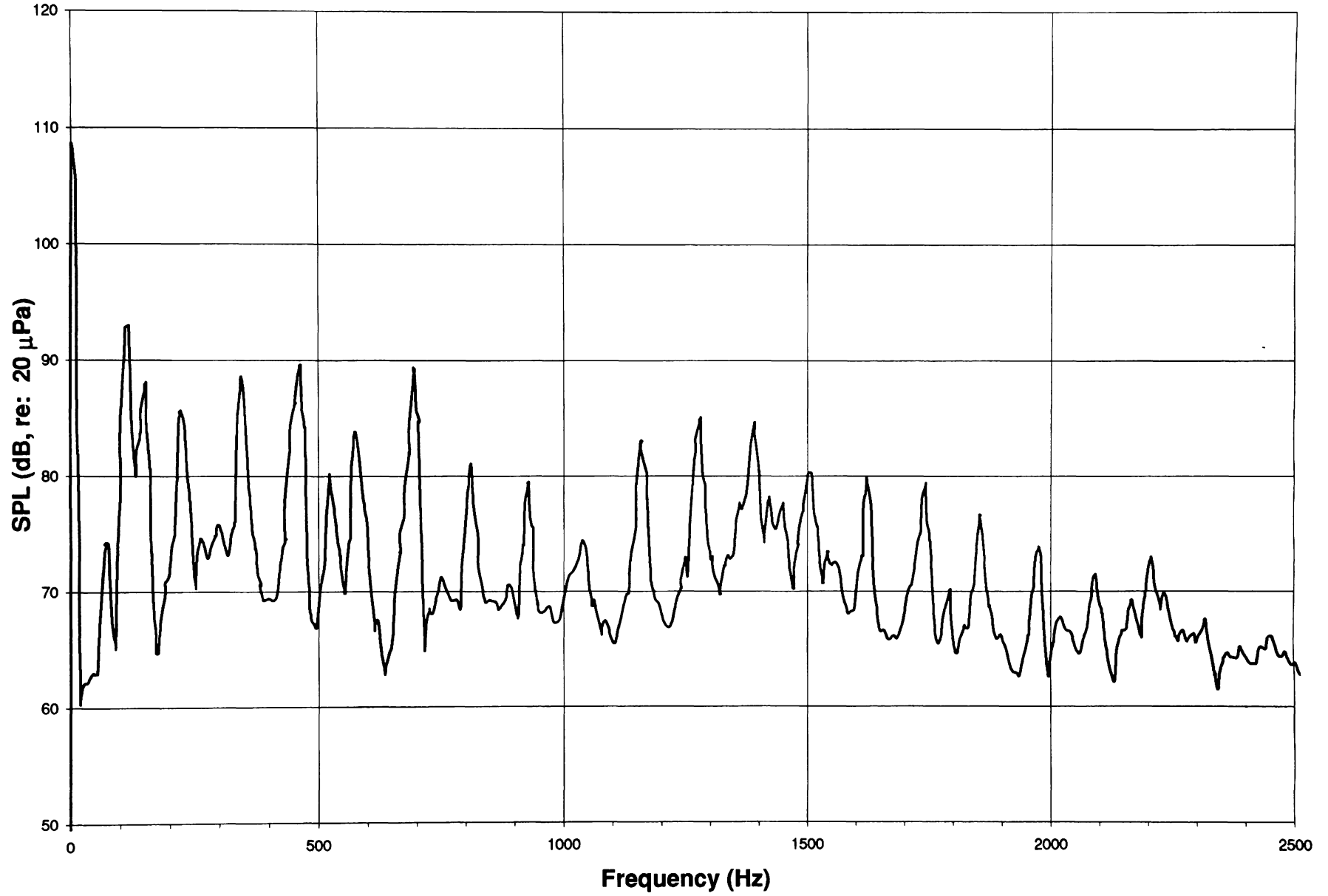
with shroud, RPM = 5000

Frequency (Hz)

SPL (dB, re: 20 μPa)

exhaust side - exh on, int on

SPL (dB, re: 20 μPa) vs Frequency (Hz)

exhaust side - exh off, int on

Frequency (Hz)

SPL (dB, re: 20 μPa)
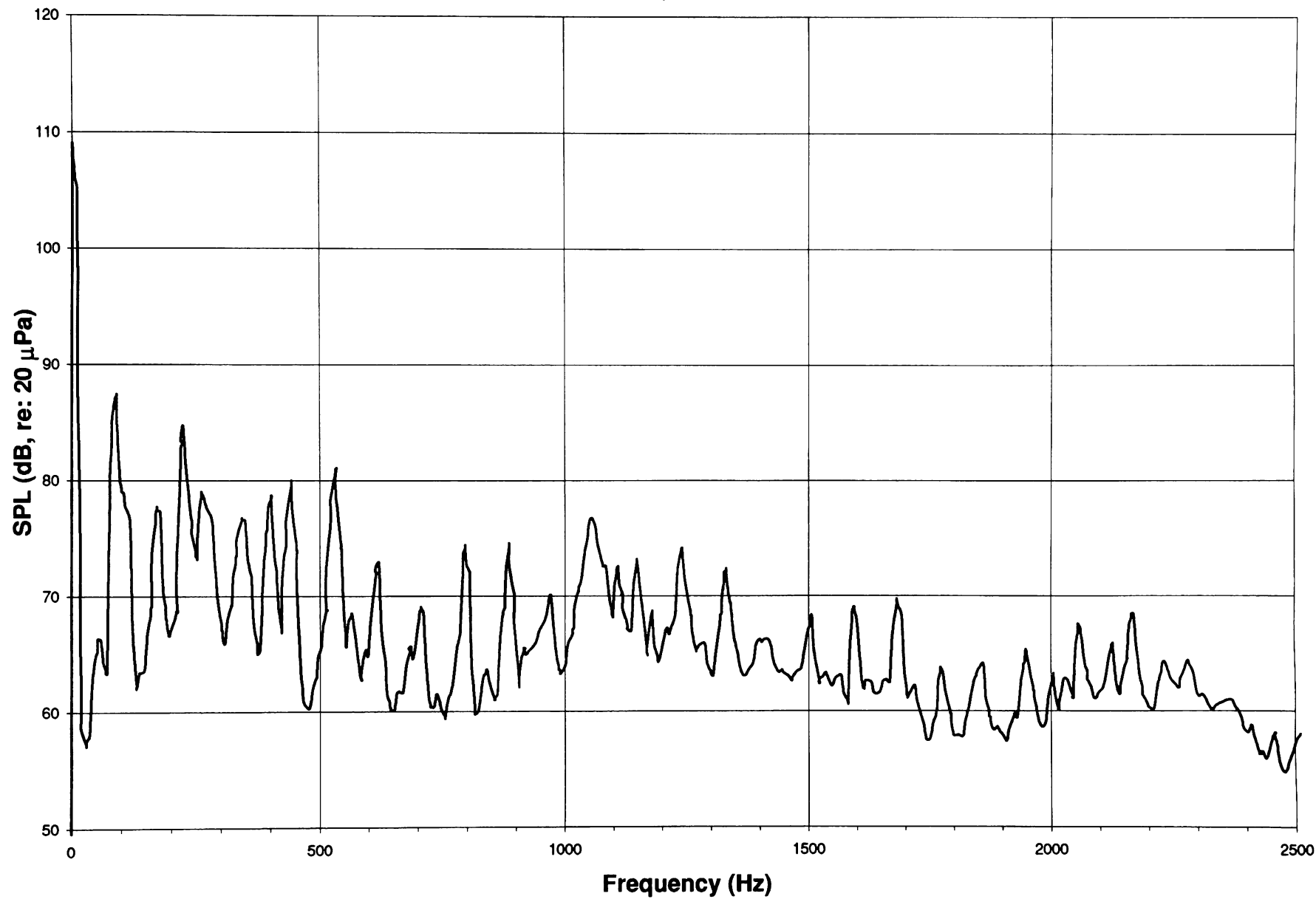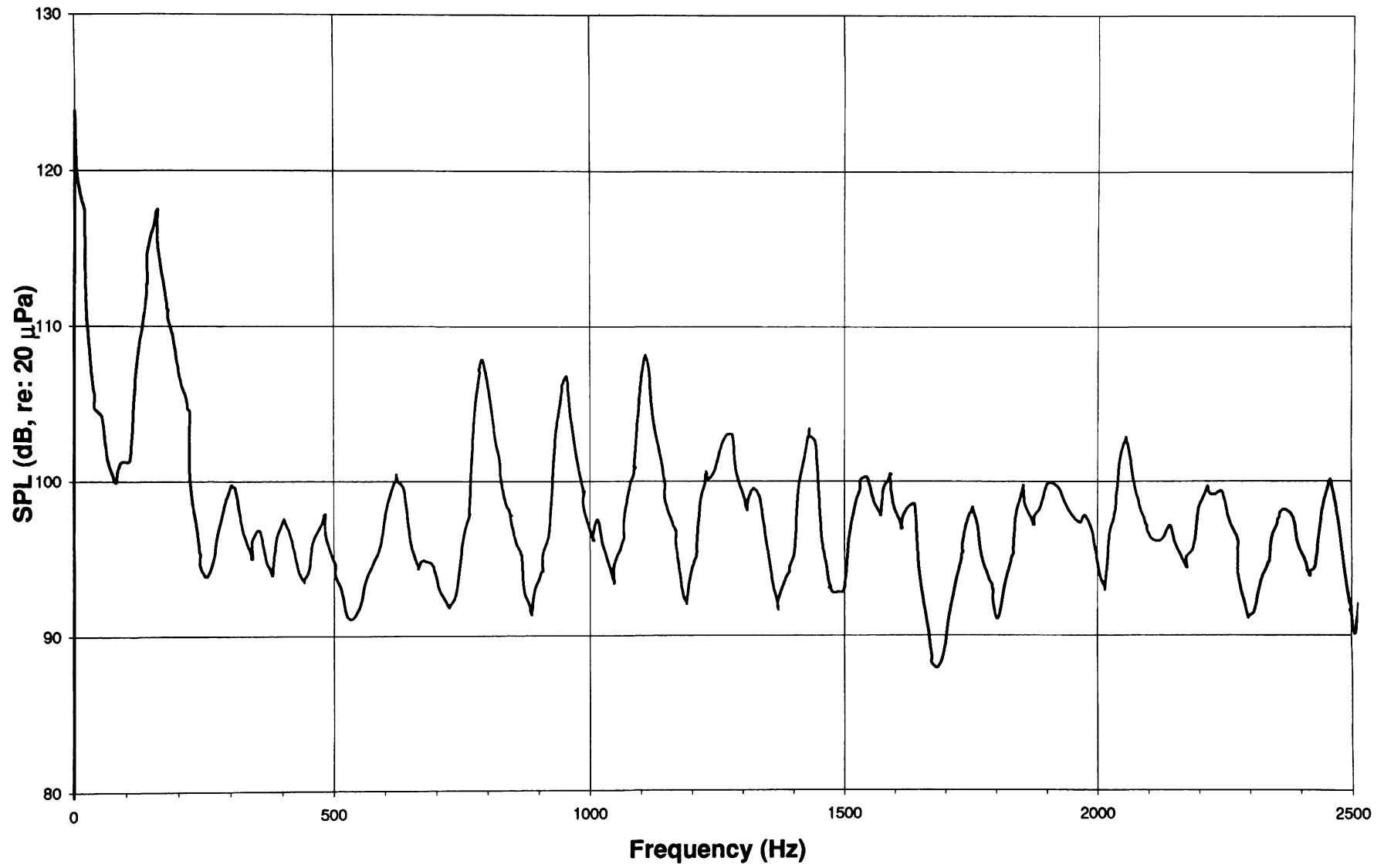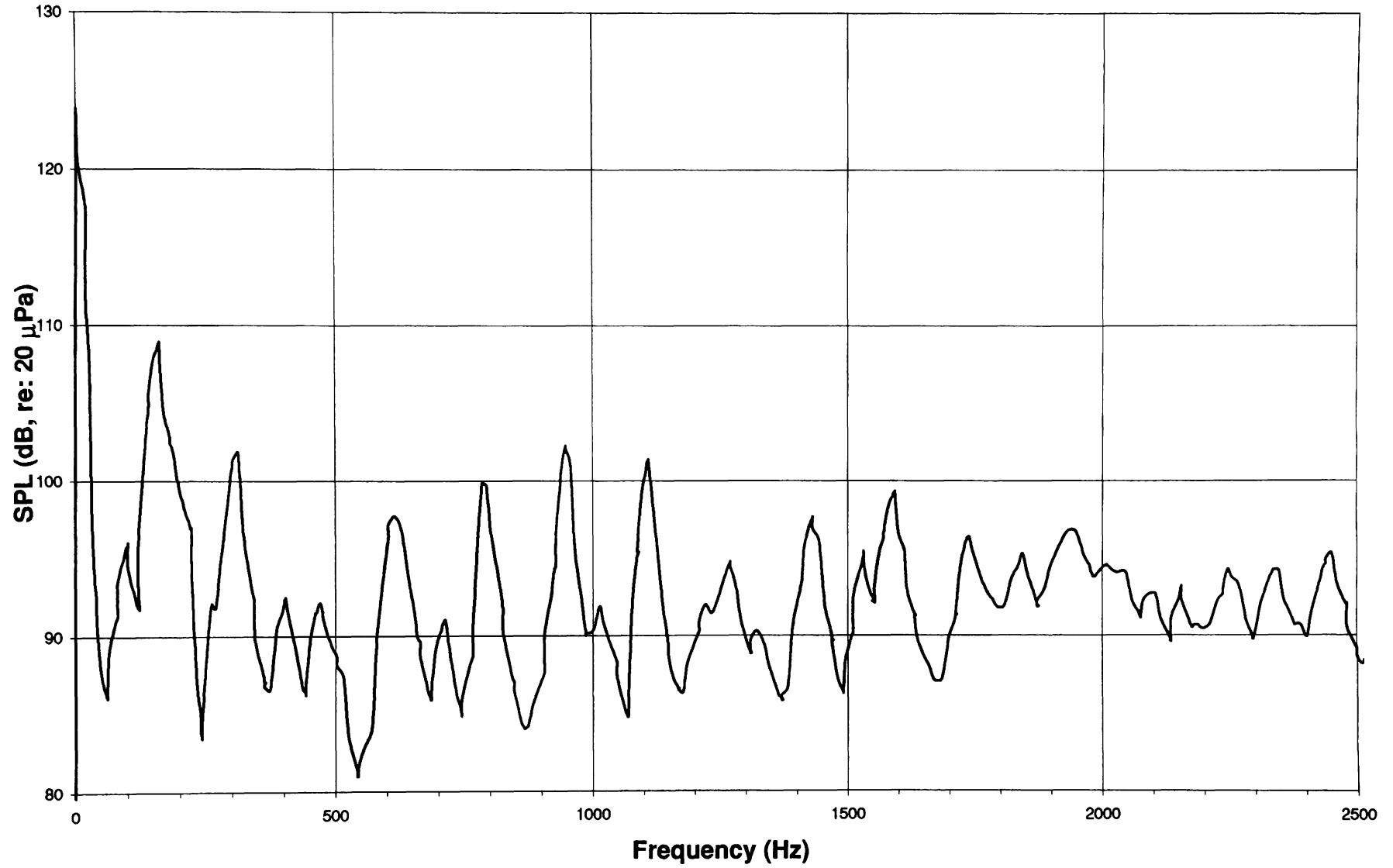
exhaust side - exh on, int off

exhaust side - exh off, int off

X-axis: Frequency (Hz)
Y-axis: SPL (dB, re: 20 µPa)

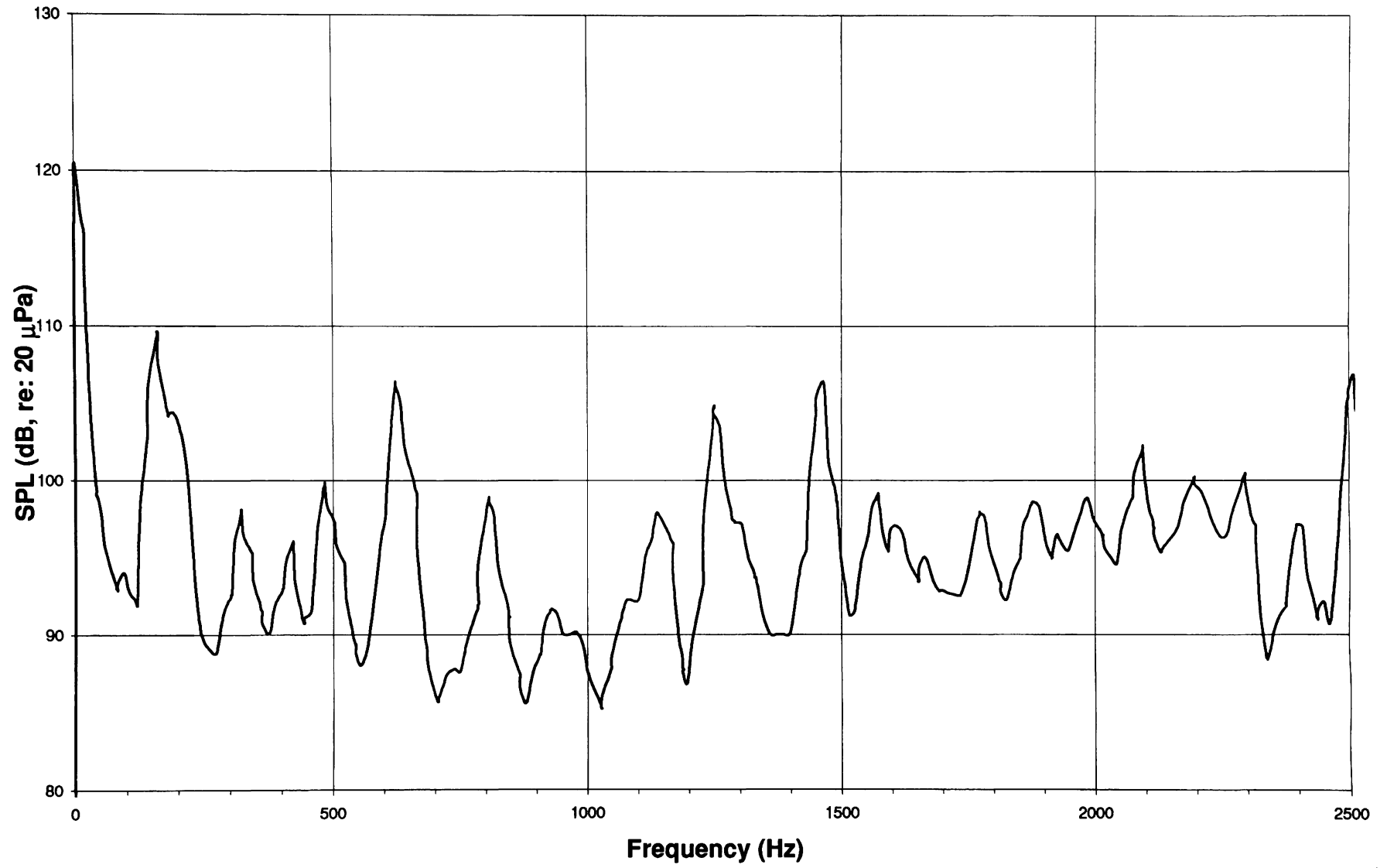# intake side - exh on, int on

Frequency (Hz)

SPL (dB, re: 20 μPa)
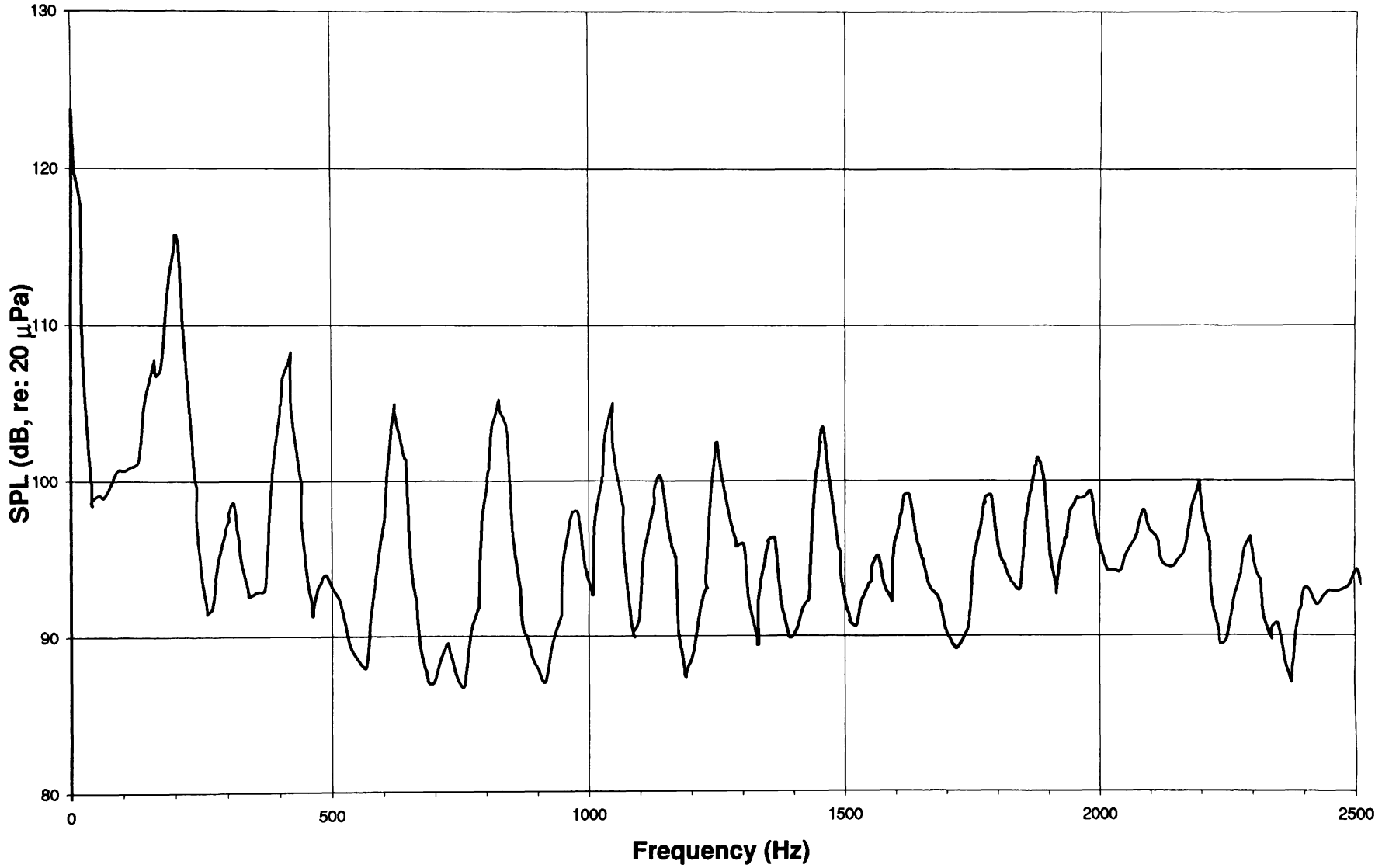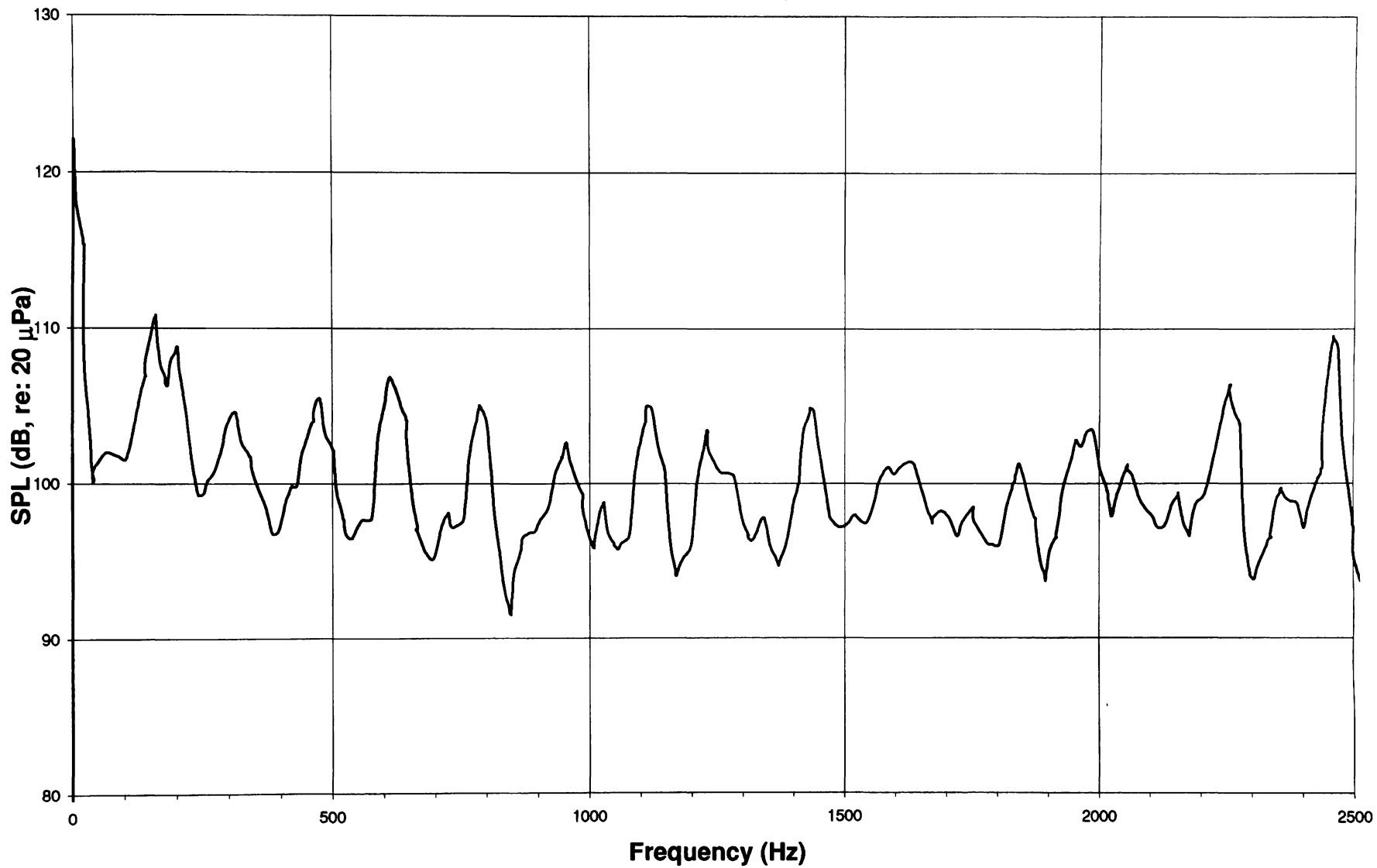
intake side - exh off, int on
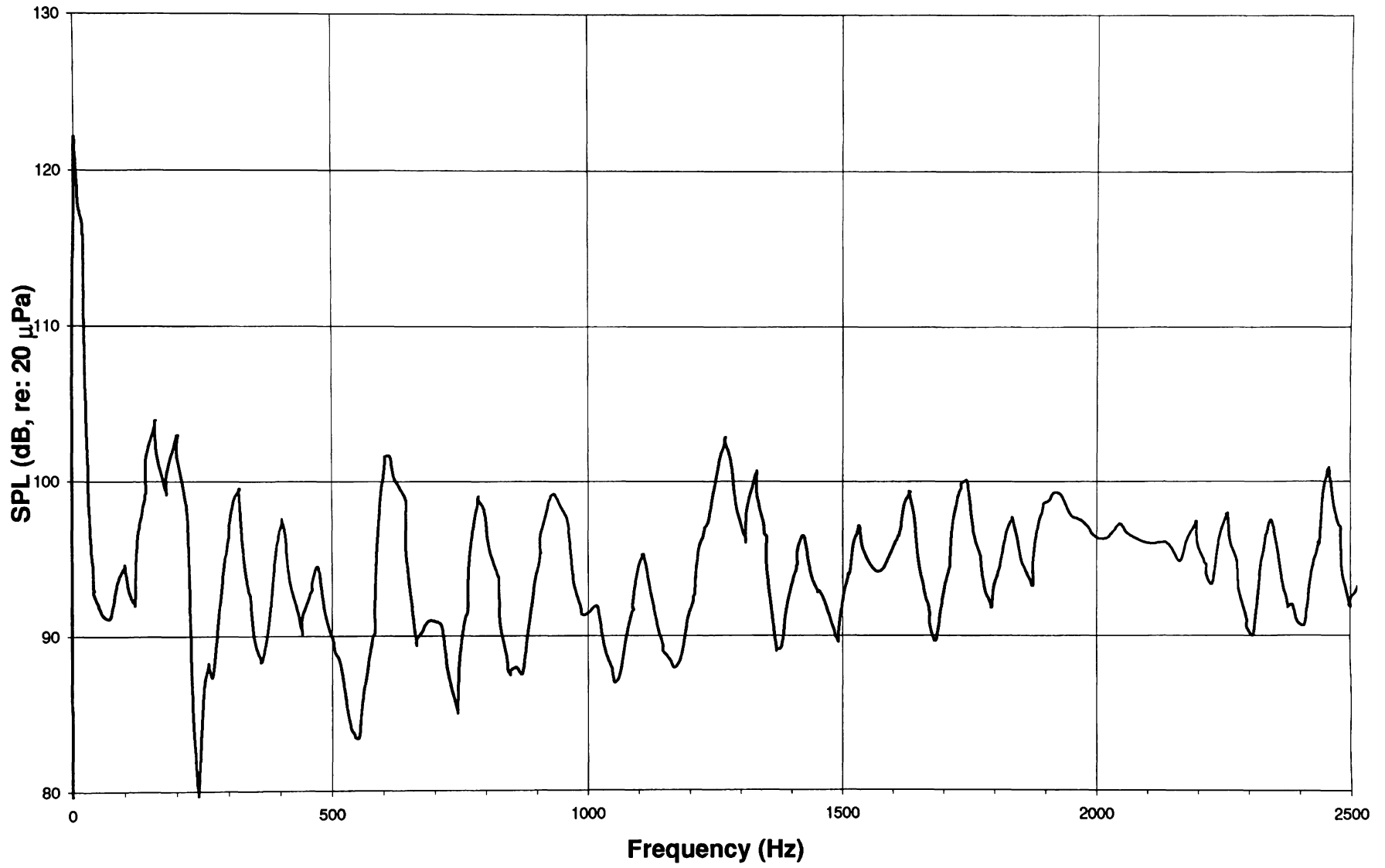
intake side - exh on, int off

intake side - exh off, int off

Chart with y-axis "SPL (dB, re: 20 μPa)" ranging from 80 to 130, and x-axis "Frequency (Hz)" ranging from 0 to 2500.

calibration signal